Abstract

TANJORE, DEEPTI. A New Application for Brookfield Viscometers: Viscoelastic Property Determination. (Under the direction of Christopher R. Daubert)

Viscoelastic properties are traditionally measured using sophisticated and expensive instruments. Brookfield YR-I is an affordable instrument, primarily developed to measure the yield stress of materials with a vane attachment. In recent years, vane attachments have gained popularity from various advantages, including elimination of wall slip, minimum disturbance to sample, quick single point determination, and easy fabrication and cleaning. Prior research has established that the vane can be used to measure elastic shear moduli of materials. This research project attempts to apply the Brookfield YR-I rheometer to the measurement of viscoelastic properties. Different concentrations of gelatin and polyacrylamide gels served as model systems for viscoelastic and elastic materials, respectively. The concepts developed were applied to the torque-time response obtained for these model systems from the Brookfield YR-I. The data compared favorably with viscoelastic data obtained from oscillatory testing with a stress controlled rheometer. The results helped establish a protocol for the Brookfield YR-I to measure viscoelastic properties. Furthermore, certain commercial products were tested using the protocol, but disagreement between the machines was observed in some materials. The effect of cup size and the position of the assumed Newtonian line are potential reasons for the disparity, and future work should focus on refining these aspects.

A NEW APPLICATION FOR BROOKFIELD VISCOMETERS: VISCOELASTIC PROPERTY DETERMINATION

By

Deepti Tanjore

A Thesis submitted to the Graduate Faculty of
North Carolina State University
in partial fulfillment of the requirements for the Degree of
Master of Science

Department of Biological and Agricultural Engineering
Raleigh, North Carolina
2005

Approved by:

_____	_____
Dr. Christopher R. Daubert Chair of Advisory Committee	Dr. Daniel H. Willits Co-chair of Advisory Committee
_____	
Dr. Jason A. Osborne Minor Representative	

DEDICATION

For MUMMY

BIOGRAPHY

Deepti Tanjore, the first daughter of Prabhakara Rao and Dhanalakshmi Tanjore, was born on August 8th, 1982 in Visakhapatnam, Andhra Pradesh, a port city on the east coast of India. She lived with her parents and younger sister, Divya for 21 years in the same city. She attended Timpany School up to 10th grade and later attended Kaizen Academy for junior college (11th and 12th grades). She had developed an immense love for Indian classical dance and music and had taken a few classes in the same. In 1999, she joined Andhra University College of Engineering for a bachelor's degree in Chemical Engineering. During the course of her undergraduate studies, she found her elective, Bio-Technology very interesting and decided to pursue her further studies in the field of Biological Engineering. After graduating in May 2003, she chose to go to NC State University, Raleigh for a masters degree in the Department of Biological and Agricultural Engineering. As a graduate student, Deepti actively participated in many student organizations including Maitri (Indian Student Association at NC State University), Food Science Club, Children Relief and You and Two Cents of Hope.

Upon completion of her master's degree, Deepti decided to follow the footsteps of her mother and pursue a PhD. She will be attending the Pennsylvania State University for a doctoral degree in the Department of Biological and Agricultural Engineering.

ACKNOWLEDGEMENTS

During the course of my graduate studies I have learnt more than I have learnt my entire life. This process was continuously supported by many and I am glad to have this opportunity to express my gratitude.

Firstly, though I cannot thank him enough, I would like to thank Dr. Christopher Daubert, for believing in me more than I believed myself. I am grateful to him for entrusting me with such an exciting project and for standing by me throughout the process. I truly appreciate the immense amount of patience he showed during my transition from an undergraduate student to a graduate researcher. It's a blessing from God to have been guided by such a brilliant and understanding professor.

I would like to express my sincere thanks to the Brookfield Engineering for sponsoring this project. I appreciate the persistent support extended by Mr. Robert McGregor throughout the course of the project.

I would like to thank my committee members including Dr. Osborne for helping with the statistical analysis and Dr. Willits for taking care of many things from my first day at NC State University.

I also want to convey my appreciation to the lab members of the Food rheology lab, including Sharon for taking care of everything, Junhua for his valuable advice, Melissa, Dr. Sankar, Jeff and John. I would also like to thank my roommates and friends who were with me through the highs and lows of my stay at Raleigh.

I would also like to take this opportunity to thank Dr. K.V. Krishna Kumar, Dr. C. Ayyanna, and Dr. V.S.R.K. Prasad whose contribution during my early stages of education is invaluable.

Lastly, I would like to show my gratitude to my family, especially my mother for making me what I am. Her constant support through these two years, from thousands of miles away, was highly inspiring. I cannot imagine doing anything without her.

TABLE OF CONTENTS

LIST OF TABLES……...x

LIST OF FIGURES……. xii

LIST OF SYMBOLS……...xvii

CHAPTER 1. EXTENDED SUMMARY…….. 1

1.1 REFERENCES…… 3

CHAPTER 2. LITERATURE REVIEW…… 4

2.1 RHEOLOGY…… 5

2.2 SHEAR STRESS AND SHEAR RATE……. 5

2.3 CHARACTERIZATION OF MATERIALS……. 7

2.4 YIELD STRESS……... 8

2.4.1 EXISTENCE OF YIELD STRESS……..... 9

2.4.2 RHEOLOGICAL MODELS……..…. 11

2.5 TIME-DEPENDENT FLOW…… 11

2.6 VISCOELASTICITY……..…. 12

2.6.1 PARAMETERS DESCRIBING VISCOELASTIC PROPERTIES..... 13

2.6.1.1 COMPLEX MODULUS…….. 13

2.6.1.2 PHASE ANGLE……..…… 13

2.6.1.3 ELASTIC MODULUS……..…….. 14

2.6.1.4 LOSS MODULUS…… 14
2.7 RHEOMETRY…….. 15
2.7.1 SLIP…… 16
2.8 VANE AND VANE RHEOMETRY…….. 17
2.8.1 ADVANTAGES AND LIMITATION OF THE USE OF VANE GEOMETRY…… 18
2.8.2 ASSUMPTIONS…….. 18
2.8.3 RIGID CYLINDER CONCEPT…….. 19
2.8.4 DEFORMATION ZONE CONCEPT…… 20
2.8.5 YIELDING AND FORMATION OF DEFORMATION ZONE… 22
2.9 VANE RHEOMETRY CALCULATIONS…….. 23
2.10 TORQUE-TIME PROFILE…… 27
2.10.1 TORQUE-TIME/STRESS-TIME PROFILE WITH A VANE IN A RATE CONTROLLED MODE…….…. 27
2.10.2 CLASSIFICATION OF YIELD STRESS……..…… 29
2.11 SHEAR MODULUS CALCULATION…….…….. 30
2.11.1 ALDERMAN ET AL. APPROACH…….……... 31
2.11.2 SHERWOOD AND MEETEN APPROACH……..... 32
2.12 BROOKFIELD ENGINEERING……..... 33
2.13 SUMMARY…… 34
2.14 REFERENCES……. 35

CHAPTER 3. ESTIMATION OF VISCOELASTIC PROPERTIES……. 73

3.1 INTRODUCTION…… 74

3.2 DETERMINATION OF TRUE STRAIN AND SHEAR MODULUS….. 75

3.2.1 NCSU APPROACH - DEFORMATION ZONE ESTIMATION.. 75

3.2.2 ALDERMAN APPROACH…… 78

3.2.3 BROOKFIELD APPROACH…….. 80

3.3 DETERMINATION OF THE PHASE ANGLE…… 80

3.4 MATERIALS AND METHODS OF EXPERIMENTATION……... 82

3.4.1 POLYACRYLAMIDE GELS…… 82

3.4.2 GELATIN GELS…….. 83

3.4.3 INSTRUMENT DESCRIPTION…… 84

3.5 RESULTS AND DISCUSSION…….. 85

3.5.1 ROTATIONAL SPEEDS SELECTION…… 85

3.5.2 CHOICE OF BROOKFIELD YR-I RHEOMETER (BETWEEN HB AND RV SERIES)…….…… 86

3.5.3 STATISTICAL ANALYSIS…… 87

3.5.4 PREFERABLE CUP SIZE…… 88

3.5.5 SUGGESTED APPROACH…….. 89

3.6 SUMMARY…… 90

3.7 REFERENCES…… 91

CHAPTER 4. DESIGN AND VERIFICATION OF PROTOCOL……. 110

4.1 INTRODUCTION…… 111

4.2 MATERIALS AND METHODS……..…… 112

4.2.1 COMMERCIAL PRODUCTS AND SAMPLE PREPARATION…….. 112

4.2.2 RHEOLOGICAL ANALYSIS……..……113

4.2.2.1 STRESS TECH……...… 113

4.2.2.2 BROOKFIELD YR-I…… 114

4.2.2.3 STATISTICAL ANALYSIS……..… 114

4.3 RESULTS……..… 114

4.3.1 SHEAR MODULUS…… 115

4.3.2 PHASE ANGLES…… 115

4.4 DISCUSSION……...115

4.5 SUMMARY……...… 117

4.6 REFERENCES……... 118

APPENDIX……...…140

LIST OF TABLES

CHAPTER 2

Table 2.1 Rheological modulus involving a Yield Stress parameter…… 50

Table 2.2 Advantages and Limitations of the vane method……..…. 51

Table 2.3 Comparison of the torque-time profiles as explained by various researchers…….. 52

Table 2.4 Spring torque constants (TK) for different models of Brookfield YR-I……..…. 53

Table 2.5 Yield Multiplier constant for different vane attachments provided with Brookfield YR-I……..... 54

Chapter 3

Table 3.1 Variances of phase angle and shear moduli data for 4% Gelatin from both the instruments at various strain rates…….. 93

Table 3.2 Comparison of data obtained for various concentrations of polyacrylamide and gelatin gels from the Brookfield YR-I with various cup sizes to the StressTech data with each of the approaches…….. 94

Chapter 4

Table 4.1 Commercial products used for testing the devised approach……121

Table 4.2 Summary of the phase angle data obtained from Brookfield YR-I and StressTech and agreement between the two instruments..... 122

Table 4.3 Summary of the shear moduli data obtained from Brookfield YR-I and StressTech and agreement between the two instruments…….. 123

Table 4.4 Categorization of the agreement between data obtained from Brookfield YR-I and StressTech……..… 124

LIST OF FIGURES

CHAPTER 2

Figure 2.1	Movement of layers of fluid on application of force.....	55
Figure 2.2	Movement of a solid on application of force……..	56
Figure 2.3	Behavior of Newtonian and yield stress fluids……...	57
Figure 2.4	Yield stress determination……..…	58
Figure 2.5	Yield stress determination at different shear rates….....	59
Figure 2.6	Stress-strain relationship of elastic and viscoelastic materials at various frequencies……	60
Figure 2.7	Strain input and stress response for a viscoelastic material……..…	61
Figure 2.8	Variation of phase angle……	62
Figure 2.9	Modulus-strain rate relationship of elastic and viscoelastic materials at various frequencies……...…	63
Figure 2.10	Effect of wall slip in a bob and cup geometry……..…	64
Figure 2.11 (a)	The vane in side view…….	65
Figure 2.11 (b)	The vane in top view……..	65
Figure 2.12	Vane in a cup……...…	66
Figure 2.13	Typical torque-time response……...	67
Figure 2.14	Deformation Zone……...	68
Figure 2.15	Flow in gap……..….	69
Figure 2.16	Torque – time response……..…	70

Figure 2.17 Classification of yield stress…….. 71

Figure 2.18 Torque-time response…… 72

CHAPTER 3

Figure 3.1 Torque-time relationship of elastic materials at various rotational speeds…….…… 95

Figure 3.2 Torque-time relationship of Newtonian materials of different viscosities at various rotational speeds at constant rate of rotation……..…… 96

Figure 3.3 Torque-time relationship of elastic, low viscosity Newtonian and viscoelastic materials at various rotational speeds…….…. 97

Figure 3.4 Various phases of a torque-time relationship of viscoelastic material……..… 98

Figure 3.5 True strain…… 99

Figure 3.6 Strain Calculation…… 100

Figure 3.7 Areas representing viscous and elastic effects of the material……. 101

Figure 3.8 Torque response at 0.1 rpm……..… 102

Figure 3.9 Torque response at 1.0 rpm……..… 103

Figure 3.10 Torque response at 5.0 rpm……..… 104

Figure 3.11 Stress Sweep at 0.05 Hz……... 105

Figure 3.12 4% Gelatin phase angle data for various cups for all three approaches…….. 106

Figure 3.13 4% Gelatin shear moduli data for various cups for all three approaches…….. 107

Figure 3.14 4% Gelatin phase angle data for the three approaches for cup 1…….. 108

Figure 3.15 4% Gelatin shear moduli data for the three approaches for cup 1…….. 109

CHAPTER 4

Figure 4.1 (a) Phase Angle data for Jell-o……... 125

Figure 4.1 (b) Shear Moduli data for Jell-o……... 126

Figure 4.2 (a) Phase Angle data for Yogurt…….. 127

Figure 4.2 (b) Shear Moduli data for Yogurt…… 128

Figure 4.3 (a) Phase Angle data for Salad Dressing……... 129

Figure 4.3 (b) Shear Moduli data for Salad Dressing……... 130

Figure 4.4 (a) Phase Angle data for Peanut Butter…… 131

Figure 4.4 (b) Shear Moduli data for Peanut Butter…… 132

Figure 4.5 (a) Phase Angle data for Grape Jelly……... 133

Figure 4.5 (b) Shear Moduli data for Grape Jelly…… 134

Figure 4.6 (a) Phase Angle data for Ketchup……... 135

Figure 4.6 (b) Shear Moduli data for Ketchup……... 136

Figure 4.7 (a) Phase Angle data for Yogurt in Cup 5……... 137

Figure 4.7 (b) Shear Moduli data for Yogurt in Cup 5…… 138

Figure 4.8 Effect of Assumed Newtonian Line…….. 139

APPENDIX

Figure A.1 10% Polyacrylamide gels phase angle data for various cups for all three approaches……..… 141

Figure A.2 10% Polyacrylamide gels shear moduli data for various cups for all three approaches……..… 142

Figure A.3 10% Polyacrylamide phase angle data for the three approaches for cup 1……..143

Figure A.4 10% Polyacrylamide shear moduli data for the three approaches for cup 1……..…144

Figure A.5 5% Polyacrylamide gels phase angle data for various cups for all three approaches……..… 145

Figure A.6 5% Polyacrylamide gels shear moduli data for various cups for all three approaches……..… 146

Figure A.7 5% Polyacrylamide phase angle data for the three approaches for cup 1……..…147

Figure A.8 5% Polyacrylamide shear moduli data for the three approaches for cup 1…….……148

Figure A.9 1.75% Gelatin phase angle data for various cups for all three approaches……..…… 149

Figure A.10 1.75% Gelatin shear moduli data for various cups for all three approaches……150

Figure A.11 1.75% Gelatin phase angle data for the three approaches for cup 1……..151

Figure A.12 1.75% Gelatin shear moduli data for the three approaches for cup 1……152

Figure A.13 1.5% Gelatin phase angle data for various cups for all three approaches……153

Figure A.14 1.5% Gelatin shear moduli data for various cups for all three approaches…….. 154

Figure A.15 1.5% Gelatin phase angle data for the three approaches for cup 1..... 155

Figure A.16 1.5% Gelatin shear moduli data for the three approaches for cup 1……..156

LIST OF SYMBOLS

- Ω Angular velocity of vane
- A Area
- G^* Complex modulus
- R_c Cup radius
- G' Elastic or Storage modulus
- F Force
- D_f Fracture diameter
- ω Frequency
- H Height
- H_v Height of the vane
- G Hookean shear modulus
- L Length
- μ Newtonian viscosity
- ε Normal strain
- γ_a Peak strain
- σ_a Peak stress
- δ Phase angle
- μ_{pl} Plastic viscosity
- γ Shear strain
- $\dot{\gamma}$ Strain rate
- σ Stress
- σ_a Stress on the horizontal ends
- σ_e Stress on vane ends
- t Time periods
- M Torque
- D_v Vane diameter
- R_v Vane radius
- θ Vane rotation angle
- η Viscosity
- G'' Viscous or Loss modulus
- γ_o Yield strain
- σ_o Yield stress

CHAPTER 1.

EXTENDED SUMMARY

A comprehensive study of the vane method literature identified the vane as an effective attachment for the measurement of yield stress, and the Brookfield YR-I viscometer uses the vane method. Many researchers have explored new methods of applying the vane to obtain additional rheological information such as the shear modulus of materials [1]. Accordingly, the NCSU approach was developed to estimate shear moduli, phase angles, and hence the viscoelastic properties of materials using Brookfield viscometry. After some preliminary tests, polyacrylamide and gelatin gels of various concentrations were selected as model systems. Three different techniques measured shear moduli of these material**:** (1) the NCSU approach, (2) Alderman approach, and (3) the Brookfield approach. The NCSU approach was based on deformation zone concept; the Alderman approach considered an alternative technique, while the Brookfield approach measured shear modulus with the stress-strain data produced by the Brookfield YR-I. Each technique was applied to the data from the model systems after testing with the Brookfield YR-I viscometer. The test samples were placed in cup sizes that ranged from 10% to 90% greater than the vane diameter. These dimensions were essential to assess the deformation zone caused by vane rotation. Statistical analysis confirmed cup 1 (radius 10% greater than vane radius) as the best selection to obtain viscoelastic data similar to that obtained from a conventional, controlled-tress rheometer, the StressTech. A comparison of the results from Brookfield YR-I and the Stress Tech machine suggested the use of the Alderman approach for shear moduli and rate calculations. A protocol was developed based on the results obtained from the model systems. To verify the use of the Brookfield

YR-I as an instrument capable of producing viscoelastic properties, certain commercial food products were also evaluated with the protocol. However, some of the results obtained from the commercial products showed distinct differences between the instruments. The shear moduli obtained from the StressTech was observed to be about an order higher than the results from the Brookfileld YR-I. The results from the model systems revealed that the shear moduli values increase with the cup size. Hence, cup 5 generated greater shear moduli values than cups 1 to 4. Nevertheless, the phase angle data from both the instruments also were in agreement. Thus, a change in the cup size could produce desirable results. Even so, the results from model systems with Cup 1 established that the Brookfield YR I can potentially deliver viscoelastic property measurements. However, certain material characteristics influence failure behavior, which in turn possibly affect the deformation zone and strain calculations. The proposed technique can immediately be applied as an empirical technique for viscoelasticity characterization, perhaps serving a quality control function. Future work should further investigate the deformation zone prediction to help adapt the procedure to more fundamental viscoelasticity measurements.

1.1 REFERENCES

[1] N. J. Alderman, G. H. Meeten and J. D. Sherwood, Vane rheometry of bentonite gels, J. Non-Newtonian Fluid Mech., 39 (1991) 291

CHAPTER 2.

LITERATURE REVIEW

2.1 RHEOLOGY

Rheology is the science of deformation and flow of matter, investigating the response of materials to applied stress or strain [1, 2]. Rheological properties describe flow characteristics and textural behavior of substances, and principles of rheology are used by industries for process design and quality control [3]. For example, food scientists use rheology when creating or re-designing food products by associating changes in texture and mouthfeel with variation in rheological properties [1, 4, 5]. Thus, rheology can be used as a vital tool for assessing product performance and consumer acceptance. However, to assess these physical properties, rheological relationships known as constitutive equations are established. The most essential parameters defining the constitutive equations are stress and strain.

2.2 SHEAR STRESS AND SHEAR STRAIN

When a material is subjected to a force (F), the sample responds by deforming, see Figures 2.1 and 2.2. Stress (σ) is defined as the amount of force applied on the material per unit area (A) of the application surface with units of Pascal (Pa) [2, 6].

$$\sigma = \frac{F}{A} \qquad [2.1]$$

The resulting deformation is measured as strain (ε or γ), computed as the relative displacement in the material. Accordingly, strain, a dimensionless quantity, is the ratio of the change in length (ΔL) to the original length (H).

$$\gamma = \tan^{-1}\left(\frac{\Delta L}{H}\right) \qquad [2.2]$$

Normal and shear are two classifications of stress categorized depending on the direction of force application. When a force is applied perpendicular to the material surface (Figure 2.1), normal stress is observed which induces a normal strain (ε). Similarly, a force applied parallel to the material surface (Figure 2.2) causes a shear stress and consequently a shear strain (γ) [2, 6].

Shear strain rate ($\dot{\gamma}$) is the time rate of change of strain occurring in the material and can be defined as the rate at which adjacent layers of a material move with respect to each other [2, 7]. Shear rate is a velocity-related parameter and is usually expressed in reciprocal seconds $\left(1/s\right)$.

$$\dot{\gamma} = \frac{d\gamma}{dt} \qquad [2.3]$$

Apparent viscosity (η) of fluids is described as the resistance to flow offered by fluid layers during the application of a shearing force and is measured according to the following equation [8].

$$\eta = \frac{\sigma}{\dot{\gamma}} \qquad [2.4]$$

Viscosity is one of many such parameters, describing stress-strain and stress-strain rate relationships, used to characterize materials.

2.3 RHEOLOGICAL CHARACTERIZATION OF MATERIALS

Rheological characterization is based on a response to an applied load, force or deformation and substances can thus be rheologically classified as, elastic (ideal solids), viscous (ideal fluids) or viscoelastic.

Ideal solids (elastic) and ideal fluids (viscous) represent extremes for rheological analyses, and substances between the two extreme scenarios are called viscoelastic materials. Ideal solids store energy gained during deformation and following the removal of the load, return to an original shape using the stored energy. Hooke's law is observed in such solids which states that the load applied to a body is directly proportional to the imposed deformation. In rheological terms, stress and strain are related linearly to each other,

$$\sigma = G\gamma \qquad [2.5]$$

where G is the Hookean shear modulus of the material, a constant unique to the material. On the other hand, ideal liquids (considered Newtonian fluids) do not store, but dissipate energy completely in the form of heat. For ideal fluids, the stress applied to the fluid is proportional to strain rate. Hence the rheological model representing ideal liquids is

$$\sigma = \mu\dot{\gamma} \qquad [2.6]$$

and μ is the Newtonian viscosity. For this ideal scenario, Newtonian viscosity is equivalent to the apparent viscosity.

Viscoelastic materials exhibit a combination of elastic and viscous effects simultaneously [6]. These materials are characterized by parameters such as phase angle(δ), elastic (G') and loss moduli(G'') and a detailed description of viscoelasticity is given in section 2.6.

2.4 YIELD STRESS

Most fluids do not display Newtonian behavior and are called non-Newtonian materials. Certain non-Newtonian materials exhibit a property known as yield stress, see Figure 2.3. Yield stress(σ_o) is defined as the minimum stress required to initiate flow [2, 9, 10, 11, 12, 13, 14, 15, 16, 17, 18, 19, 20]. Accordingly, these non-Newtonian materials are expected to be a viscoelastic solid prior to yielding and viscoelastic liquid post yielding [21, 21, 22]. Yield stress is often a desirable property and is accountable for functional performance of many products [10, 11, 12, 23, 24, 25, 26, 27, 28, 29, 30, 31, 32, 33, 34, 35, 36, 37, 38]. For example, paints are required to be suitably thin for application purposes. At the same time, paints are also required to exhibit a yield stress to supply sufficient resistance to avoid sagging or flow after application. Numerous food products, including ketchup, mayonnaise, and salad dressings, are specifically designed to impart a yield stress. For example, a salad dressing is expected to be thick and not flow freely from a

container, but at the same time should not require high stresses to initiate flow. Thus, the application and intensity of yield stress are significant components for product quality [23].

Barnes (1999) extensively discussed the concept of yield stress in a review paper [9]. Some noteworthy features are that yield stress has been traditionally measured as the stress where a significant decrease in the viscosity is observed. However, a logarithmic plot of viscosity against the logarithm of applied stress shows that material flow occurs in a range of stress values and not at a unique stress, see Figure 2.4 [9, 22, 39]. Hence, when the time of observation is extended to geological scale, even mountains flow [40].

2.4.1 EXISTENCE OF YIELD STRESS

Barnes and Walters (1985) stated that yield stress is an ideal concept, one that does not exist in reality [19, 41]. A Newtonian plateau is perceived both at low and high shear rates for high viscosity materials, and power-law type behavior is noticed at intermediate shear rates. Also, materials known to have a unique yield stress displayed flow below the yield stress when tested with modern equipment, like controlled stress rheometers at low rates [42, 43, 44, 45, 46]. Finally, Barnes and Walters (1985) stated that experimental verification of yield stress would involve an infinite amount of time, and therefore be impossible to perform [47].

The proposed concept by Barnes and Walters received criticism [41, 48, 49] from Hartnett and Hu (1989), who identified yield stress as an ‘engineering reality’ [50,

51]. In their approach, Hartnett and Hu (1989) used a falling ball technique and observed no change in the position of a nylon ball after several months as it was allowed to drop through a solution of high viscosity. Thus, the solution used for the experiment exhibited a significant yield stress [50]. Barnes (1999), defending their position on yield stress, suggested the use of a microscope to observe the change in position [9]. Astarita (1990) and Evans (1992) built a bridge between the extreme theories stating that the entire concept revolves around the order of distance measured and experimental time scale [47, 48]. Accordingly, the existence of yield stress depends on the nature of the experiment being conducted. Schurz (1992) and Cheng (1986), similar to Evan's theory, affirmed that an "apparent yield stress," which would be distinguished according to a significant measurable time and lowest possible shear rate, is more meaningful [32, 52]. Therefore, yield stress is believed to be a time-dependent property, varying inversely with the time period employed for the test [12, 32]. A longer measurement time (lower rate) will generate a smaller yield stress value [31, 53]. Accordingly, a higher strain rate would produce a higher yield stress and vice versa, see Figure 2.5 [22, 31, 54]. Uhlherr et al. (2005) believed that the material yielding is determined by a critical strain, the yield strain (γ_o), rather than by a critical stress or critical shear rate [54]. The measurement device employed for the test is also believed to affect the yield stress value [19, 31]. The yield stress concept might be in debate, but the application of the theory and models developed based on the rheological behavior of several materials that do not exhibit free flow in small ranges of stress values is significant in many practical engineering circumstances [39, 54].

2.4.2 RHEOLOGICAL MODELS

Numerous rheological models for non-Newtonian fluids incorporate a yield stress factor to predict flow phenomena more accurately, see Table 2.1. The Bingham plastic model has a yield stress term (σ_o) in addition to the general Newtonian model. Accordingly, the shear rate and hence a Newtonian flow will be perceived only after the yield stress is achieved. Other models including a yield stress term are the Herschel-Bulkley and Casson models. The Hershel-Bulkley model is an extension of the power law model with an additional yield stress parameter. Model constants and yield stress values depend on the range of rates during the analysis. The parameters in each of the above models do not vary with strain rates and accordingly time. Thus, such materials do not exhibit time-dependent nature.

2.5 TIME-DEPENDENT FLOW

Time-dependent materials exhibit a variation in the rheological properties with frequency and stress history. Certain materials, though tested at similar test conditions, do not assume behavior identical to that observed prior to shearing [55]. Time-dependent materials whose viscosity decreases with time at a constant shear rate are known as thixotropic. Thixotropy arises from structure deformation caused by disruption of weak, intermolecular forces, such as hydrogen bonding. Rheopexy (or anti-thixotropy) is the opposite behavior to thixotropy and thus the viscosity of a rheopectic material increases with time at a steady shear rate. Viscoelastic

materials, unlike purely elastic and viscous materials, do not display similar rheological properties when tested at different frequencies or rates. Therefore, viscoelastic materials are frequency-dependent, and accordingly time-dependent in nature [56].

2.6 VISCOELASTICITY

Typically, most materials lie between the ideal scenarios defining viscous fluids and elastic solids and are called viscoelastic materials [57]. Liddell and Boger (1996) explain viscoelasticity as the property observed in materials during transition from solid-like behavior to liquid-like behavior or vice versa [11, 39]. Figure 2.6 illustrates the behavior of an elastic and viscoelastic material with different frequencies (ω) or time periods (t).

A typical viscoelastic material exhibits an initial linear stress-strain relationship called the linear viscoelastic behavior (extended in the Figure 2.6 for clarity) followed by a non-linear dependence of strain and stress called the non-linear viscoelastic behavior of the material [58]. The extent of the linear viscoelastic region is based on a unique critical limit for each material, beyond which the non-linear behavior is observed [59]. Examples of viscoelastic materials include bread dough, polymer melts, and gels.

Concepts of viscoelasticity are essential to study the behavior of these complex materials at different conditions [60]. Numerous industrial products including food

products, polymers, etc. are viscoelastic in nature, and consequently the knowledge of the viscoelastic properties of the products is considerably significant in industry as well [31, 61].

2.6.1 PARAMETERS DESCRIBING VISCOELASTIC PROPERTIES

The degree of viscoelasticity is characterized by parameters which are generally obtained through dynamic or oscillatory testing. In such tests, a stress or strain varying in a sinusoidal fashion is allowed into the material, and the resulting strain or stress respectively, is assessed, see Figure 2.7 [62]. The amplitude of the input stress or strain is the peak stress (σ_a) or strain (γ_a) during oscillation.

Viscoelastic parameters include the complex modulus (G*), the phase angle (δ), elastic (or storage) modulus (G′), and viscous (or loss) modulus (G′′).

2.6.1.1 Complex modulus is the ratio of the amplitude stress and strain determined in the linear viscoelastic region [62, 63, 64].

$$G^* = \frac{\sigma_a}{\gamma_a} \qquad [2.7]$$

2.6.1.2 Phase angle can be defined as the ratio of the viscous effects to the elastic effects. In the linear viscoelastic region, when a strain is input into a material, phase angle is the angle with which the responding shear stress deviates from the input strain, see Figure 2.7 [65, 66]. For a perfectly elastic solid, the stress is in phase with the strain without any

lag, and hence the phase angle is 0°. For a perfectly viscous liquid, the strain and stress are totally out of phase, and the phase angle is 90° [67, 68]. Mathematically, phase angle is determined as

$$\delta = \tan^{-1}(G'' / G') \qquad [2.8]$$

Thus, a large value of elastic modulus, G′, in comparison with loss modulus, G″, indicates a more elastic material, while a larger value of G″ indicates a more viscous material. A material with a phase angle between 0° and 90° is deemed viscoelastic in nature [64, 65], see Figure 2.8.

2.6.1.3 The elastic modulus or the storage modulus (G′) represents the energy stored within the material and corresponds to the elastic behavior of the sample. Mathematically, storage modulus is computed as the product of complex modulus and the cosine of the phase angle

$$G' = G^* \left(\cos\delta\right) = \frac{\sigma_a}{\gamma_a}\left(\cos\delta\right) \qquad [2.9]$$

2.6.1.4 The loss modulus (G″) is used as a measure of the energy lost through dissipation and accordingly describes the viscous behavior of the sample. Loss modulus is the product of complex modulus and sine of the phase angle.

$$G'' = G^* \left(\sin\delta\right) = \frac{\sigma_a}{\gamma_a}\left(\sin\delta\right) \qquad [2.10]$$

Consequently, complex modulus can be re-written as a combination of the elastic and loss modulus which form the real and imaginary parts defined as,

$$G^* = G' + iG'' \qquad [2.11]$$

Therefore, the magnitude of G^* can be computed as,

$$G^* = \sqrt{G'^2 + G''^2} \qquad [2.12]$$

The equations for computations of the moduli are applicable in the linear viscoelastic region alone as the linear relationship between stress and strain is invalid beyond the region [69]. In the linear region, an increase in the magnitude of stress is nullified by a corresponding increase in strain or vice versa. Accordingly in the linear region, for a given strain rate, material functions are independent of varying stress or strain which maintains the validity of the above equations. A logarithmic plot of modulus and strain rate gives a better understanding of the linear viscoelastic behavior, see Figure 2.9.

Viscoelastic property data and other rheological properties are obtained by testing materials on sophisticated instruments called rheometers [2].

2.7 RHEOMETRY

Rheometry is the study of rheological property measurement. Rheometers can be placed into two general categories: rotational type and tube type [3, 69]. Rotational type rheometers drive an attachment at a constant rate or constant stress and measure the resistance offered by the material. The attachment is usually connected to a spring or a torque bar which acts to measure this resistance [3, 70]. Some of the important sensors used for rotational type rheometers are parallel

plate, cone and plate, mixer type, and bob-in-cup (coquette and searle) geometries. The choice of geometry is primarily based on the type of material being tested and the test conditions considered. Another type of geometry, which has gained popularity over the recent years, is the vane. A vane geometry is often used to study the low shear rate properties of plastic fluids and has the advantage of eliminating slip [10, 37, 71].

2.7.1 SLIP

Substances that exhibit yield stress are typically multiphase systems which, due to the formation of a three-dimensional network, resist instant flow [3, 10, 11, 12, 15, 18, 29, 36, 43, 53, 54, 72, 73, 74, 75, 76]. Typically, such multi phase systems exhibit the problem of slip when tested at low shear rates with smooth surfaces geometries [26, 38, 77]. Displacement of the dispersed phase from solid boundaries cause the formation of a thin, particle-depleted, low-viscosity boundary layer initiating the slip of the material during experimentation, see Figure 2.10 [20, 53].

A considerably smaller value of viscosity, or a pseudo yield stress, is observed when slip occurs. The cone and plate, parallel plate, and wide gap bob-in-cup geometries are more vulnerable to slip due to a higher particle-wall interaction observed with these geometries. Slip is minimized by roughening the geometry, e.g., serrated systems or by chemically treating the sides of the geometry so that

the particles adhere to the walls [53]. Slip can be also minimized using the vane geometry.

2.8 VANE AND VANE RHEOMETRY

A vane is a rheological tool with thin blades spaced at equal angles around a cylindrical axial rod [11, 12, 18, 26, 27, 31, 37, 43, 69, 71, 72, 75, 78, 79, 80, 81]. Figure 2.11 (a) depicts a vane with four blades, but the number of blades can vary. The vane rotated in a material circumscribes a cylindrical shape, see Figure 2.11 (b). Similar to the bob in the couette geometry, the vane is placed centrally in a cup for experimental purposes, see Figure 2.12.

The vane is generally operated in a rate-controlled mode, where the vane is immersed into the material and rotated at a constant speed. The torque observed on the vane is measured with time and the corresponding stress is evaluated [81, 82]. The stress at the peak point of the torque-time profile is, in general, referred to as the yield stress of the material, see Figure 2.13 [10, 11, 17, 18, 43, 83, 84].

The vane was initially used to study coagulation in clay soils, and the method was adopted for the measurement of in situ shear strength and compactness of the soils [11, 16, 26, 29, 43, 72, 80, 83, 85, 86, 87]. Later, the vane geometry was adopted for various viscometers to avoid problems associated with slip phenomena. Over the last 25 years, vane rheometry has been extensively used for yield stress measurements of non-Newtonian materials in varied systems such as ice slurries, filamentous fermentation broths, particle suspensions, cements, and several other

industrially significant substances [9, 30, 53, 83, 88, 89]. The yield stress measured using the vane technique was similar to those obtained from extrapolation of shear stress-shear rate data acquired from other geometries [29, 43, 69, 71, 81, 90, 91, 92]. Oscillatory experiments were also conducted with the vane-in-cup geometry, and results similar to concentric bob and cup were observed [92, 93, 94].

2.8.1 ADVANTAGES AND LIMITATIONS ON THE USE OF VANE GEOMETRY

Barnes and Nguyen (2001) emphasized the increasing popularity of the vane technique in their review paper on rotating vane rheometry. Some of the advantages of using the vane rheometer have been discussed elaborately with emphasis on various fields, where the vane technique has been adopted due to these advantages [83]. A summary of the advantages and limitations of the use of vane technique found in respected literature is tabulated in Table 2.2.

2.8.2 ASSUMPTIONS

A summary of the assumptions for the vane method follows [10, 12, 28, 29, 31, 43, 69, 86]:

(i) The vane forms a rigid cylinder with the material trapped within the blades
(ii) The material trapped within the blades rotates along with the vane during rotation, and hence no secondary flow occurs between the blades
(iii) The yield surface has a cylindrical shape
(iv) The stress distribution is uniform over the surface of the vane cylinder
(v) The vane geometry is considered to be two-dimensional since the vane length is assumed to be infinitely long

2.8.3 RIGID CYLINDER CONCEPT

The vane and material held within the blades develops into a cylindrical body upon rotation. The cylindrical body is called a “rigid cylinder” with the yielding surface equivalent to the cylindrical surface of the vane [9, 10, 11, 12, 17, 26, 41, 43, 85, 86, 95, 96, 97, 98, 99]. The rigid cylinder behaves similar to that of a bob in the couette geometry, see Figure 2.14 [31, 61].

Keentok et al. (1985) used the finite element method to analyze the stress distribution of vane rotation in a Bingham Plastic model fluid for three different vanes with 2, 3, and 4-blades. The results for the 2 and 3-bladed vanes were slightly irregular, but the yield surface for a 4-bladed vane was approximately cylindrical. Photographs of a transparent Bingham liquid confirmed the occurrence of a cylindrical yielding surface, strengthening the rigid cylinder assumption [85]. Yan and James (1997) also conducted finite element analysis on Herschel-Bulkley and Casson materials. A mesh, which was considerably finer than that used by Keentok et al. (1985), analyzed the yielding surface. The strain in the fluid occurred only at the edges of the vane and nowhere inside the rigid cylinder [10]. The rigid cylinder is a valid concept and has been accepted by numerous researchers [9, 10, 11, 17, 26, 43, 85, 86, 95, 96, 97].

2.8.4 DEFORMATION ZONE CONCEPT

The flow behavior using a vane has been studied by researchers considering materials of different behavior [43, 85, 93, 95, 100]. The studies proved the validity of the "rigid cylinder concept," but also brought into light the fact that a finite area beyond the rigid cylinder observes some movement due to vane rotation [10, 11, 13, 17, 28, 29, 43, 69, 85, 93, 95, 97, 100, 101, 102, 103]. Hence the concept of a deformation zone was developed which indicated that the diameter of the affected area due to vane rotation is larger than the rigid cylinder (vane) diameter. The implementation of the vane diameter in the computations of the shear strength in such cases would lead to a magnified value [102]. The shaded area in Figure 2.14 represents the deformation area.

Keentok et al. (1985) demonstrated the presence of a deformation zone using viscoelastic greases and gelatin gels which exhibited the Herschel-Bulkley behavior. Keentok et al. and many other researchers call the deformation zone as the "fracture zone." This zone is the affected area surrounding the vane when the vane is rotated in the material until fracture. The ratio of the fracture zone diameter to the vane diameter $\left(D_f / D_v \right)$ was estimated to be approximately 1.05 for greases while for gelatin gels the ratio was approximately 2. The shear surfaces of gelatin gels were found to be approximately cylindrical. An attempt was made to establish a relation between the ratio of yield stress and viscosity of the fluids $\left(\sigma_o / \eta \right)$ and the

ratio $\left(D_f / D_v \right)$; however no conclusive results could be drawn. Numerical simulations were also performed as an analytical support to the observed behavior and the $\left(D_f / D_v \right)$ value thus obtained was 1.025 for greases [85].

Yan and James (2000) conducted a study on the stress distribution in a vane-in-cup geometry with a power law fluid which confirmed that the material around the circular circumference of the vane participated in the movement due to vane rotation [10, 43]. An enhanced numerical approach to the stress profile of the region around the vane blades agreed with the fracture zone concept [10]. The concept of fracture zone is believed to exist, so to determine the actual strain in the material, the knowledge of the fracture zone is necessary [93].

Olsen (1999) called the fracture zone diameter as the effective cutting diameter of the vane, and the cutting diameter for clay was observed to be much larger than the vane cylinder [102]. Troung and Daubert (2001) observed a distinct fracture zone area when testing tofu and gellan gums with the vane rheometer [104]. The extent of the fracture zone depends upon the material being tested and the rotational speed. A more solid-like material or a higher rotational speed would cause a larger fracture zone [80, 85]. Thus, the vane method is not a very appropriate fundamental method due to the ambiguity in computing the actual strain [105]. Therefore, to overcome the uncertainty caused by the fracture zone, the implementation of a correction factor involving the extent of fracture zone in the stress computations has been suggested [17, 85, 95, 102, 104, 105].

2.8.5 YIELDING AND FORMATION OF DEFORMATION ZONE

The following discussion gives a brief description of yielding and formation of deformation zone within a vane-in-cup rheometer. The area between the vane cylinder and cup wall is generally referred to as gap, see Figure 2.15. The flow of material observed in the gap, when the vane is subjected to rotation, is more complicated and the stress distribution is more non-uniform than in simple bob-in-cup geometry [10, 12, 28, 43, 53, 85, 106]. The shear stress decreases with distance from the vane cylinder, but within the cylinder the stress increases from the center of the vane to the vane edge, see Figure 2.16. Accordingly, the maximum value of stress is observed at the cylindrical surface of the vane. The finite element analysis of the stress distribution for the present scenario determined that the stress peaks at the tips of the vane [10, 28, 43, 85,106, 107]. Until the stress at the vane tips is lesser than the yield stress, no flow is observed in the gap. When the peak stress exceeds the yield stress, yielding of material is observed at the tips of the vane. Yielding is observed throughout the vane cylinder only on further rotation of the vane. Thus at complete yielding, the peak stress observed will be higher than the yield stress.

As stated earlier, the stress decreases radially from the vane cylinder. Consequently, within the gap, at a point closer to the vane, the yield stress of the material is observed at complete yielding. A layer of material entrapped between the vane cylinder and the point of yield stress observation experiences a stress greater than the yield stress. The layer is the deformation zone and terminates at a

point where stress lower than the yield stress occurs [10, 23]. Thus the yielding layer of the cylinder is a layer of fluid trapped between two solid layers of material between the blades and the material past the fracture zone. The width of the yielding layer depends on the shear rate and the material [10, 98].

Though the concept of stress peaking at the vane tips has been proven, the yield stress computations are based on the assumption that the stress observed throughout the entire vane cylinder is uniform. Materials become non-linear at the tips of the vane but the total torque measured is affected only when the non-linearity is considerable [72]. Yan and James (1997) used numerical approximations to prove that the assumption of cylindrical yielding surface is applicable to various types of fluids, while Dzuy and Boger stated that the assumption is valid only at the moment of yielding [10, 28, 29, 86, 95]. After yielding, the material fractures and hence the assumption does not prevail. Furthermore, for shear-thinning liquids, the flow in the gap is found to be similar to that observed in concentric-cylinder geometry [43, 108]. Therefore, most vane rheometry computations exclude the concepts of stress distribution and the fracture zone of the vane rheometer in spite of the prominence of the theories [83, 100].

2.9 VANE RHEOMETRY CALCULATIONS

The computation of yield stress using the vane rheometer is based on the geometry of the vane. Certain specifications have been established for the positioning of the vane during experimentation [11, 28, 29, 69], see Figure 2.12.

(i) ratio of the vane length (H_v) to vane diameter (D_v) should lie within 1.5 and 4.0, i.e. $1.5 \geq H_v/D_v \geq 4.0$

(ii) depth of the vane surface from the surface of material (Z_1) can be 0 or the ratio of Z_1 to the diameter should be greater than 1.0, i.e. $Z_1 = 0$ or $Z_1/D_v \geq 1.0$ (the yield stress computation would differ accordingly)

(iii) ratio of the height of vane from bottom of cup (Z_2) to vane diameter (D_v) should be greater than 0.5, i.e. $Z_2/D_v \geq 0.5$
The ratio ensures that the end effects at the top and bottom of the vane are negligible.

(iv) the vane blades are assumed to be infinitely thin to avoid complications in yield stress computations [31, 78, 83]

The total torque (M_o) required to surmount the yield stress of the fluid can be broken down into two parts,

(i) torque (M_c) required for the vane's cylindrical surface,

$$M_c = \left[\left(\pi D_v H_v\right)\left(\sigma_o\right)\right]\left[\frac{D_v}{2}\right] = \frac{\pi h D_v^{\,2}}{2}\sigma_o \qquad [2.13]$$

In the expression above, ($\pi D_v H_v$) represents the area of stress application (cylindrical surface area), and $D_v/2$ is the distance from the point of force application to the vane's cylindrical surface (radius of the vane, R_v)

(ii) the torque (M_h) required for the upper and lower horizontal surfaces of the vane,

$$M_h = 2\int_0^{\frac{D_v}{2}} 2\pi r^2 dr\sigma_e \qquad [2.14]$$

where, σ_e is the shear stress on the vane ends. The area of stress application (upper and lower horizontal surfaces of the vanes) is represented by $2\pi r^2$

Assuming σ_e varies with the radius (r) according to a power-law relationship,

$$\sigma_e = \left(\frac{2r}{D_v}\right)^m \sigma_o \qquad [2.15]$$

Substituting the value of σ_e in Eq [2.14],

$$M_h = 4\pi\int_0^{\frac{D_v}{2}} r^2\left(\frac{2r}{D_v}\right)^m \sigma_o dr \qquad [2.16]$$

$$= \frac{2^m \left(4\pi\sigma_o\right)}{D_v^m} \int_0^{\frac{D_v}{2}} r^{2+m} dr$$

Substituting r = $D_v/2$,

$$M_h = \frac{2^{m+2}\pi\sigma_o}{D_v^m} \frac{\left(D_v/2\right)^{3+m}}{3+m} \qquad [2.17]$$

$$= \frac{\pi\sigma_o D_v^{\,3}}{2\left(3+m\right)}$$

Hence, the total torque can be determined as,

$$M_o = M_c + M_h \qquad [2.18]$$

$$M_o = \frac{\pi h D_v^2}{2}\sigma_o + \frac{\pi\sigma_o D_v^3}{2\left(3+m\right)} \qquad [2.19]$$

$$M_o = \frac{\pi\sigma_o D_v^2}{2}\left(H_v + \frac{D_v}{3+m}\right) \qquad [2.20]$$

$$= \frac{\pi\sigma_o D_v^3}{2}\left(\frac{H}{D_v} + \frac{1}{m+3}\right)$$

Re-writing the above expression, the yield stress of the material (σ_o) can be determined as,

$$\sigma_o = \frac{2M_o}{\pi D_v^3}\left(\frac{H_v}{D_v} + \frac{1}{m+3}\right)^{-1} \qquad [2.21]$$

Substituting 'm' as zero is usually satisfactory and errors in using Eq [2.21] for m>1 decreases with larger values of $\left(H_v/D_v\right)$. If m=1, errors ≤ 3.7% may be obtained with $\left(H_v/D_v\right)$>2 [9]. Conventionally, 'm' is assumed to be zero.

Equation [2.21] is valid when $Z_1/D_v \geq 1.0$, while when $Z_1 = 0$ the yield stress computation is,

$$\sigma_o = \frac{2M_o}{\pi D_v^3}\left(\frac{H_v}{D_v}+\frac{1}{6}\right)^{-1} \qquad [2.22]$$

Various researchers used Eq [2.21] in different forms [11, 12, 16, 27, 28, 29, 31, 37, 63, 69, 93, 104, 105, 106, 109]. For example, Barnes and Nguyen (2001) also calculated the stress from the peak torque observed. The total torque (M_o) was computed as the sum of the torque on the cylindrical surfaces (M_c) and the horizontal edges (M_h) of the cylinder. However, M_c and M_h were defined as follows,

$$M_c = 2\pi\sigma_o H_v R_v^2 \qquad [2.23]$$

$$M_h = \left(\frac{4\pi\sigma_o R_v^3}{3}\right) \qquad [2.24]$$

The total torque according to Eq [2.18] would be,

$$M_o = \left(2\pi H_v R_v^2\right)\sigma_o + \left(\frac{4\pi R_v^3}{3}\right)\sigma_o \qquad [2.25]$$

$$= 2\pi R_v^3 \sigma_o \left(\frac{H_v}{R_v}+\frac{2}{3}\right) \qquad [2.26]$$

Re-arranging the above equation, yield stress would be calculated as,

$$\sigma_o = \frac{M_o}{2\pi R_v^3}\left(\frac{H_v}{R_v}+\frac{2}{3}\right)^{-1} \qquad [2.27]$$

Sherwood and Meeten (1991) calculated the torque for a two-bladed vane to be,

$$M = 2\pi D_v^3 \mu\Omega(\hat{l}+0.66) \qquad [2.28]$$

where, μ is the viscosity of sample, Ω is the vane's angular velocity, i.e. $d\theta/dt$, and

$\hat{l} = H_v/R_v$

The torque per unit length on an n-bladed vane of infinite length was indicated as,

$$M = 2\pi D_v^2 \mu\Omega(2 - 2n^{-1}) \qquad [2.29]$$

A vane with an infinite number of blades is equivalent to a solid cylinder [78, 100]. All the above calculations are relevant to complete yielding. However, the stage of the material prior to complete yielding provides much rheological information about the material. The dynamic torque-time profile of the vane is used to study the various phases observed in the material during vane rotation.

2.10 TORQUE-TIME PROFILE

2.10.1 TORQUE-TIME/STRESS-TIME PROFILE WITH VANE IN RATE CONTROLLED MODE

When the vane is immersed into a material and rotated, the material renders some amount of resistance to the movement of the vane. The torque sensor attached to the vane winds up due to the resistance. The sensor wind up, measured as torque, is the measure of the resistance and accordingly the stress observed in the material. Once the yield stress is attained, the vane rotates until the material yields along the entire vane cylinder after which the material does not offer any resistance. Thus, the torque at which the material yields is the peak torque observed in the

torque-time profile, and the peak torque is associated with the yield stress [10, 11, 17, 43, 83, 84, 98].

A typical torque-time profile is represented in Figure 2.13. The stresses and strains experienced in the material can be estimated by substituting the corresponding torque-time value in Eq [2.21]. Hence, a corresponding stress-time profile or stress-strain profile are analogous to the torque-time profile.

Alderman et al. (1991) divided the torque time response into various segments to explain the behavior of the material in each phase [72]. Similarly, the torque-time response has been divided into the following regions, see Figure 2.13:

1. AB region – An initial transient response is observed as the vane is rotated from rest. Several torque-time profiles depicted by various researchers do not have the AB region as a part of the response. A definite amount of time may be required for elastic deformation of the network bonds present in the material and consequently causes a delay in experimental response [23]. At rotational speeds higher than 1.0 rpm, a prominent AB region has been observed for the Brookfield YR-I viscometer (details in section 3.5.1).

2. BC region – A linear response is observed in the BC region and according to most researchers, an elastic deformation occurs here [10, 11, 31, 37, 39, 43, 53, 72, 85, 109]. Sometimes a non-linear response is observed due to an inconsistency in the vane assumptions. Other reasons for non-linear behavior include material property of non-linear elastic behavior prior to yielding and sometimes a substantial creep flow observed below the yield stress of material [53, 83].

3. CD region – The non-linear response originates at C and reaches a maximum torque value of D. The stress corresponding to the torque value of D is defined as the yield stress as material starts to flow beyond D. Viscoelastic flow is believed to be observed in the CD region [68]

4. DE region – Viscous flow is observed in the DE region [22].

5. EF region – The determination of the slope and the final level of the EF curve is usually not possible. Knowledge of the extent of fracture zone may be required for the further assessment of the curve [98].

The rate of stress development (i.e., the torque-time gradient) is dependent on the rotational speed, the measuring system stiffness (the spring constant in the case of Brookfield YR-I), and the vane size. Thus, variations in the above stated variables produce a BC region of desirable extent [11]. To observe a longer linear BC region, a lower rotational speed with a weaker stiffness of the measuring sensor is preferred. Vane size does not affect the magnitude of yield stress measured, but affects the rate of torque development and consequently the shape of the torque-time profile. A vane with smaller dimensions gives a sharper torque-time response i.e, reaches the peak value earlier than a relatively larger vane [11].

The torque-time profile has been exclusively discussed by Lidell and Boger (1996) (see Figure 2.17), Alderman et al. (1990) (see Figure 2.18), Yan and James (1997) (see Figure 2.16) and Zhu et al. (2001) [10, 11, 53, 72]. Lidell and Boger (1996) present a similar illustration as that of Dzuy and Boger (1983) for the stress-time profile (which is equivalent to the torque-time profile) based on the network bonds within the material [11, 22, 29]. Details are tabulated in Table 2.3. Torque-time profiles have been utilized to observe and define many standard rheological aspects exhibited by the material by the above mentioned researchers.

2.10.2 CLASSIFICATION OF YIELD STRESS

Traditionally, yield stress is categorized into two types, static and dynamic yield stress [22]. When a material is tested after a prolonged rest period, a relatively higher yield stress is observed which is called the static yield stress. The reason for

the observed behavior is the formation of a network in the material with time caused by the action of diffusion forces like Brownian motion [11, 18]. Dynamic yield stress is determined after breaking the bonds of any such weak network that may be present by shearing the material [11, 18, 32, 54].

Lidell and Boger (1996) classified yield stresses on the basis of the transition of the torque-time profile from one region to the other, see Figure 2.17. The static yield stress $\left(\sigma_{o_A}\right)$ is defined as the stress corresponding to the transition between fully elastic and viscoelastic behavior of the material. i.e., the stress observed at point C. Prior to C, the vane is static and hence no movement is observed in the material. The dynamic yield stress is defined as the difference between the static yield stress and the peak stress corresponding to the transition observed between viscoelastic behavior of the material to fully viscous behavior i.e., the stress observed at point D, the peak stress [11, 22]. Thus, dynamic yield stress is the difference between peak stress and static yield stress $\left(\sigma_{o_A} - \sigma_{o_B}\right)$. Beyond C, the vane starts rotating in the viscoelastic region and hence is in a dynamic position. The speed of vane rotation equals that of the applied rotational speed when the fully viscous region is reached (DE region).

2.11 SHEAR MODULUS CALCULATION

Alderman et al. (1990), Sherwood and Meeten (1991) and Bagdassarov and Pinkerton (2004) have demonstrated methods to obtain an estimate for shear modulus G, of materials using the vane technique [72, 100, 110].

2.11.1 ALDERMAN ET AL. APPROACH

Alderman et al. (1990) provided a new dimension to vane rheometry by developing a method to obtain rheological data. A method was developed to determine shear modulus (G) and the yield strain (γ_o) [72]. A distinct stress value was calculated for shear modulus computations. The stress evaluated, though not the same as illustrated in Eq [2.21], is computed similarly based on the torque balance equation for the vane.

Though the angular vane rotation was used in the computations, the value was not considered equivalent to the shear strain observed in the material. The shear strain estimation followed the shear modulus calculation and was evaluated as the ratio of shear stress to shear modulus. The shear modulus has been computed as the slope of the linear region in the torque-time response. The computational procedure adopted for the estimation of shear modulus and shear strain is as follows. The material was assumed to be sheared between two concentric cylinders (rigid cylinder concept) of height H and inner radius equivalent to the vane radius, R_v, and the outer radius equivalent to the cup radius, R_c. According to the torque balance equation, for a torque value (M) and an applicable radius (r), the corresponding shear stress (σ) can be evaluated as,

$$\sigma = \frac{M}{2\pi r^2 H_v} \qquad [2.30]$$

where, $R_v \le r \le R_c$

If θ is the vane rotation angle, the strain is calculated based on the assumption of simple shear flow in the annular gap [111],

$$\gamma = r\frac{d\theta}{dr} \qquad [2.31]$$

and the shear modulus is evaluated as,

$$G = \frac{\sigma}{\gamma} \qquad [2.32]$$

Substituting the value of γ, σ, and re-arranging and integrating the expression with the corresponding radius values produces,

$$\int_0^{\theta(R)} d\theta = \frac{M}{2\pi H_v G}\int_{R_v}^{R_c}\frac{dr}{R^3} \qquad [2.33]$$

Solving and rearranging the integral in Eq [2.33] provides the following equation,

$$G = \frac{M}{4\pi H_v \theta}\left(\frac{1}{R_v{}^2} - \frac{1}{R_c^2}\right) \qquad [2.34]$$

Shear strain (γ) is then calculated as,

$$\gamma = \frac{\sigma_o}{G} \qquad [2.35]$$

Substituting the value of yield stress from Eq [2.27] and the value of G from Eq [2.34], shear strain is,

$$\gamma = \frac{\frac{M_o}{2\pi R_v^3}\left(\frac{H_v}{R_v} + \frac{2}{3}\right)^{-1}}{\frac{M}{4\pi H_v \theta}\left(\frac{1}{R_v{}^2} - \frac{1}{R_c^2}\right)} \qquad [2.36]$$

2.11.2 SHERWOOD AND MEETEN APPROACH

Assuming that the end effects are negligible and no slip occurs at the edges of the vane, the torque required to rotate the vane is,

$$M = 2\pi R_v^2 G\theta \qquad [2.37]$$

The torque required to rotate a cylinder of the same radius will be,

$$M = 4\pi R_v^2 G\theta \qquad [2.38]$$

As stated earlier, in the non-linear region, vane rotation causes a larger yielding region. The consideration of the non-linear region affects the computation of G from torque and hence, only the linear region is applied for the above computation. The concept of identification of the linear region is similar to Alderman et al.'s approach (1991) where the slope of the linear region of the torque-time response for shear modulus calculations is considered.

2.12 BROOKFIELD ENGINEERING

Brookfield viscometers are the most commonly used rotational viscometers in the world. They are smaller and more affordable than other rotational viscometers [64]. The principle behind most Brookfield viscometers is based on the measurement of scale deflection or spring wind up observed due to the rotation of a spindle in the test material [2, 112, 113, 114, 115]. The Brookfield YR-I rheometer was primarily developed to measure yield stress (σ_o) of substances, using a 4-bladed vane spindle and a spring for torque detection. The spring wind up due to the resistance offered by the material to vane rotation produces torque. The dynamic torque response thus observed is measured with time and can also be converted to a

shear stress and strain behavior based on attachment geometry, rotational speed, and time. The shear stress is computed according to Eq [2.21] and is given as,

$$\sigma_o = \frac{TK \times YMC \times \%M}{10} \qquad [2.39]$$

where, TK is the model torque constant, YMC is the yield multiplier constant and %M is % Torque reading. The manual to the Brookfield YR-I contains each of the above stated values for different vane sizes, see Tables 2.4 and 2.5 [84].

The strain (γ) observed in the material, as reported by Brookfield YR-I, is calculated according to the following equation which is applicable only for viscometers with a spring wind up [16],

$$\gamma = \theta - S \times (\%M) \qquad [2.40]$$

where, θ is the angular displacement of the vane (rad) and S is the radial spring factor (rad / %torque). The product (%M) x S is the rotation of the spring for a completely stationary vane.

2.13 SUMMARY

The knowledge of the rheological properties of various products is necessary for understanding and assessing the texture of the product. Moreover, rheological properties are required for the design of flow processes for quality control to help predict storage and stability of the product [1]. Most industrial materials and products are viscoelastic in nature and thus viscoelasticity is a important rheological

concept. Traditionally, sophisticated and expensive rheometers have been a requirement for measuring viscoelastic properties, thereby limiting the application of such measurements. Brookfield viscometers, on the other hand, are cost effective instruments widely found throughout all industries for rapid viscosity detection. The aim of the project is to adapt the affordable Brookfield YR – I for viscoelastic property measurement.

2.14 REFERENCES

[1] P. K. W. Herh, S. M. Colo, N. Roye, K. Hedman, in International Scientific Communications, Inc.**,** Rheology of foods: New techniques, capabilities, and instruments, 16-20 June 2000, American Laboratory News.

[2] V. A. Hackley and C. F. Ferraris, in NIST Special Publication 946, Guide to Rheological Nomenclature: Measurements in Ceramic Particulate Systems, Department of Commerce, January 2001, National Institute of Standards and Technology (NIST), Technology Administration, U.S, Gaithersburg, 2001.

[3] F. S. Baker, Rheology-A practical approach to Quality Control, Rheology Conference, Shrewsbury (1998), Paper 1, 1-6

[4] G.T. Munizaga and G. V. B. Canovas, Rheology for the food industry, J. of Food Engineering, 67 (2004) 147

[5] R. L. Keith, L. G. Margaret and A. Martin, Rheological and Structural Properties of Model Composite Foods, Third European Rheology Conference and Golden Jubilee Meeting of the British Society of Rheology, 1990, p. 301

[6] S. S. Nielsen, Food Analysis, in Aspen Publishers, Rheological Principles for Food Analysis, Second Edition, Gaithersburg, 1998, Chapter 34

[7] D. W. Hadley and J. D. Weber, Rheological Terminology, Rheologica Acta, 14 (1975) 1098

[8] W. L. McCabe, J. C. Smith and P. Harriott, Unit Operations of Chemical Engineering, International Editions, McGraw-Hill, Singapore, 1993, Chapter 3

[9] Barnes H A, The yield stress – a review or 'παντα ρει' – everything flows?, J of Non-Newtonian Fluid Mechanics, 81(1&2) (1999) 133

[10] Yan J., James A.E., The yield surface of viscoelastic and plastic fluids in a vane viscometer, J. Non-Newtonian Fluid Mech., 70 (1) (1997) 237

[11] Liddell P.V. and Boger D.V., Yield stress measurements with the vane, J. of Non-Newtonian Fluid Mechanics, 63 (1996) 235

[12] Stokes J. R. and Telford J. H., Measuring the yield behavior of structured fluids, J. of Non-Newtonian Fluid Mechanics, 124 (2004) 137

[13] B. D. Besses, A. Magnin and P. Jay, Viscoplastic flow around a cylinder in an infinite medium, J. of Non-Newtonian Fluid Mechanics, 115 (2003) 27

[14] K. Sekimoto, Motion of the yield surface in a Bingham fluid with a simple – shear geometry, J. of Non-Newtonian Fluid Mechanics, 46 (1993) 219

[15] P. Doremus and J.M. Piau, Yield stress fluid. Structural model and transient shear flow behaviour, J. of Non-Newtonian Fluid Mechanics, 39 (1991) 335

[16] C. R. Daubert et al., Quantitative Measurement of Food Spreadability using the Vane Method, J. of Texture Studies, 29 (1998) 427

[17] M. Keentok, The measurement of the yield stress of liquids, Rheologica Acta, 21 (1982) 325

[18] C. Gallegos and J. M. Franco, The Measuring of Yield Stress Liquids, Progress and Trends in Rheology V, Proc. of fifth European Rheology Conference, Portoroz 1998, p. 203

[19] C.R. Meier, Yield Stress Measurements, Third European Rheology Conference and Golden Jubilee Meeting of the British Society of Rheology, Rhevisco,1990, 347

[20] R.G. Larson, The structure and Rheology of complex fluids, Oxford University Press, New York, 1999, p. 30-35

[21] A.Y. Malkin, Rheology Fundamentals, ChemTec Publishing, Ontario, 1994, p.119

[22] J. Guo, C. Tiu, P.H.T. Uhlherr and T.-N. Fang, Yielding behavior of organically treated anatase TiO_2 suspension, Korea-Australia Rheology Journal, 15 (1) (2003) 9

[23] X. M. Zhang and Q. D. Nguyen, Movement of the Yield Boundary of Time-Dependent Yield Stress Fluids in Couette Flow, Proc. 12th Congress on Rheology, Quebec City (Quebec), 1996, p. 560

[24] P. Coussot, S. Proust and C. Ancey, Rheological interpretation of deposits of yield stress fluids, J. of Non-Newtonian Fluid Mechanics, Volume 66 (1996) 55

[25] A. Magnin and J.M. Piau, Shear Rheometry of Fluids with a Yield Stress Volume, J. of Non-Newtonian Fluid Mechanics, 23 (1) (1987) 91

[26] S. Savarmandet al., Rheological properties of concentrated aqueous silica suspensions: Effects of pH and ions content, J. of Rheology, 47 (5) (2002) 1113

[27] H.M. Yoshimura and K. Prud'homme, A Comparison of Techniques for Measuring Yield Stresses, J. of Rheology, 31 (8) (1987) 699

[28] N.Q. Dzuyand D.V. Boger, Direct Yield Stress Measurement with the Vane Method, J. of Rheology, 29 (3) (1985) 335

[29] N.Q. Dzuy and D.V. Boger, Yield Stress Measurement for Concentrated Suspensions, J. of Rheology, 27 (4) (1983) 321

[30] J. R. Stokes, J. H. Telford and A. M. Williamson, The flowability of ice suspensions, J. of Rheology, 49 (1) (2005) 139

[31] Q. D. Nguyen and D. V. Boger, Measuring the Flow Properties of Yield Stress Fluids, Annual Review of Fluid Mechanics 24 (1992) 47

[32] D. C–H. Cheng, Yield stress-A time-dependent property and how to measure it, Rheologica Acta, 25(5) (1986) 134

[33] P. Coussot and J.–M. Piau, On the behavior of fine mud suspensions Rheologica Acta, 33 (1994) 175

[34] J.F. Hutton, On using the Weissenberg rheogoniometer to measure normal stresses in lubricating greases as examples of materials which have a yield stress, Rheologica Acta, 14 (1975) 979

[35] H. P. Romngsen, Yield Stress Measurements on Waxy North Sea Crude Oils with Controlled Stress Rheometers and Model Pipeline, Third European

Rheology Conference and Golden Jubilee Meeting of the British Society of Rheology Rhevisco,1990, 410

[36] P. Coussot, Q. D. Nguyen, H. T. Huynh and D. Bonn, Avalanche Behavior in Yield Stress Fluids, Phys. Rev. Lett. 88 (17) (2002) 175501

[37] M. Krulis, and H. Rohm, Adaption of a vane tool for the viscosity determination of flavoured yoghurt, Eur Food Res Technol 218 (2004) 598

[38] H. J. Walls, S. B. Caines, A. M. Sanchez and S. A. Khan, Yield Stress and Wall Slip Phenomena, J. of Rheology 47 (4) (2003) 847

[39] H. A. Barnes, The Myth of Yield Stress Fluids, Progress and Trends in Rheology V, Proc. of fifth European Rheology Conference, Portoroz, 1998, p. 201

[40] M. Reiner, in Physics Today, The Deborah Number, Fourth International Congress on Rheology, 62 (1964)

[41] H.A. Barnes and K. Walters, The yield stress myth, Rheological Acta, 24 (4) (1985) 323

[42] H. A. Barnes, A Brief History of the Yield Stress, Applied Rheology, 9(6) (1999) 262

[43] H.A. Barnes and J.O. Carnali, The vane-in-cup as a novel rheometer geometry for shear thinning and thixotropic materials, J. of Rheology, 34 (6) (1989) 841

[44] B.H.A.A. Brule and S.E. Kadijk, A simple constant-stress rheometer, J. of Non-Newtonian Fluid Mechanics, 43 (1) (1992) 127

[45] W. M. Hipp, Measuring yield points instead of calculating, Third European Rheology Conference and Golden Jubilee Meeting of the British Society of Rheology, Rhevisco,1990, 540

[46] H.A. Barnes and D. Bell, Controlled-stress rotational rheometry: An historical review, Korea-Australia Rheology Journal, 15 (4) (2003) 187

[47] I. D. Evans, Letter to the Editor: On the nature of the yield stress, J. of Rheology, 36 (7) (1992) 1313

[48] G. Astarita, Letter to the Editor: The engineering reality of the yield stress, J. Rheology 34 **(**2) (1990) 275

[49] D.D. Kee and C.F.C.M. Fong, Letter to the Editor: A true yield stress?, J. of Rheology, Volume 37 (4) (1993) 775

[50] J.P. Hartnett and R.Y.Z. Hu., Technical Note: The Yield Stress – An Engineering Reality, J. of Rheology, 33 (4) (1989) 671

[51] D. Tatsumi, S. Ishioka and T. Matsumoto, Effect of Fiber Concentration and Axial Ratio on the Rheological Properties of Cellulose Fiber Suspensions, Journal of Society of Rheology, Japan, 30 (1) (2002) 27

[52] J. Schurz, Letter to the Editor: A yield value in a true solution?, J. of Rheology, 36(7) (1992) 1319

[53] L. Zhu et al., A slotted plate device for measuring static yield stress, J. of Rheology, Volume 45 (5) (2001) 1105

[54] P. H. T. Uhlherr, J. Guo, G. Tiu, X.-M. Zhang, J. Z.-Q. Zhou and T.-N. Fang, The shear-induced solid-liquid transition in yield stress materials with

chemically different structures, J. of Non-Newtonian Fluid Mechanics, 125 (2005) 101

[55] D. B. Braun and M.R. Rosen, Rheology Modifiers Handbook - Practical Use and Application, William Andrew Publishing, Norwich, 19 (1999) 1

[56] C. Ancey, Role of lubricated contacts in concentrated polydisperse suspensions, J. of Rheol., 45 (6) (2001) 1421

[57] H. A. Barnes, J. F. Hulton and K. Walters, An Introduction to Rheology, First Edition, Elsevier Publications, Amsterdam, 1989, Chapter 3.

[58] J. Minster, Short Communications, Wissenschaftliche Kurzrichte, A note on the application of the stress-time analogy methods, Rheologica Acta, 18 (1979) 424

[59] N. W. Tschoegl, The Phenomenological Theory of Linear Viscoelastic Behavior-An Introduction, First Edition, Springer-Verlag Berlin Heidelberg, New York, 1989, Chapter 2

[60] S. M. Schmalholz and Yu. Podladchikov, Buckling versus Folding: Importance of Viscoelasticity, Geophysical Research Letters, 26 (17) (1999) 2641

[61] J. M. Maia and J. A. Covas, Non-Conventional Rheological Monitoring of Polymer Processing, Rheology-A practical approach to Quality Control, Rheology Conference, Shrewsbury, 1998, Paper 7, p. 1

[62] Q. Zhong, Cooling Effects on the Functionality and Microstructure of Processed Cheese, Ph.D. Thesis, Department of Food Science, North Carolina State University, 2003, p. 14-17

[63] M. H. Tunick and D. L. Van Hekken, Torsion Gelometry of Cheese, J. Dairy Science, 85 (2002) 2743

[64] L. Papageorge, J. Zhang, J. Powell and J. Gayo, Food Rheology Class Project, NC State University 2002 http://legacy.ncsu.edu/classes/fs785001/Lectures&handouts/projects/viscoelasticity-report.pdf

[65] J. M. Aguilera and D. W. Stanley, Microstructural Principles of Food Processing and Engineering, Second Edition, Aspen Publications, Gaithersburg, 1999, p. 140

[66] J. D. Ferry, Viscoelastic Properties of Polymers, Third Edition, John Wiley and Sons Inc., New York, 1979, 12

[67] J. J. Benbow, F. N. Cogswell and M. M. Cross, On the dynamic response of viscoelastic fluids, Rheologica Acta, 15 (1976) 231

[68] E.K. Walsh, Viscoelasticity and Rheology, Proc. of a symposium conducted by the Mathematics Research Center, University of Wisconsin-Madison, 1984, p. 36

[69] J.F. Steffe, Rheological Methods in Food Process Engineering, Second Edition, Freeman Press, East Lansing, 1996, p. 2, 158, 200-201, 296, 316-317

[70] D.R. Dinger, Rheology for Ceramists, First Edition, Morris Publishing, Kearney, 2002, p. 163

[71] P.H.T. Uhlherr, J. Guo, T.-N. Fang and C. Tiu, Static measurement of yield stress using a cylindrical penetrometer, Korea-Australia Rheology Journal, 14 (1) (2002) 17

[72] N. J. Alderman, G. H. Meeten and J. D. Sherwood, Vane rheometry of bentonite gels, J. Non-Newtonian Fluid Mech., 39 (1991) 291

[73] K. Tanaka, K. Ichizawa, R. Akiyama and A. Kubono, Simultaneous Measurement of Rheological Behavior and Conduction Current for and Electro – Rheological Suspension with Cation Exchange Resin Particles, J. of the Society of Rheology, Japan, 29(3) 2001 105

[74] H. See, Towards an Understanding of the Rheological Response and Microstructure of Electro-Rheological Fluids and Concentrated Particulate Suspensions, J. of Society of Rheology, Japan Volume 30 (5) (2002) 259

[75] P. McFadyen, Relationship of Beach Slope to Yield Stress, Undergraduate Thesis, Department of Chemical Engineering, The University of Queensland, 1998

[76] G.P. Roberts, H.A. Barnes, New measurements of the flow-curves for Carbopol dispersions without slip artifacts, Rheologica Acta 40 (2001) 499

[77] T. Dobbie, D. J. Fleming and J. Busby, Wall Slip: Measuring and Flow Modelling for Processing, Rheology-A practical approach to Quality Control, Rheology Conference, Shrewsbury, 1998, Paper 11, p. 1-5

[78] C. Atkinson and J.D. Sherwood, The torque on a rotating n-bladed vane in a newtonian fluid or linear elastic medium, Proceedings of Royal Society London, Series A – Math. Phys. Eng. Sci, 438, (1992), p.183-196

[79] N. Cunningham, Rheology School (2005), http://www.rheologyschool.com/inc/sp.asp?c=/artlist.asp

[80] C. Ancey, Role of particle network in concentrated mud suspensions, in Rickenmann & Chen (eds), Debris-Flow Hazards Mitigation: Mechanics, Prediction, and Assessment, Millpress, Rotterdam, 2003, Volume 1, p. 257

[81] D.J. Pollard, G. Hunt, T.K. Kirschner and P.M. Salmon, Rheological characterization of a fungal fermentation for the production pneumocandins, Bioprocess Biosyst Eng 24 (2002) 373

[82] C. Harris, M.C.R. Davies and J.-P. Coutard, Rates and Processes of Periglacial Solifluction: An experimental approach, Earth Surface and Landforms 22 (1997) 849

[83] H. A. Barnes and Q. D. Nguyen, Rotating vane rheometry — a review, J. Non-Newtonian Fluid Mech, 98(1) (2001) 1

[84] Brookfield YR – I Rheometer Operating Instructions, Manual No. M/02 – 215, Brookfield Engineering Laboraties, Inc

[85] M. Keentok, J. F. Milthorpe and A. E. Donovan, On the shearing zone around rotating vanes in plastic liquids: theory and experiment, J. Non-Newtonian Fluid Mech., 17 (1) (1985) 23

[86] C.W. Pernell, E.A. Foegeding and C.R. Daubert, Measurement of the Yield Stress of Protein Foams by Vane Rheometry, J. of Food Science, Volume 65 (1) (2000) 110

[87] A.F. Richards, Vane Shear Strength Testing in Soils, International Symposium on Laboratory and Field Vane Shear Strength, Tampa, Florida, 1987

[88] G. H. Meeten, Effects of plate roughness in squeeze-flow rheometry, J. of Non-Newtonian Fluid Mechanics, Volume 124 (2004) 51

[89] Z. Kemblowski, P. Budzynski and P. Owczarz, On-line Measurements of the Rheological Properties of Fermentation Broth, Third European Rheology Conference and Golden Jubilee Meeting of the British Society of Rheology (1990) 265 – 300

[90] A.W. Saak, H.M. Jennings, S.P. Shah, The influence of wall slip on yield stress and viscoelastic measurements of cement paste, Cement and Concrete Research 31 (2001) 205

[91] G. H. Meeten, Constant-force squeexe flow of soft solids, Rheologica Acta, 41, 557-566 (2002)

[92] F. Da Cruz, F. Chevoir, D. Bonn and P. Coussot, Viscosity bifurcation in granular materials, foams, and emulsions, Physical Review E 66 (2002) 051305 (1-7)

[93] S. Carozza, C. Servais and I. Roberts, Oscillatory Vane Rheometry for complex materials, XIIIth International Congress on Rheology, Cambridge, 3 (2000) 321

[94] B. Balzer, Martin K. M. Hruschka and L. J. Gauckler, In Situ Rheological Investigation of the Coagulation in Aqueous Alumina Suspension, J. American Ceramic Soc. 84 (8) (2001) 1733

[95] T.A. Glenn III, K.M. Keener and C.R. Daubert, A Mixer Viscometry Approach to use vane tools as steady shear rheological attachments, J. of Applied Rheology, 10 (2) (2000) 80

[96] X. D. Zhang, D. W. Giles, V. H. Barocas, K. Yasunaga and C. W. Macosko, Measurement of foam modulus via a vane rheometer, J. of Rheology, Volume 42 (4) (1998) 871

[97] S. Junus and J. L. Briggs, Vane sensor system in small strain oscillatory testing, J. of Applied Rheology, 11 (3) (2001) 264

[98] Gebhard Schramm, A Practical Approach to Rheology and Rheometry, Gebrneder Haake Rheometers, Karlsruhe, (1994) 203

[99] C. W. Macosko, Rheology, Principles, Measurements, Wiley-VCH, New York, 222-225, (1994)

[100] J.D. Sherwood and G.H. Meeten, The use of the vane to measure the shear modulus of linear elastic solids, J. of Non-Newtonian Fluid Mechanics, Volume 41 (1991) 101

[101] K. Meaney, Undergraduate Thesis, Department of Chemical Engineering, The University of Queensland (1998) http://www.cheque.uq.edu.au/ugrad/theses/1998/pdf/Karl.pdf

[102] R. S. Olsen, The Field Vane Shear Web Page (1999), http://www.liquefaction.com/insitutests/vane/

[103] D. Patel, The mixing of 'Yield Stress' fluids, Progress and Trends in Rheology V, Proc. of fifth European Rheology Conference, Portoroz (1998) 208

[104] V. D. Troung and C. R. Daubert, Textural Characterization of Cheeses using Vane Rheometry and Torsion Analysis, J. of Food Science, Volume 66 (5) (2001) 716

[105] V.D. Troung, C. R. Daubert, M. A. Drake and S. R. Baxter, Vane Rheometry for Textural Characterization of Cheddar Cheeses: Correlation with Other Instrumental and Sensory Measurements, LWT Food Science and Technology, 35 (2002) 305

[106] J. Keating and D.J. Hannant, The Effect of Rotation Rate on Gel Strength and Dynamic Yield Strength of Thixotropic Oil Well Cements Measured Using a Shear Vane, J. of Rheology, 33 (7) (1989) 1011

[107] L. Rubart, Finite Element Analysis of Shear-Thinning Flow Problems in Mixing Vessels, Third European Rheology Conference and Golden Jubilee Meeting of the British Society of Rheology (1990) 301

[108] H.A. Barnes, A review of the slip (wall depletion) of polymer solutions, emulsions and particle suspensions in viscometers: its cause, character, and cure, J. of Non-Newtonian Fluid Mechanics, 56 (1995) 221

[109] P. J. Scales, S. B. Johnson and T. W. Healy, Shear Yield Stress of Partially Flocculated Colloidal Suspensions, AIChE Journal, 43 (3) 1998 538

[110] N. Bagdassarov and H. Pinkerton, A review and investigation of the Non-Newtonian properties of lavas based on laboratory experiments with analogue materials, J. of Volcanology and Geothermal Research, 45 (3) (2004) 197

[111] A. Apelbat, J. C. Healy and M. Joly, Shear rate in the Couette viscometer with a narrow annular gap between cylinders, A new approximate formula, Rheologica Acta, A new approximate formula, 14 (1975) 976

[112] T.C. Patton, A new method for the Viscosity Measurement of Paint in the Settling, Sagging, Leveling and Penetration Shear Rate Range of 0.001 to 1.0 reciprocal seconds using a Cone/Plate Spring Relaxation Technique, J. of Paint Technology, Volume 38 (502) (1966) 656

[113] R.W. Williams, Determination of viscometric data from the Brookfield R.V.T. viscometer, Rheologica Acta, 18 (1979) 345

[114] Y. Ozturk and R.W. Williams, Further consideration to the determination of viscometric data from the Brookfield Syncho – Lectric Viscometer, Rheologica Acta,19 (1980) 488

[115] M. Mitschka, A simple conversion of Brookfield R.V.T. readings into viscosity functions, Rheologica Acta, 21 (1982) 207

[116] A. E. James, D. J. A. Williams and P. R. Williams, Direct Measurement of static yield properties of cohesive suspensions, Rheologica Acta, 26 (1987) 437

[117] Q. K. Tran and L. Glumac, Study on filtered mud conveying at an alumina refinery, Kaiser Engineers Pty Ltd., Perth (2002)

[118] P.F.G. Banfill, The Rheology of Fresh Cement and Concrete-A Review, Proc 11th International Cement Chemistry Congress, Durban, 2003

[119] Y. K. Leong and Y. L. Yeow, Relation between viscoelasticity an shear-thinning behaviour in liquids, Rheologica Acta (2003) 42, 365-371

[120] M. A. Rao and H. J. Cooley, Determination of Effective Shear rates in Rotational Viscometers with Complex Geometries, J. of Texture Studies, 15 (1984) 327

[121] V. H. R. Garrido, J. P. Gonjalez and L.A.V.A. Montalaban, Vane rheometry of an aqueous solution of worm-like micelles, Revista Mexicana De Fisica, 44 (1) (2003) 40 http://www.ejournal.unam.mx/revmexfis/no491/RMF49107.pdf

Table 2.1: Rheological modulus involving a Yield Stress parameter

Model Name	Model Equation
Bingham-plastic	$\sigma = \sigma_0 + \mu_{pl}\dot{\gamma}$
Herschel-Bulkley	$\sigma = \sigma_0 + K\dot{\gamma}^n$
Casson Model	$\sqrt{\sigma} = \sqrt{\sigma_0} + \sqrt{K_1\dot{\gamma}}$

Note: K, K_1 and n are constants unique to each material and model

Table 2.2: Advantages and Limitations of the vane method

Sl. No.	Advantages	Limitations
1	Elimination of wall-slip effects [10, 11, 16, 27, 29, 30, 31, 37, 43, 53, 69, 72, 76, 78, 79, 83, 86, 90, 92, 93, 96, 99, 100, 103, 105, 106, 108, 116, 117, 118,] - Yielding surface or the shear surface is present within the material which eliminates wall depletion (slip).	At high rotational speeds due to the possibility of the development of secondary flow behind the vane and slip [9, 43, 53, 108]
2	Minimum disturbance to the sample [16, 30, 31, 37, 43, 72, 79, 83, 93, 95, 96, 98, 99,116] - The thin blades of the vane cause minimal damage to the sensitive network developed in a material, which is significant when testing weak gels, thixotropic materials, or foam-like materials [12, 26, 29, 53, 86, 91, 106, 110].	With low viscosity fluids as the inertial effects become more prominent and cause vortices [99] - The dissipation of energy associated with the vortices would indicate a higher viscosity [83]
3	Larger gap provides less problems raised due to particulate material and reduces viscous heating greatly compared to bob and cup [12, 30, 37, 43, 53, 75, 80, 83, 93, 96, 109, 116, 117, 119]	With materials having lower yield stress - Materials with a minimum value of yield stress (around 10 Pa) are suitable. Minimum value depends upon the number of blades of the vane [31, 72].
4	Quick single point determination of yield stress [12, 16, 29, 31, 83, 98]	When the end effects are prominent - End effects in a couette geometry are avoided by modifying the bob's contour which cannot be used with the vane due to the constraints of vane geometry [43].
5	Higher shear rates can be obtained than cone and plate and Couette geometry due to minimum slip and larger surface area [121]	With materials containing high measure of particulate matter - The vane is not extremely reliable when assessing non-Newtonian fluids containing high measure of solids even at very low shear rates [101].
6	Larger surface area - The method of matching viscosities provides lesser error for geometries with larger surface areas and thus can be used with vane geometry with higher number of blades [120].	With expensive samples – Larger gap requires higher amounts of sample which is not preferable with expensive materials.
7	Can perform in situ yield stress measurements [29, 93, 94]	
8	Simple sample preparation [105]	
9	Simple attachment, easily fixed to an existing rheometer [83]	
10	Simplicity of fabrication [83, 108]	
11	Simple to clean [83, 108]	

Table 2.3: Comparison of the torque-time profiles as explained by various researchers

Region	Alderman et al.	Liddell and Boger	Yan and James	Zhu et al.
AB	Attributed to gear train play as acknowledged by the Haake rheometer manufacturers			
BC	Hookean elastic response. Slope represents elastic modulus of suspension, G	Elastic deformation of the network bonds	Material deforms elastically	Slope is linear (or almost linear for some materials) representing elastic nature. Yield stress determined at C is almost constant, not dependent on strain rate
CD	Non-hookean behavior of material	Viscoelastic flow (creep flow) of material	Viscoelastic behavior. Behavior of material in this stage is important to explain its properties	Non linear elastic behavior associated with structural rearrangement
At D	Yield stress is computed as stress observed at the maximum torque point, D	Most of the network bonds are broken and material begins to flow	The yielding process is complete	Peak stress observed. Yield stress determined at D is a strong function of strain rate
DE	The sheared sample has transformed to a fluid from a gel	A steady decrease in stress occurs which finally results in the collapse of the entire network structure	Material flows plastically	Represents the thixotropic nature of the sample. Material starts to flow
EF				If strain is stopped at E, a stress relaxation is observed at F associated with residual stress.

Table 2.4: Spring torque constants (TK) for different models of Brookfield YR-I

Model	Model Code on YR-I Screen	TK
RV YR-I	RV	1
HB YR-I	HB	8
5HB YR-I	5HB	40

Table 2.5: Yield Multiplier constant for different vane attachments provided with Brookfield YR-I

Spindle	Spindle Code	YMC
V-71	71	0.5
V-72	72	2.0
V-73	73	10.0

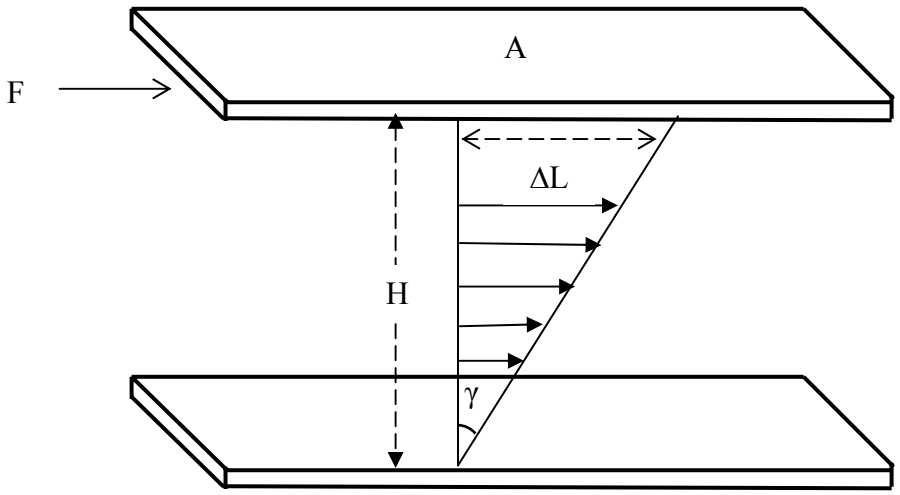


Fig. 2.1 Movement of layers of fluid on application of force, (Nielsen S. S., 1998)

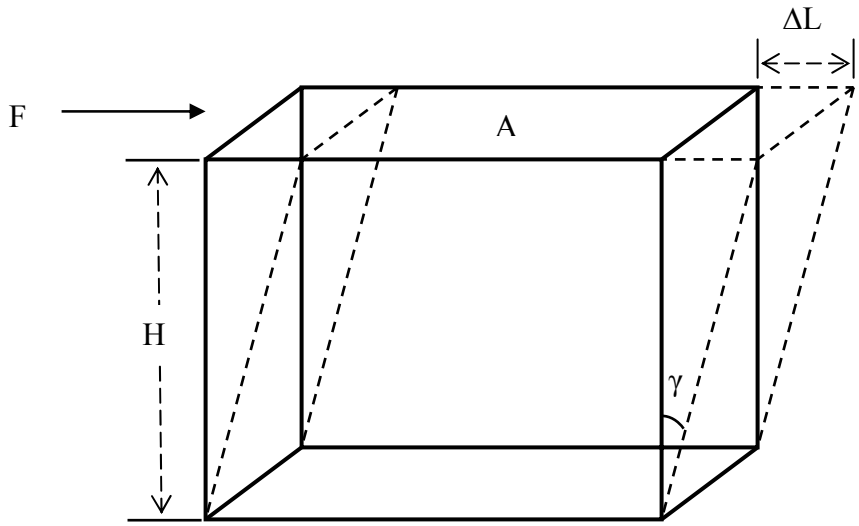


Fig. 2.2 Deformation of a solid on application of force, (Nielsen S. S., 1998)

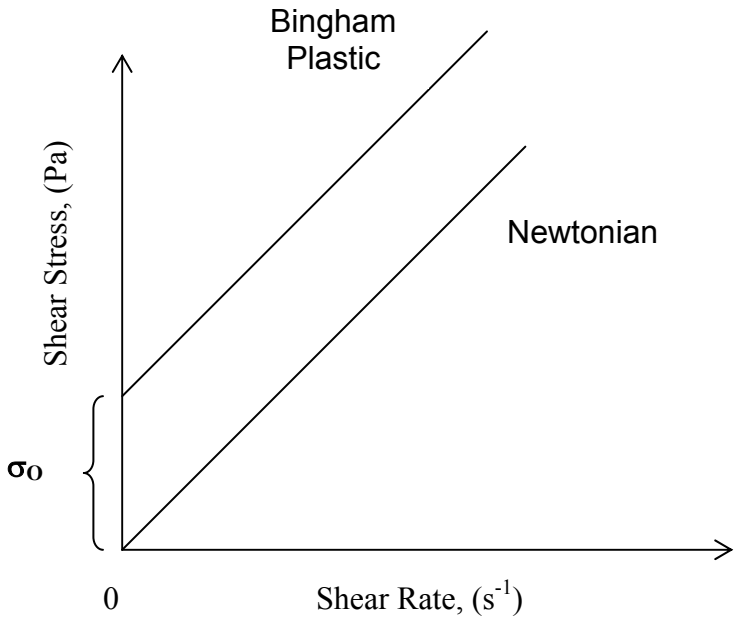


Fig. 2.3 Behavior of Newtonian and yield stress fluids,
(Mc Cabe W. L., Smith J.C. and Hariott P., 1998)

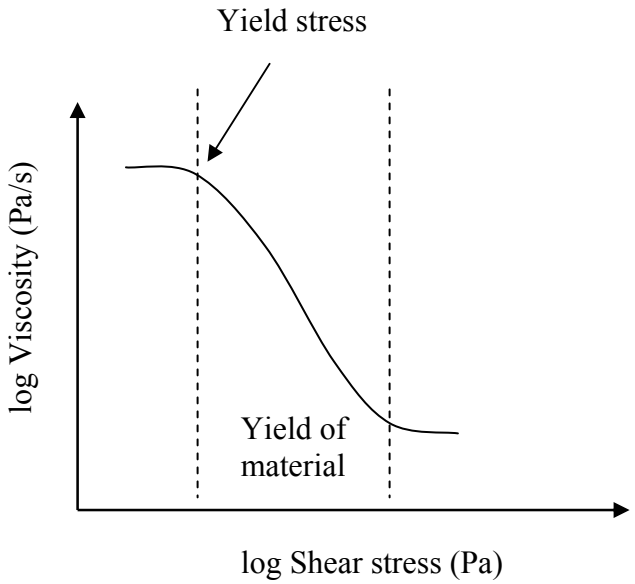


Fig. 2.4 Yield stress determination, (Barnes H. A., 1999)

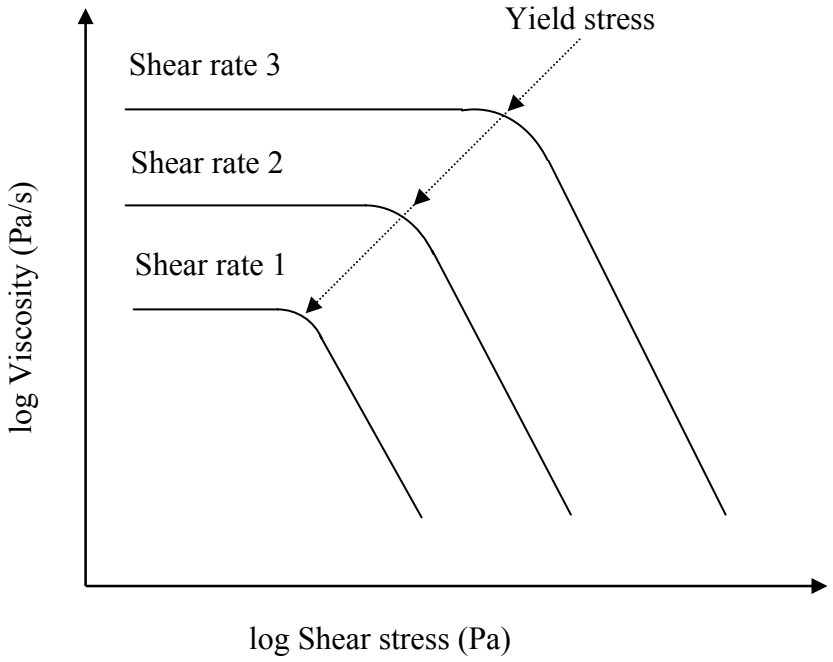


Fig. 2.5 Yield stress determination at different shear rates

Note: Shear rate 1< Shear rate 2 < Shear rate 3

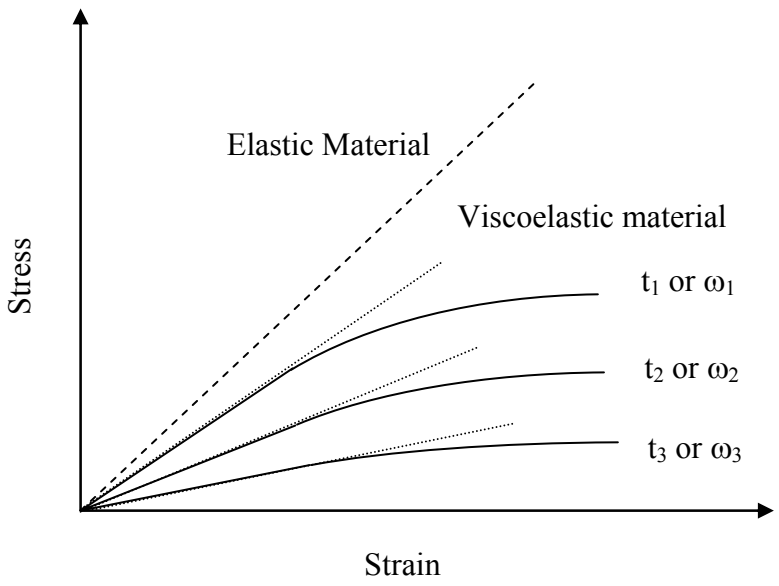


Fig. 2.6 Stress-strain relationship of elastic and viscoelastic materials at various frequencies

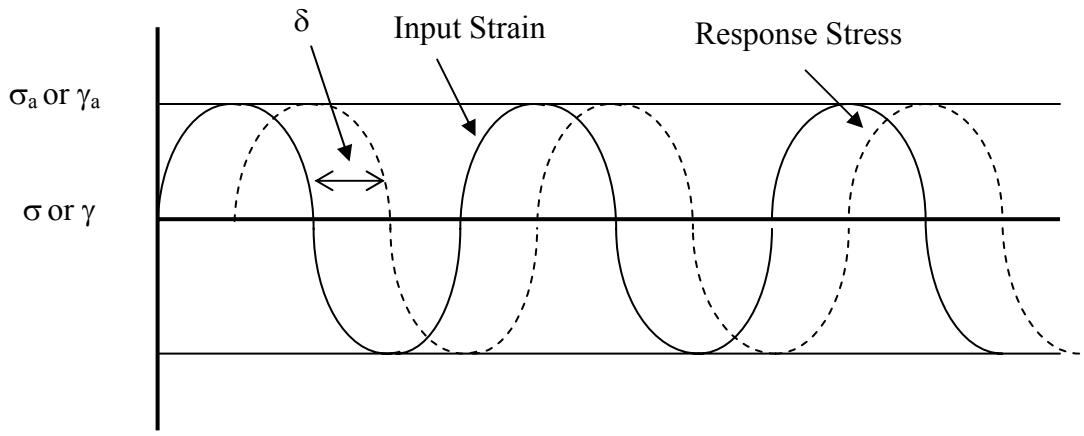


Fig. 2.7 Strain input and stress response for a viscoelastic material (Ferry J. D., 1980)

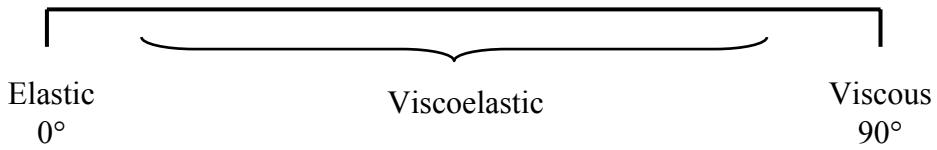


Fig. 2.8 Variation of phase angle

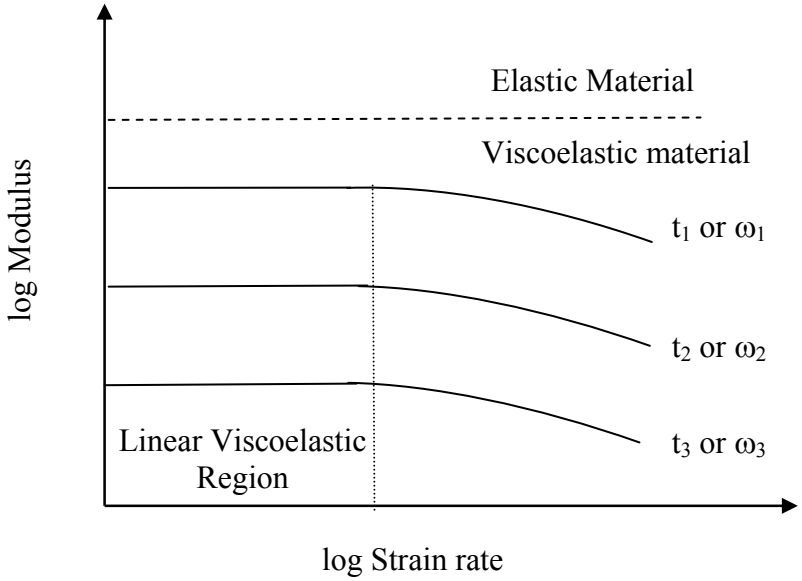


Fig. 2.9 Modulus-strain rate relationship of elastic and viscoelastic materials at various frequencies

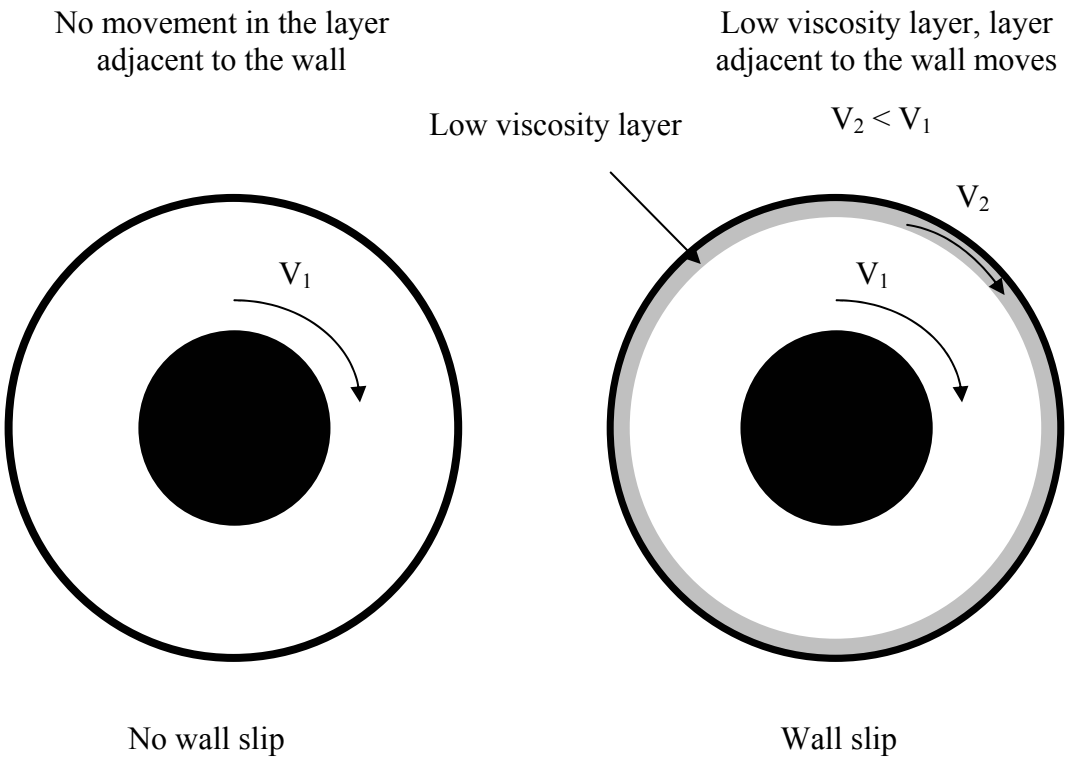
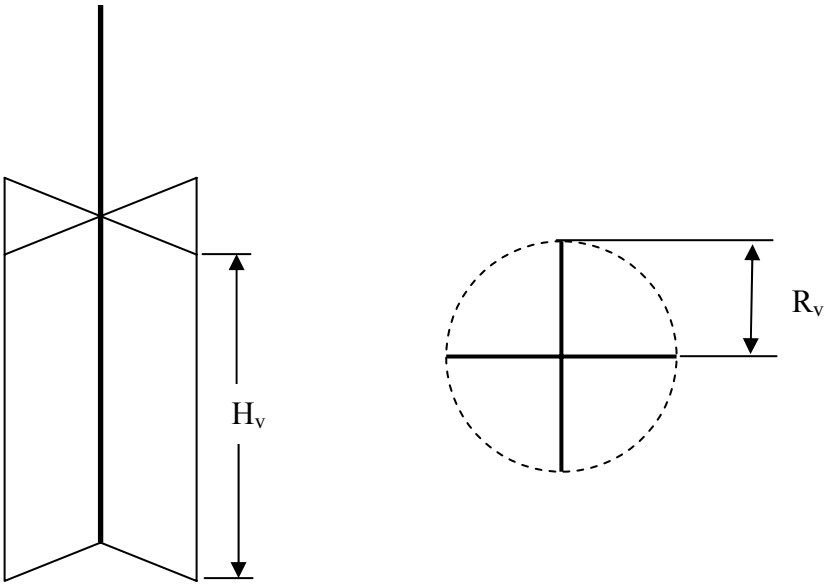


Fig. 2.10 Effect of wall slip in a bob and cup geometry



Side (a)

Top (b)

Fig. 2.11 The vane in side and top view

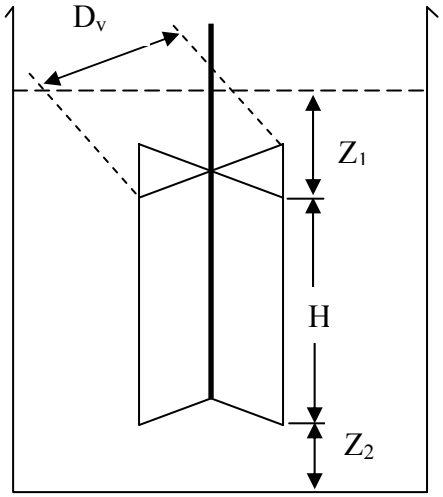


Fig. 2.12 Vane in a cup

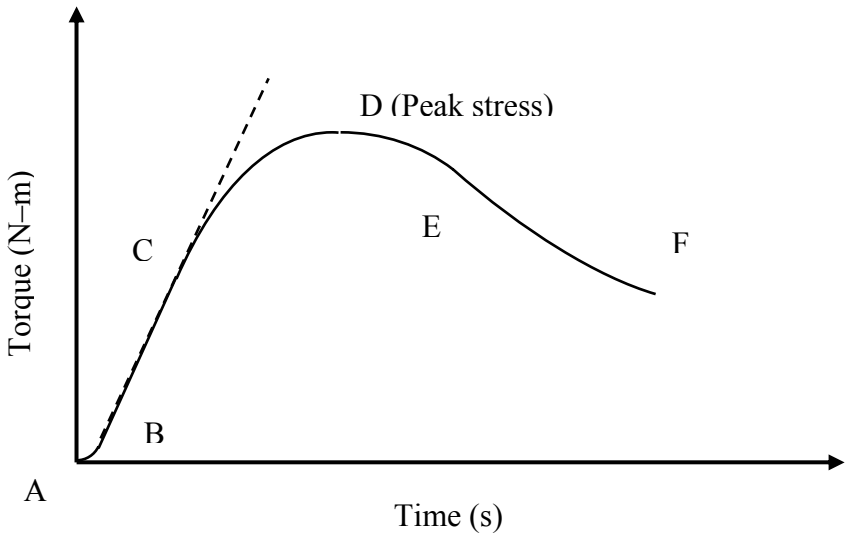


Fig. 2.13 Typical torque-time response,
(Alderman et al. 1991)

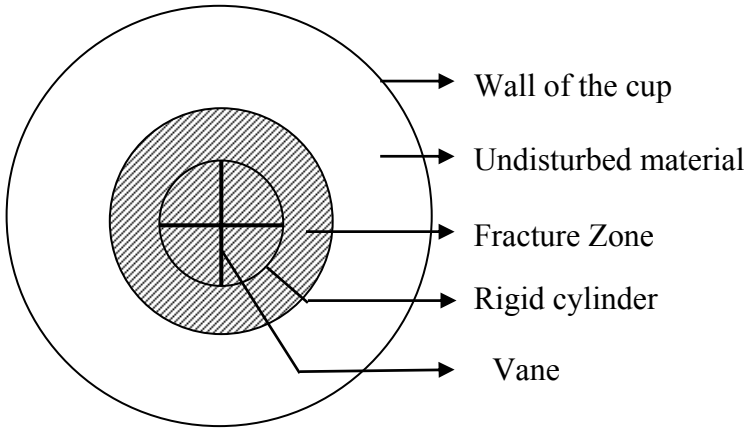


Fig. 2.14 Deformation Zone

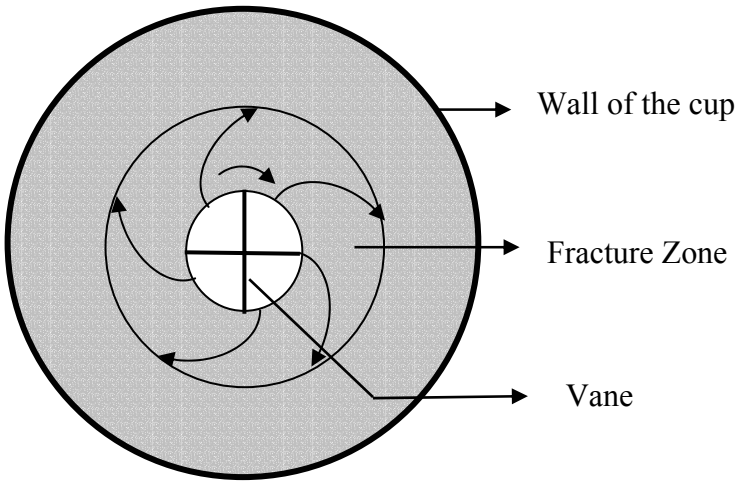


Fig. 2.15 Flow in gap

Note: Gap

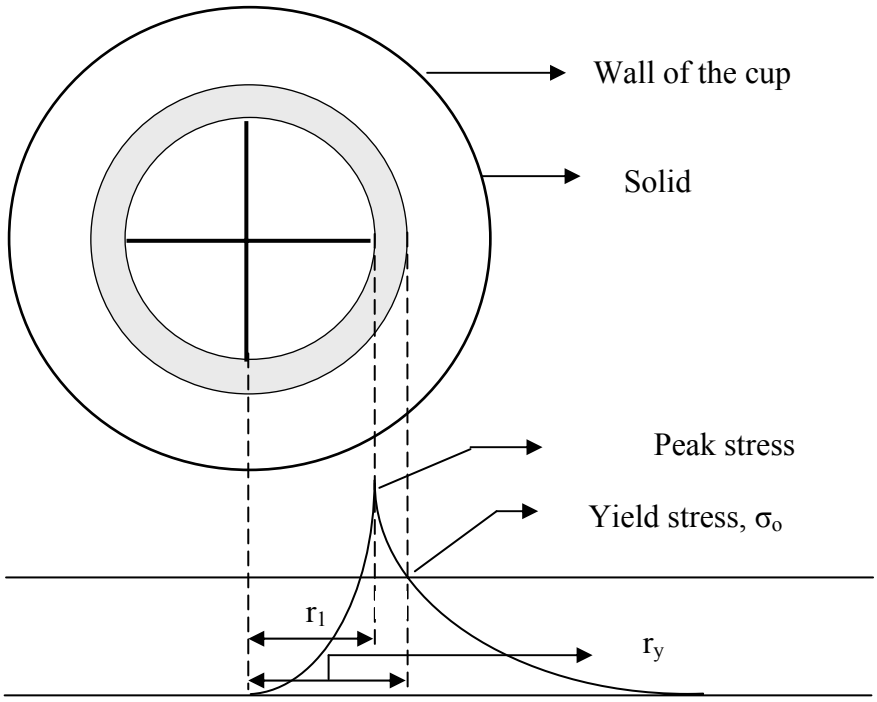


Fig. 2.16 Torque – time response
(Yan and James, 1997)

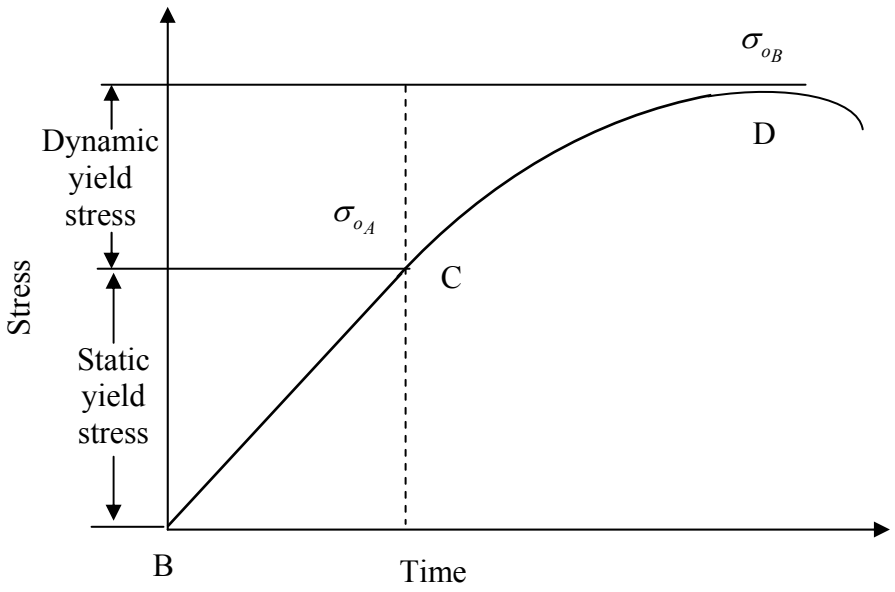


Fig. 2.17 Classification of yield stress
(Liddell and Boger, 1996)

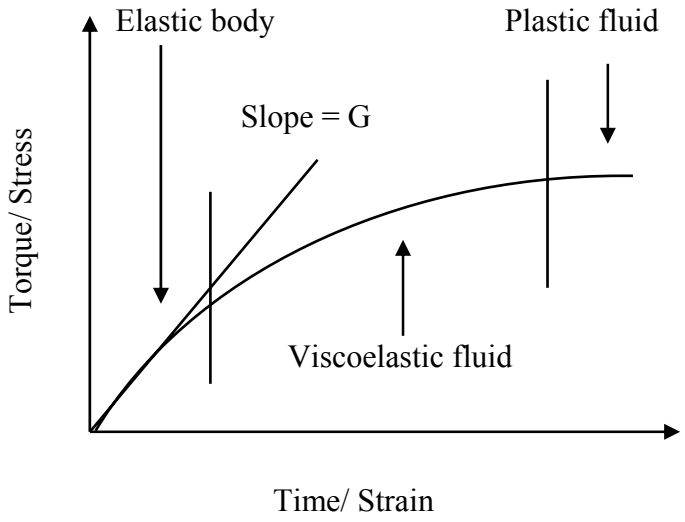


Fig. 2.18 Torque-time response (Alderman etal. 1991 and Liddell and Boger, 1996)

CHAPTER 3.

ESTIMATION OF VISCOELASTIC PARAMETERS

3.1 INTRODUCTION

The torque-time profile obtained from the Brookfield YR-I is similar to the torque-time profiles acquired from a rate controlled test with any rheometer using the vane geometry. If the Brookfield YR-I measures the yield response of an ideal elastic material, the observed torque response (ideal elastic line) follows the spring windup line - a perfectly linear, elastic response with no yielding, see Figure 3.1. No deviation from the spring windup line is observed, as energy dissipation does not occur in ideal elastic materials. All the energy applied to the material through vane rotation is stored in the spring during wind up.

Contrarily, if the YR-I measures the yield response of an ideal liquid, the response would be parallel to the abscissa. Low viscosity Newtonian fluids dissipate nearly all the energy applied to the material in the form of heat, and negligible energy is used for spring wind up. However, higher viscosity Newtonian fluids may display a parallel response significantly different from the abscissa, see Figure 3.2. When a viscoelastic material is tested on the rheometer, an intermediate torque-time response is observed. Viscoelastic materials store some energy for spring windup and dissipate the remaining energy. Consequently the torque-time curve for a viscoelastic material lies between the spring windup line and the abscissa. Viscoelastic materials are time-dependent in nature, and hence the response varies with frequency, rotational speed, strain rate, or other time-related parameters. Accordingly, when a viscoelastic material is tested, the torque response of the Brookfield YR-I rheometer depicts the typical behavior of a material, which varies

with rotational speeds, see Figure 3.3. At higher rotational speeds a more elastic response, a curve closer to the elastic line, is observed.

For a viscoelastic material, the torque-time response is normally composed of three regions, as shown in Figure 3.4. Many researchers believe that the initial linear response of the torque-time profile of a viscoelastic material is due to elastic deformation [1, 2, 3, 4, 5, 6, 7, 8, 9, 10]. The linear region is followed by a non-linear response, related to the viscoelastic phase of the material. Further increase in torque causes yielding of material. Yielding is related to the microstructural destruction of the material network, resulting in the initiation of flow. The torque response, especially the linear response, is an important basis for many theories developed for the vane method [7, 8].

The objectives of this research were to develop the theory behind the application of Brookfield viscometers for viscoelastic property measurement. The theory will be applied towards measuring the viscoelastic properties of several model systems with the Brookfield YR1 and validating with a stress-controlled rheometer.

3.2 DETERMINATION OF TRUE SHEAR STRAIN (γ) AND SHEAR MODULUS (G)

3.2.1 NCSU APPROACH - DEFORMATION ZONE ESTIMATION

The effect of vane rotation is observed not only in the material trapped within the vane blades but also extends a finite distance from the vane edge into the material. The affected layer around the vane due to rotation is called the deformation zone [1, 9].

Shear modulus (G) is computed as the ratio of the shear stress (σ) value to the shear strain (γ) value.

$$G = \frac{\sigma}{\gamma} \qquad [3.1]$$

Accordingly, the estimation of the deformation zone becomes imperative for the calculation of true strain and therefore the shear modulus of the material.

A proposed procedure to compute the true strain value at the yield point follows: after angular rotation of the vane (θ), a strain value of γ is observed in the material, see Figure 3.5. If the radius of the vane and the radius of the deformation zone are R_v and R_d, the strain can be approximated according to the following equation for small angles of vane rotation, see Figure 3.6,

$$\tan\gamma = \frac{a}{\left(R_d - R_v\right)} \qquad [3.2]$$

where *a* is the extent of horizontal displacement of the material. Also from Figure 3.6,

$$\tan\theta = \frac{a}{R_v} \qquad [3.3]$$

$$a = R_v \tan\theta \qquad [3.4]$$

By substituting the value of a from Eq [3.4] in Eq. [3.2],

$$\tan\gamma = \frac{R_v \tan\theta}{\left(R_d - R_v\right)} \qquad [3.5]$$

A rearrangment produces the strain value as,

$$\gamma = \tan^{-1}\left[\frac{R_v \tan\theta}{\left(R_d - R_v\right)}\right] \qquad [3.6]$$

The equation can now be rewritten as,

$$\gamma = \tan^{-1}\left[\frac{\tan\theta}{(R_d / R_v)-1}\right] \qquad [3.7]$$

The stress value (σ) reported by the Brookfield is based on a torque balance for the vane around its circular circumference and is determined according to Eq [2.19]. The NCSU approach considers the stress value to be the shear stress applied by the vane on the test material during rotation.

$$\sigma = \frac{2M}{\pi D_v^{\,3}}\left(\frac{H}{D_v}+\frac{1}{3}\right)^{-1} \qquad [3.8]$$

where H is height of the vane, M is the torque observed, and D_v is the diameter of the vane.

Thus, substituting the values of stress and strain from Eq [3.8] and Eq [3.7] respectively in shear modulus calculation according to Eq [3.1],

$$G = \frac{\sigma}{\gamma} = \frac{\frac{2M}{\pi D_v^{\,3}}\left(\frac{H}{D_v}+\frac{1}{3}\right)^{-1}}{\tan^{-1}\left[\frac{\tan\theta}{(R_d / R_v)-1}\right]} \qquad [3.9]$$

and substituting $D_v = 2R_v$,

$$G = \frac{\frac{M}{2\pi R_v^3}\left(\frac{H}{R_V}+\frac{2}{3}\right)^{-1}}{\tan^{-1}\left[\frac{\tan\theta}{(R_d / R_v)-1}\right]} \qquad [3.10]$$

The angular rotation of the vane is a function of time for a controlled rate test,

$$\theta = \omega t - \%MS \qquad [3.11]$$

where ω is the rotational speed of the vane, t is time taken for the rotation to occur, %M is the percentage full-scale torque, and S is the spring constant.

Hence, rewriting Eq [3.6] for true strain by substituting the value of angular vane rotation from Eq [3.11],

$$\gamma = \left\{ \tan^{-1} \left[\frac{R_v \tan\left(\omega t - \%MS\right)}{\left(R_d - R_v\right)} \right] \right\} \qquad [3.12]$$

Strain rate of the material can be computed by differentiating strain with respect to time, i.e.,

$$\dot{\gamma} = \frac{d\gamma}{dt} = \frac{d}{dt} \left\{ \tan^{-1} \left[\frac{R_v \tan\left(\omega t - \%MS\right)}{\left(R_d - R_v\right)} \right] \right\} \qquad [3.13]$$

Solving and rearranging Eq [3.13] produces strain rate as,

$$\dot{\gamma} = \left(\frac{R_v}{R_d - R_v} \right) \omega \left(\frac{\cos^2 \gamma}{\cos^2 \theta} \right) \qquad [3.14]$$

3.2.2 ALDERMAN APPROACH

Alderman et al. (1991) calculated a distinct stress value for shear modulus computations. The stress evaluated is based on the torque balance equation for the vane, but different from the stress reported by the Brookfield viscometers. The approach uses the angular vane rotation value, but does not consider the value to be equivalent to shear strain observed in the material. The shear strain estimation follows the shear modulus calculation and is evaluated as the ratio of shear stress to shear modulus. The equations used for shear modulus and strain calculations are as follows,

$$G = \frac{M}{4\pi H \theta} \left(\frac{1}{R_v^{\,2}} - \frac{1}{R_c^2} \right) \qquad [3.15]$$

$$\gamma = \frac{\sigma}{\frac{M}{4\pi H\theta}\left(\frac{1}{R_v^2} - \frac{1}{R_c^2}\right)} \qquad [3.16]$$

where, M represents torque observed, R_c is the radius of the cup, and R_v is the radius of the vane.

The approach uses the following calculation for stress (σ),

$$\sigma = \frac{M}{2\pi R_v^2 H} \qquad [3.17]$$

Substituting the value of shear modulus and stress from Eq [3.15] and Eq [3.17] respectively in the strain calculation of Eq [3.16],

$$\gamma = \frac{\frac{M}{2\pi R_v^2 H}}{\frac{M}{4\pi H\theta}\left[\frac{1}{R_v^2} - \frac{1}{R_c^2}\right]} \qquad [3.18]$$

Rearranging,

$$\gamma = \frac{\frac{1}{R_v^2}}{\frac{1}{2}\left[\frac{1}{R_v^2} - \frac{1}{R_c^2}\right]} \times \theta \qquad [3.19]$$

Substituting the value of θ from Eq [3.11] and rearranging,

$$\gamma = \frac{2}{\left[1 - \frac{R_v^2}{R_c^2}\right]}\left(\omega t - \%MS\right) \qquad [3.20]$$

Thus, strain rate can be calculated by differentiating strain with respect to time,

$$\dot{\gamma} = \frac{d\gamma}{dt} = \frac{2\omega}{\left[1 - \frac{R_v^2}{R_c^2}\right]} = \frac{2\omega R_c^2}{R_c^2 - R_v^2} \qquad [3.21]$$

3.2.3 BROOKFIELD APPROACH

The Brookfield YR – I reports an apparent strain value equivalent to the rotation of the vane (θ) during the course of the experiment. The reported strain value is considered to be the true strain (γ) observed in the material, i.e.,

$$\gamma = \theta = \omega t - \%MS \qquad [3.22]$$

The stress value (σ) reported by the Brookfield is based on a torque balance for the vane and is considered to be the shear stress applied by the vane on the test material during rotation, computed according to Eq [3.8]

Thus, the shear modulus (G) is calculated as the ratio of the shear stress to the shear strain, and the strain rate as the change in the strain with respect to time.

$$G = \frac{\sigma}{\gamma} = \frac{\dfrac{2M}{\pi D_v^{\,3}}\left(\dfrac{H}{D_v} + \dfrac{1}{3}\right)^{-1}}{\theta} \qquad [3.23]$$

$$\dot{\gamma} = \frac{d(\gamma)}{dt} = \frac{d(\omega t - \%MS)}{dt} = \omega \qquad [3.24]$$

3.3 DETERMINATION OF THE PHASE ANGLE (NCSU APPROACH)

An elastic material, when tested on a Brookfield YR-I, would assume the spring windup line. Any deviation from the ideal elastic line can be attributed to viscous effects present in the material. The initial linear viscoelastic region is extended as a straight line. The straight line, called as the extended linear viscoelastic response has a clear deviation from the ideal elastic line, see Figure 3.7. As a reasonable

deduction, the area between the extended linear viscoelastic response and the ideal elastic line, A″ correspond to the viscous effect of the material while the area between the extended linear viscoelastic response and the Newtonian line, A′ represents the elastic effect. In other words, A″ represents the energy dissipated, and A′ represents the energy stored. Similar to the phase angle calculation in dynamic measurement using storage modulus (G′) and loss modulus (G″) [see Eq. 2.8], the phase angle from Brookfield YR-I data can be calculated as the ratio of the energy dissipated to the energy stored, i.e.,

$$\delta = \tan^{-1}\left(\frac{A''}{A'}\right) \qquad [3.25]$$

Hence, the phase angle of the viscoelastic material can be determined using the torque-time response exhibited by the material when tested on the Brookfield YR-I.

The shear modulus of the material can be calculated according to Eq. [3.10], Eq [3.15] or Eq [3.23] which is equated to the complex modulus (G^*) of the material [11].

$$G^* = G \qquad [3.26]$$

As stated in the previous chapter, viscoelastic parameters, G′ and G″, can be calculated as a function of complex modulus and phase angle according to Eq [2.9] and Eq [2.10]. Therefore, the viscoelastic properties of the material can be obtained by substituting the shear modulus (G) instead of the complex modulus (G*) according to Eq [3.26].

$$G' = G\cos\delta \quad [3.27]$$

$$G'' = G\sin\delta \quad [3.28]$$

Thus, viscoelastic parameters can be obtained from the torque-time response of the Brookfield YR-I.

3.4 MATERIALS AND METHOD OF EXPERIMENTATION

Various model systems used to verify the NCSU Concept included starch, agar gels, gelatin gels and polyacrylamide, each at different concentration levels. Polyacrylamide and gelatin gels were ultimately selected as the model systems because of a longer linear viscoelastic region. Longer linear regions are suitable for the present experimental conditions as a clear deviation from a linear response can be observed. Polyacrylamide is used to represent perfectly elastic solids [12], while gelatin gels of various concentrations represent linear viscoelastic materials with phase angles dependent on gelatin concentration.

3.4.1 POLYACRYLAMIDE GELS

Polyacrylamide (PAAm) gels were prepared using 30% Acrylamide/ Bis solution (37.5:1), ammonium persulfate and N,N,N,N′-tetramethyl ethylenediamine (TEMED) from Bio-Rad, Hercules, CA. The acyrlamide/ bis solution is a combination of the monomer and the crosslinker respectively, while ammonium persulfate and TEMED are used to initiate the polymerization at room temperature. Two concentrations of

polyacrylamide gels were prepared by initially diluting acrylamide/ bis solution with deionized water at different levels such that acrylamide/ bis solution constitutes 5% and 10% of the final solutions. The final solutions, for both the concentrations, also constituted ammonium persulfate solution and TEMED at concentrations of 0.075% w/v and 5ppm v/v, respectively. Ammonium persulfate solution is prepared by dissolving ammonium persulfate crystals in deionized water. The prepared solution was added to dilute acrylamide/ bis solution which was continuously stirred at a speed of 200 rpm. Later, TEMED was added to the blending solution and was weighed for desired final weight. If the desired weight was not obtained, deionized water was further added. The final solution started gelling 2 to 3 minutes after TEMED was added, and complete gels were obtained after 3 hrs. Accordingly, the final solutions were quickly transferred into the rheometers and left undisturbed for 3 hours prior to testing, permitting the formation of a uniform gel around the attachment. Two concentrations were chosen for polyacrylamide gels: 10% and 5% (w/w) solutions in water.

3.4.2 GELATIN GELS

Different amounts of gelatin crystals were mixed with warm deionized water (at around 50° C) to obtain various concentrations of the solution. The solutions were mixed on a hot plate at a speed of 300 rpm until a temperature of 40° C was observed. At 40° C, the solutions were cooled in the rheometers at room

temperature for 6 hours prior to testing. Three concentrations chosen for gelatin solutions were 4%, 1.75% and 1.5% (w/w) in water.

3.4.3 INSTRUMENT DESCRIPTION

A controlled stress rheometer, StressTech (Rheologica Instruments AB, Lund Sweden), was selected as the control rheometer. The geometry used with the StressTech was a serrated bob-cup, while the Brookfield YR – I, (Brookfield Engineering, Middleboro, Massachusetts) used the vane attachment, V – 72, with cups of various sizes. The cups were designed specifically for this study by Brookfield Engineering at diameters 10%, 30%, 50%, 70%, and 90% greater than the diameter of the vane spindle (V – 72). The cups were numbered from 1 to 5 with increasing radius. i.e., the cup with radius 10% greater than the vane radius is Cup 1 while that with radius 30% greater is Cup 2, etc. The different cups represented the radius R_c in Eq [3.15] for the Alderman approach, while for the NCSU approach the cup sizes were the radius of the different deformation zones, i.e., $R_d = R_c$ in Eq [3.10].

Strain controlled experiments produce specific strains compared with stress controlled frequency sweeps. Stress controlled produce variable strains at desired levels of stress. Hence strain controlled frequency sweeps were conducted with frequencies required to match the strain rates obtained from the Brookfield. The tests were conducted at similar conditions of temperature and pressure for both the

rheometers and polyacrylamide and gelatin solutions used in both rheometers were from the same lot.

Each of the model systems was tested at 5 rotational speeds (0.1, 0.3, 0.5, 0.7 and 1.0 rpm) on the Brookfield YR-I and at 5 frequencies in the linear viscoelastic region of the model system on the StressTech. The frequencies on the StressTech were chosen such that the strain rates from both the Brookfield YR-I and the StressTech were in the same range and comparable. Each model system was tested 5 times on the selected set of rotational speeds and frequency, which were called trials. A second lot of the same model system was tested in similar way, called a separate set. Thus, for each model system, two sets of 5 trials were conducted such that each trial consisted of 5 strain rates on both Brookfield YR-I and StressTech.

3.5 RESULTS AND DISCUSSION

3.5.1 ROTATIONAL SPEEDS SELECTION

Polyacrylamide was chosen as a model system to represent perfectly elastic solids with a phase angle of 0 degrees. The torque-time response obtained from the Brookfield YR-I at various rotational speeds facilitated the identification of the range of speeds feasible for these experiments. The torque response of polyacrylamide at higher rotational speeds suggested that the sample exhibits a phase angle greater than zero. On closer examination, the torque values below 10% full scale torque were questionable, and these data were discarded. The phase angles obtained on

the application of the NCSU concept following removal of the questionable data showed a better agreement with the standard data for rotational speeds below 1.0 rpm, see Figures 3.8 and 3.9. Rotational speeds greater than 1.0 rpm did not provide reliable data, even after the elimination of the questionable torque data, see Figure 3.10. The new set of rotational speeds recommended for subsequent experiments ranged between 0.1 rpm and 1.0 rpm.

3.5.2 CHOICE OF BROOKFIELD YR-I RHEOMETER (BETWEEN HB AND RV SERIES)

Initially, starch samples prepared at concentrations between 8% to 10% w/w in water were tested on both Brookfield YR – I (HB series) and a controlled stress rheometer, StressTech. The StressTech affirmed that the linear viscoelastic region of the starch sample fell below a stress level of approximately 10 Pa, see Figure 3.11. The HB series has a stronger spring with maximum measurable yield stress of 150 Pa with vane spindle V-72. Hence, the Brookfield YR – I (HB series) attained stress levels similar to that of StressTech prior to attaining a 10% torque value when tested at rotational speeds between 1.0 rpm to 5.0 rpm. The values below 10% torque level, as illustrated in section 3.5.1, were questionable and were not used to establish the phase angle or other viscoelastic properties. This disparity between the rates of stress development in both machines eliminated the selection of starch as a model system. Starch was tested on a more sensitive viscometer such that the linear viscoelastic region fell more within the range of equipment sensitivity, and the

Brookfield YR – I (RV) was used. Thus, it was concluded that materials with higher yield stress, with the linear viscoelastic region extending beyond 30 Pa, should be tested on the HB series of Brookfield YR-I. Accordingly, weaker materials with lower yield stress should be evaluated with the RV series of the Brookfield YR-I, which is 8 times more sensitive than the HB series.

For the model systems, the HB series of Brookfield YR-I was used with polyacrylamide and 4% w/w gelatin gels due to their strength and high yield stress values (greater than 150 Pa). The weaker structure and lower values of yield stress (less than 20 and 30 Pa respectively) of 1.5% and 1.75% w/w gelatin gels required a more sensitive rheometer that could vividly depict the linear viscoelastic regime of the gels. Accordingly, the Brookfield YR-I RV series was used to measure the viscoelastic properties of these model systems.

3.5.3 STATISTICAL ANALYSIS

Various statistical methods were considered to analyze the data obtained from both the machines. SAS, a popular statistical software, was chosen to perform the analysis. The GLM (general linear models) procedure is one of the procedures used for multiple linear regression models and analysis of variance, and the method assumes the variances of both machines are the same. The variance of Brookfield YR-I is observed to be two orders higher than the StressTech, see Table 3.1. Accordingly, the assumption of equal variances is not accurate, and the process of combining data and testing with GLM procedure for instrument effect is not

possible. To consider fitting individual models for both machines, the data obtained from each machine should be linear. Certain materials showed linear behavior with the StressTech, but there was no evidence of linear association from the Brookfield for any material. Again, confidence bands can be developed around a series of data points only when linearity is observed, and hence was not possible. A t-test cannot be performed on the data since obtaining response for the same strain rates is not possible for the machines. The strain rates for the machines can be kept in close proximity but cannot be the same. Therefore, the best approach for a statistical analysis for the present data was to develop confidence intervals for the mean of the individual responses and visually assess the proximity of the areas within the intervals. Though the smooth lines used to join the confidence intervals do not necessarily predict the behavior of the material within strain rates, the lines are of assistance for visual assessment.

3.5.4 PREFERABLE CUP SIZE

The model systems were tested both on the Brookfield YR-I and the StressTech at similar conditions of temperature, pressure, and shear rate. The torque-time responses obtained from the Brookfield YR-I for each rotational speed were transformed into shear modulus and phase angle for the corresponding strain rates according to sections 3.2 and 3.3. The parameters were then marked on the same plot as that for various strain rates obtained from the StressTech, for easier comparison.

Figures 3.12 and 3.13 describe the behavior of 4% gelatin with strain rate for different cup sizes. The plots clearly show that the results obtained from the Brookfield YR-I with Cup 1 coincided well with the data obtained from the StressTech. A gradual increase in the Brookfield YR-I values of phase angle and shear modulus was observed with increasing cup size. Recurrence of the observation with 5% polyacrylamide, 10% polyacrylamide, 1.75% and 1.5% gelatin gels established that using Cup 1 with Brookfield YR-I produced data most comparable to the data obtained with the StressTech machine. The relevant plots describing the data obtained from the aforementioned model systems are presented in the appendix. The level of correspondence of the data for different model systems from the StressTech and Brookfield YR-I for various cups was tabulated in Table 3.2. The relative comparability of the Brookfield data of various cups was suggested in the tables. A cross (X) indicates that a marked difference between the data from both the instruments was observed, whereas a tick (√) suggests that the data from the Brookfield YR-I for that cup with the StressTech data was comparable.

3.5.5 SUGGESTED APPROACH

Confidence intervals at a 95% level were developed for the phase angle and shear moduli data obtained from Brookfield YR-I-cup 1 combination and StressTech for each approach and a smooth line joined the data. An overlap of the areas within

the lines connecting the confidence intervals signified similarity between the data produced by both machines.

Figures 3.14 and 3.15 describe the behavior of 4% gelatin for all three approaches considered. Though the Brookfield approach produced similar phase angle data as the StressTech, similar shear moduli data was not observed, while the Alderman and NCSU approaches provided similar phase angle and shear moduli data. However, the NCSU approach did not have a clear strain rate value corresponding to each rotational speed. The strain rate value depends upon the strain observed in the material each time and so replication of data at the same strain rate was not easy. Thus, desired strain rates were not observed with the NCSU approach. Also, better estimations of shear moduli were observed with the Alderman approach for other cups too. Similar behavior was observed with other model systems including 10% polyacrylamide, 5% polyacrylamide, 1.75% gelatin, and 1.5% gelatin which are presented in the form of similar plots in the appendix. Thus, the Alderman approach for shear moduli calculation along with the NCSU approach for phase angle determination is the best combination for viscoelastic property determination.

3.6 SUMMARY

The torque-time profile obtained by testing a material on the Brookfield YR-I was used to develop the NCSU approach for the determination of phase angle and shear moduli data. Other methods, including the Alderman approach and the Brookfield approach, were also considered. Cups of different sizes were used with

the Brookfield YR-I to represent the cup and deformation zone radii in the Alderman and NCSU calculations. Different concentrations of polyacrylamide and gelatin gels were selected as the model systems, and were tested on both instruments, followed by the application of the aforementioned approaches for viscoelastic property determination. The results obtained from the tests determined the appropriate test conditions required for the measurement of viscoelastic properties. Cup 1 (radius of cup 10% greater than vane radius) should be used with Brookfield YR-I, and rotational speeds below 1.0 rpm should be applied. The choice between Brookfield YR-I HB and RV series depends upon the strength of the material. A statistical analysis confirmed the Alderman technique as the better selection for shear moduli and rate calculations. Thus, viscoelastic parameters of materials can be obtained with the Brookfield YR-I by adopting the proposed experimental protocol.

3.7 REFERENCES

[1] Yan J., James A.E., The yield surface of viscoelastic and plastic fluids in a vane viscometer, J. Non-Newtonian Fluid Mech., 70 (1) (1997) 237

[2] Liddell P.V. and Boger D.V., Yield stress measurements with the vane, J. of Non-Newtonian Fluid Mechanics, 63 (1996) 235

[3] Q. D. Nguyen and D. V. Boger, Measuring the Flow Properties of Yield Stress Fluids, Annual Review of Fluid Mechanics 24 (1992) 47

[4] M. Krulis, and H. Rohm, Adaption of a vane tool for the viscosity determination of flavoured yoghurt, Eur Food Res Technol 218 (2004) 598

[5] H. A. Barnes, The Myth of Yield Stress Fluids, Progress and Trends in Rheology V, Proc. of fifth European Rheology Conference, Portoroz, 1998, p. 201

[6] H.A. Barnes and J.O. Carnali, The vane-in-cup as a novel rheometer geometry for shear thinning and thixotropic materials, J. of Rheology, 34 (6) (1989) 841

[7] L. Zhu et al., A slotted plate device for measuring static yield stress, J. of Rheology, Volume 45 (5) (2001) 1105

[8] N. J. Alderman, G. H. Meeten and J. D. Sherwood, Vane rheometry of bentonite gels, J. Non-Newtonian Fluid Mech., 39 (1991) 291

[9] M. Keentok, J. F. Milthorpe and A. E. Donovan, On the shearing zone around rotating vanes in plastic liquids: theory and experiment, J. Non-Newtonian Fluid Mech., 17 (1) (1985) 23

[10] P. J. Scales, S. B. Johnson and T. W. Healy, Shear Yield Stress of Partially Flocculated Colloidal Suspensions, AIChE Journal, 44 (3) 1998 538

[11] J.F. Steffe, Rheological Methods in Food Process Engineering, Second Edition, Freeman Press, East Lansing, 1996, p. 317

[12] J. Zhang, C. R. Daubert and E. A. Foegeding, Fracture Analysis of alginate gels, Journal of Food Science (in press) 2005

Table 3.1.Variances of phase angle and shear moduli data for 4% Gelatin from both the instruments at various strain rates

Strain Rate	Brookfield YR-I		StressTech	
Parameter	Phase Angle	Shear Modulus	Phase Angle	Shear Modulus
0.13	0.914	3039.02	0.003	2.435
0.39	0.008	214.199	0.003	2.602
0.65	0.06	560.665	8.86E-16	3.038
0.91	0.191	199.975	0.007	2.647
1.30	0.344	158.410	0.003	3.365

Table 3.2.Comparison of data obtained for various concentrations of polyacrylamide and gelatin gels from the Brookfield YR-I with various cup sizes to the StressTech data with each of the approaches.

Cup Size	Alderman		NCSU		Brookfield	
Parameter	Phase Angle	Shear Modulus	Phase Angle	Shear Modulus	Phase Angle	Shear Modulus
Cup 1	√	√	√	√	√	X
Cup 2	X	√	X	X	X	X
Cup 3	X	√	X	X	X	X
Cup 4	X	√	X	X	X	X
Cup 5	X	√	X	X	X	X

Note: The cup size which generates best comparable parameters with that of StressTech data is denoted as a tick (√), while the other cups are marked with a cross (X)

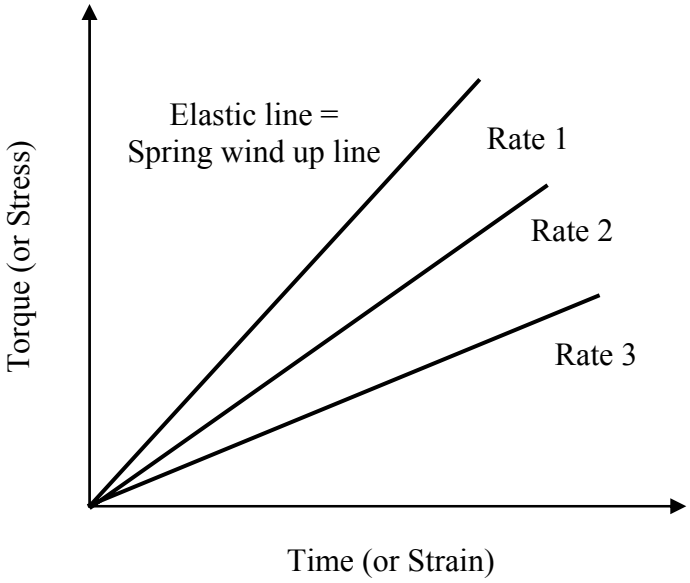


Fig. 3.1 Torque-time relationship of elastic materials at various rotational speeds
Rate 1 > Rate 2 > Rate 3

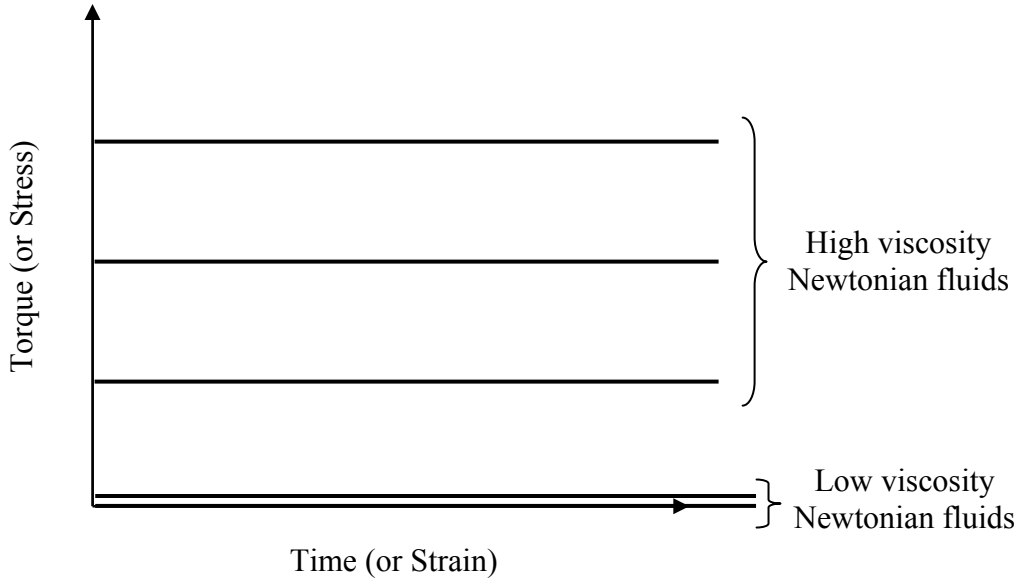


Fig. 3.2 Torque-time relationship of Newtonian materials of different viscosities at various rotational speeds at constant rate of rotation

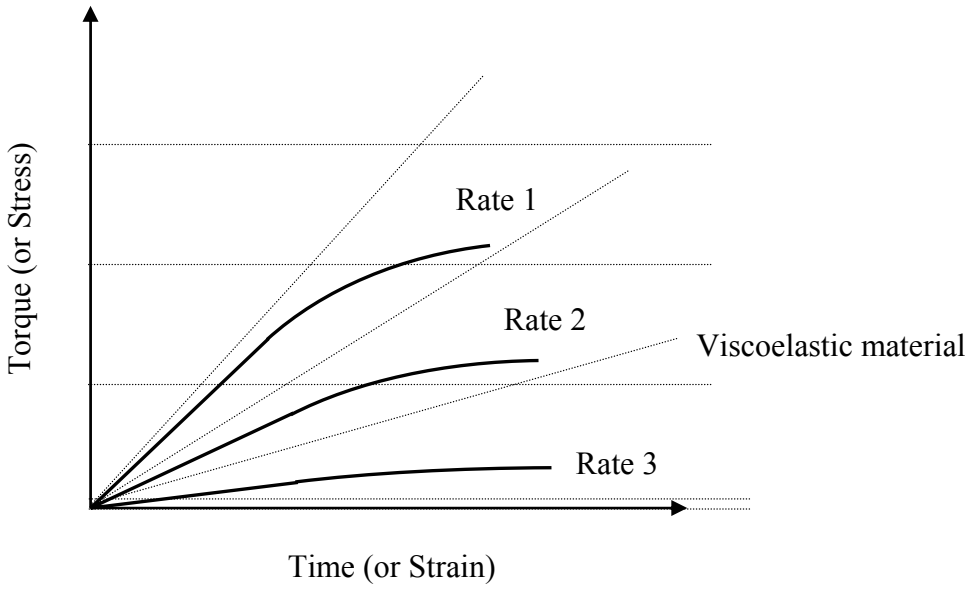


Fig. 3.3 Torque-time relationship of elastic, low viscosity Newtonian and viscoelastic materials at various rotational speeds
Rate 1 > Rate 2 > Rate 3

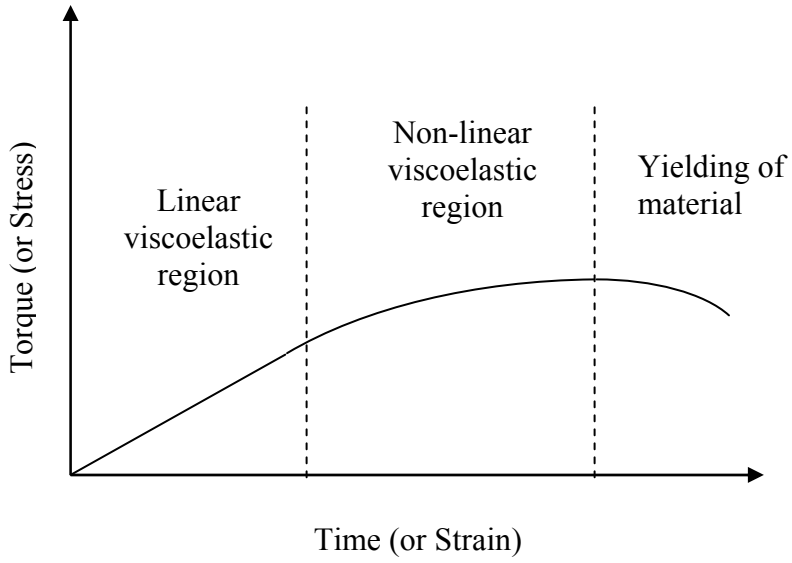
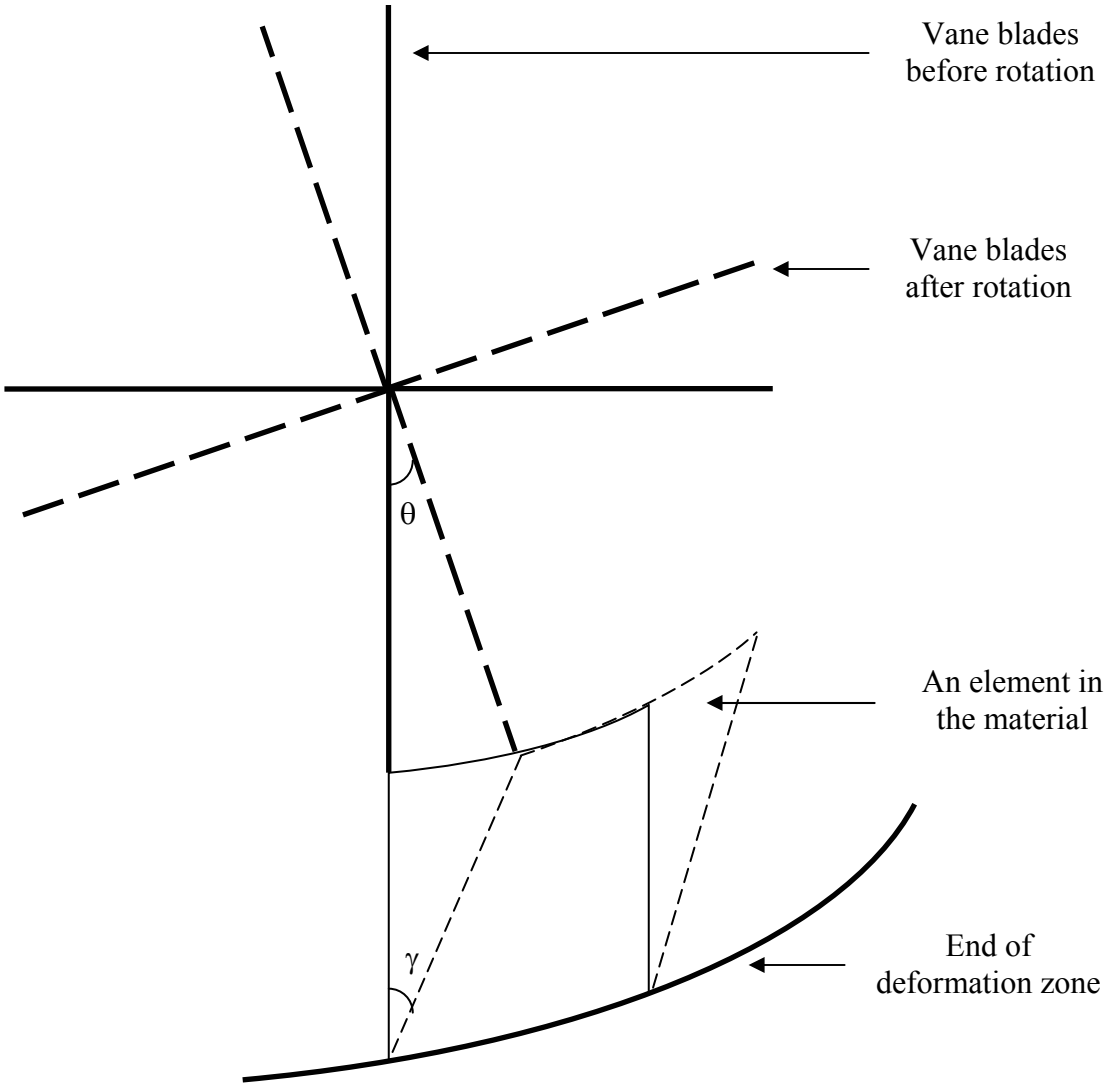


Fig. 3.4 Various phases of a torque-time relationship of viscoelastic material, (Zhang 2004)



Note: γ - True strain in NCSU approach
θ - Vane rotation, strain in Brookfield approach

Fig. 3.5 True strain

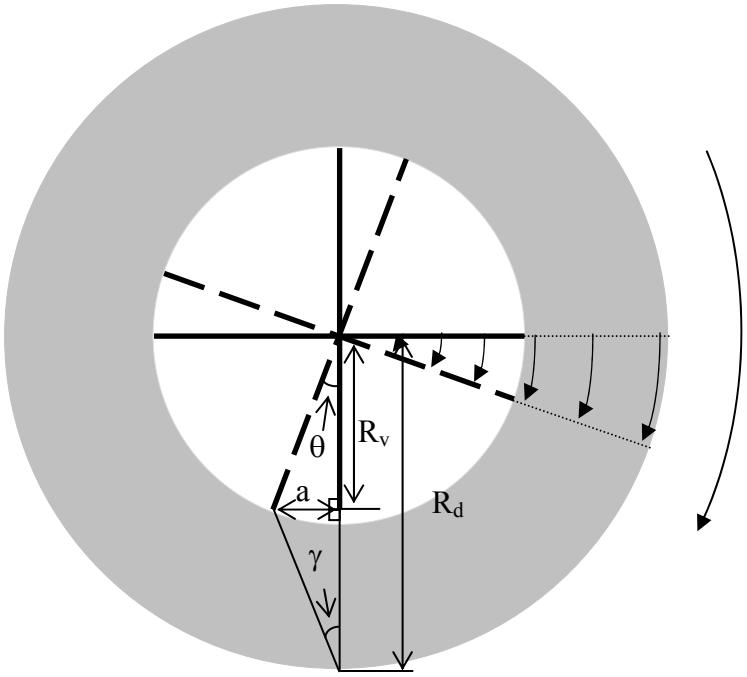


Fig. 3.6 Strain Calculation

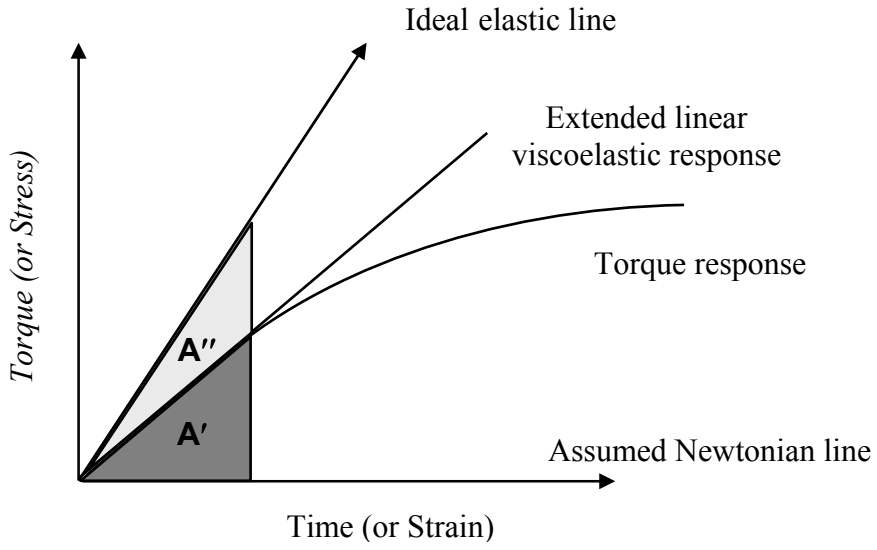


Fig. 3.7 Areas representing viscous and
elastic effects of the material

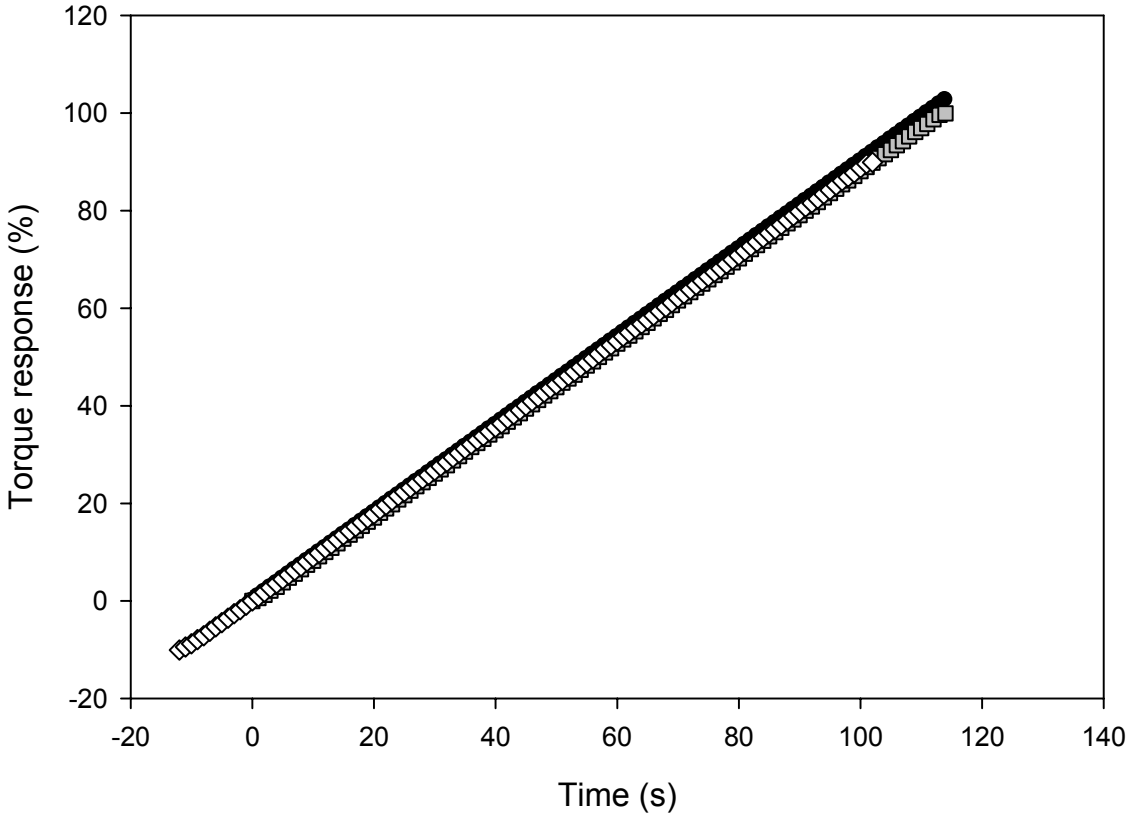


Fig. 3.8 Torque response at 0.1 rpm; ● Elastic Line; □ Torque response; ◇ Corrected torque response;

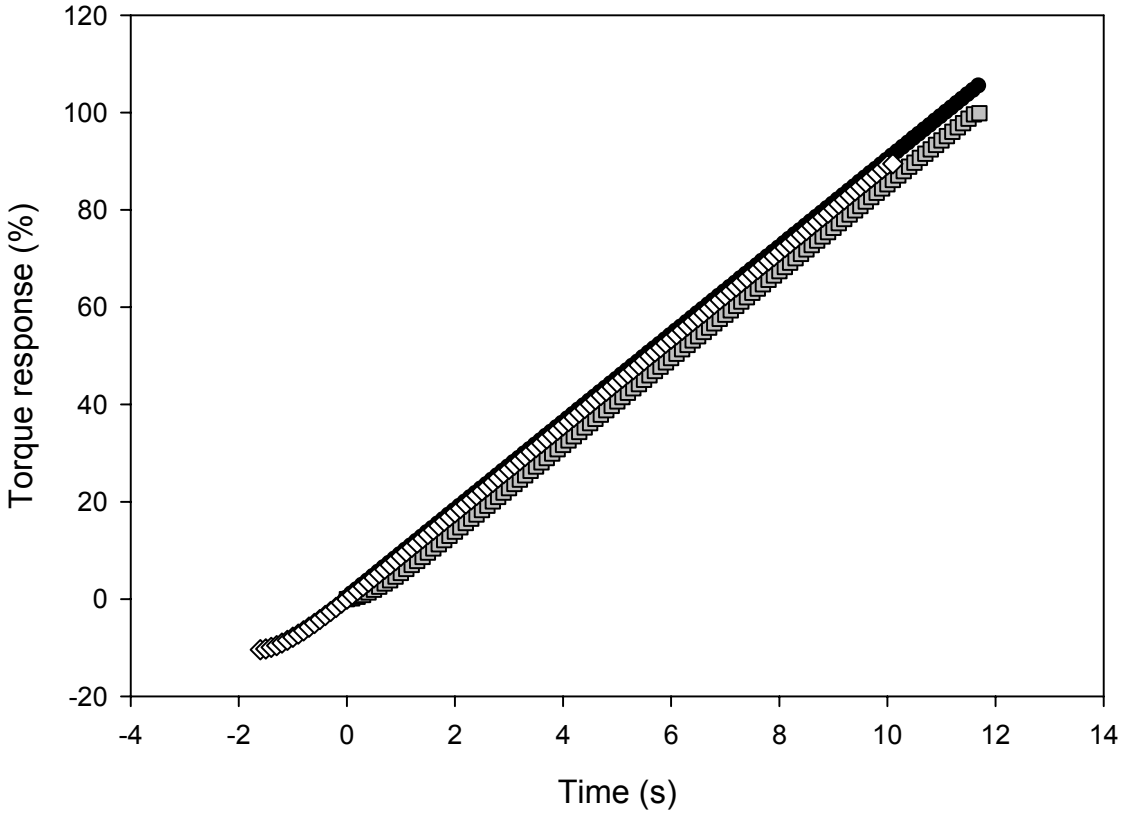


Fig. 3.9 Torque response at 1.0 rpm; ● Elastic Line; ▫ Torque response; ◇ Corrected torque response;

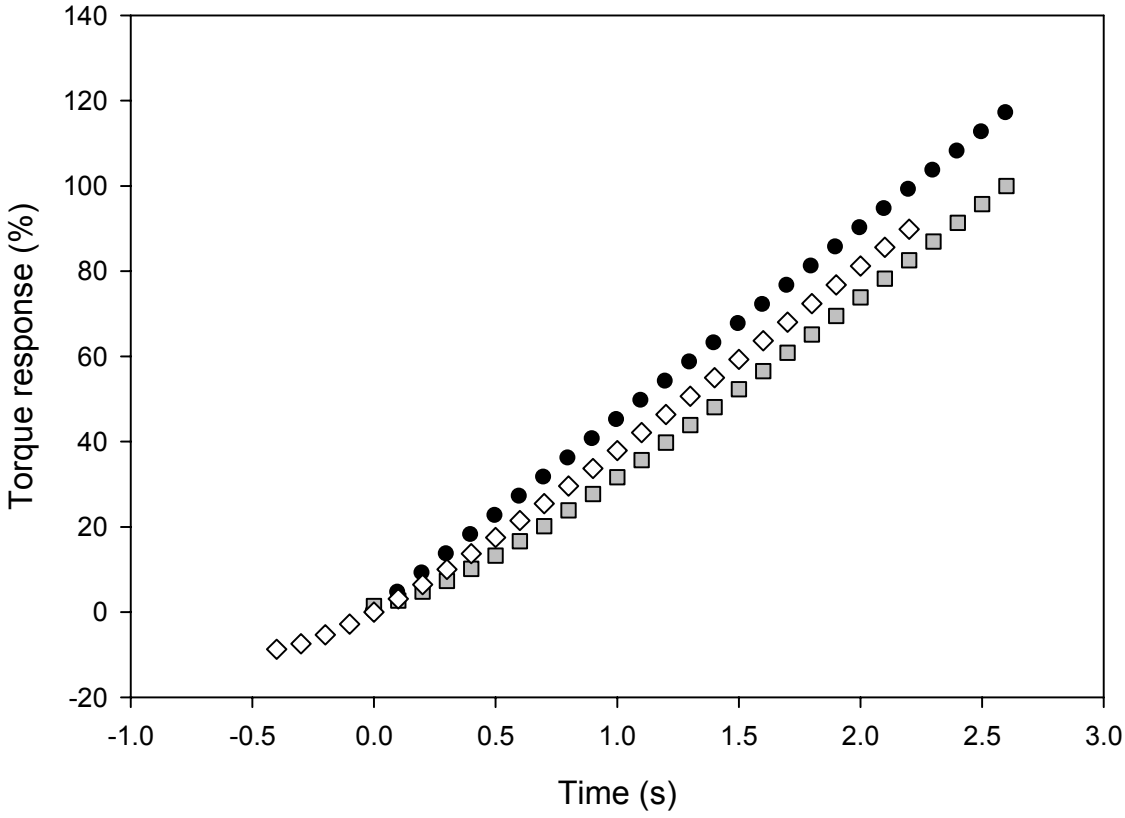


Fig. 3.10 Torque response at 5.0 rpm; ● Elastic Line; ▫ Torque response; ◇ Corrected torque response;

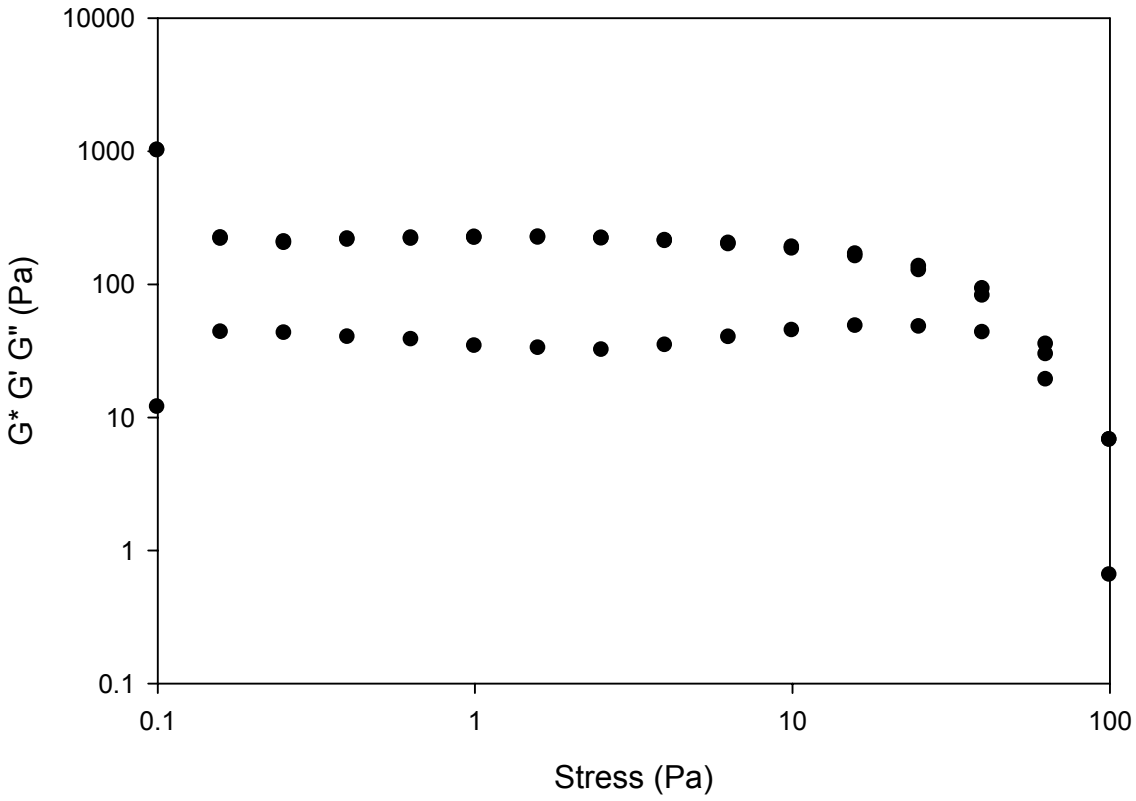


Fig. 3.11 Stress sweep at 0.05 Hz; ● G* G' G";

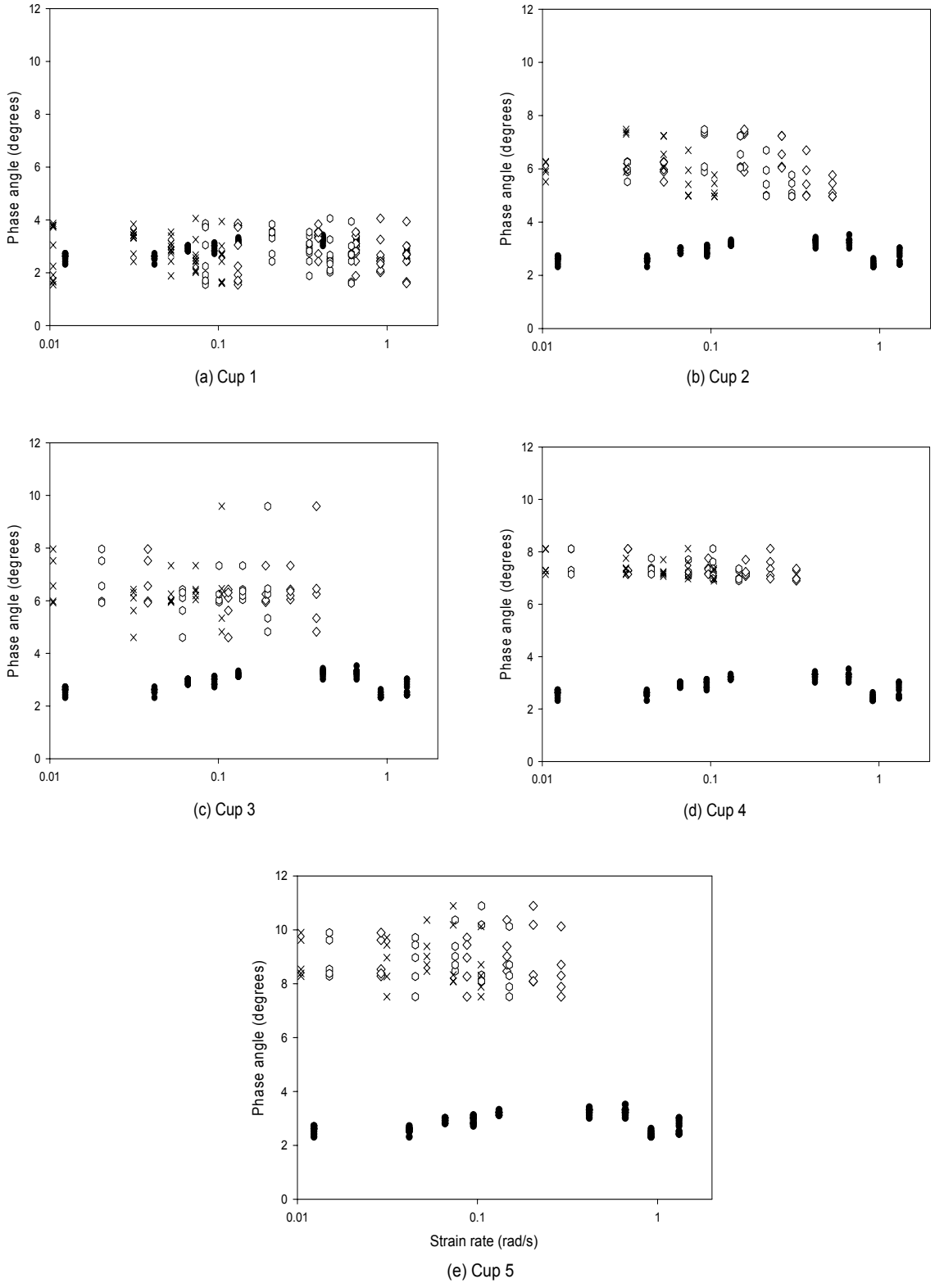


Fig. 3.12 Gelatin 4% - phase angle data for various cups for all three approaches; • StressTech data; ◇ Alderman approach; ⎔ NCSU Approach; × Brookfield Approach

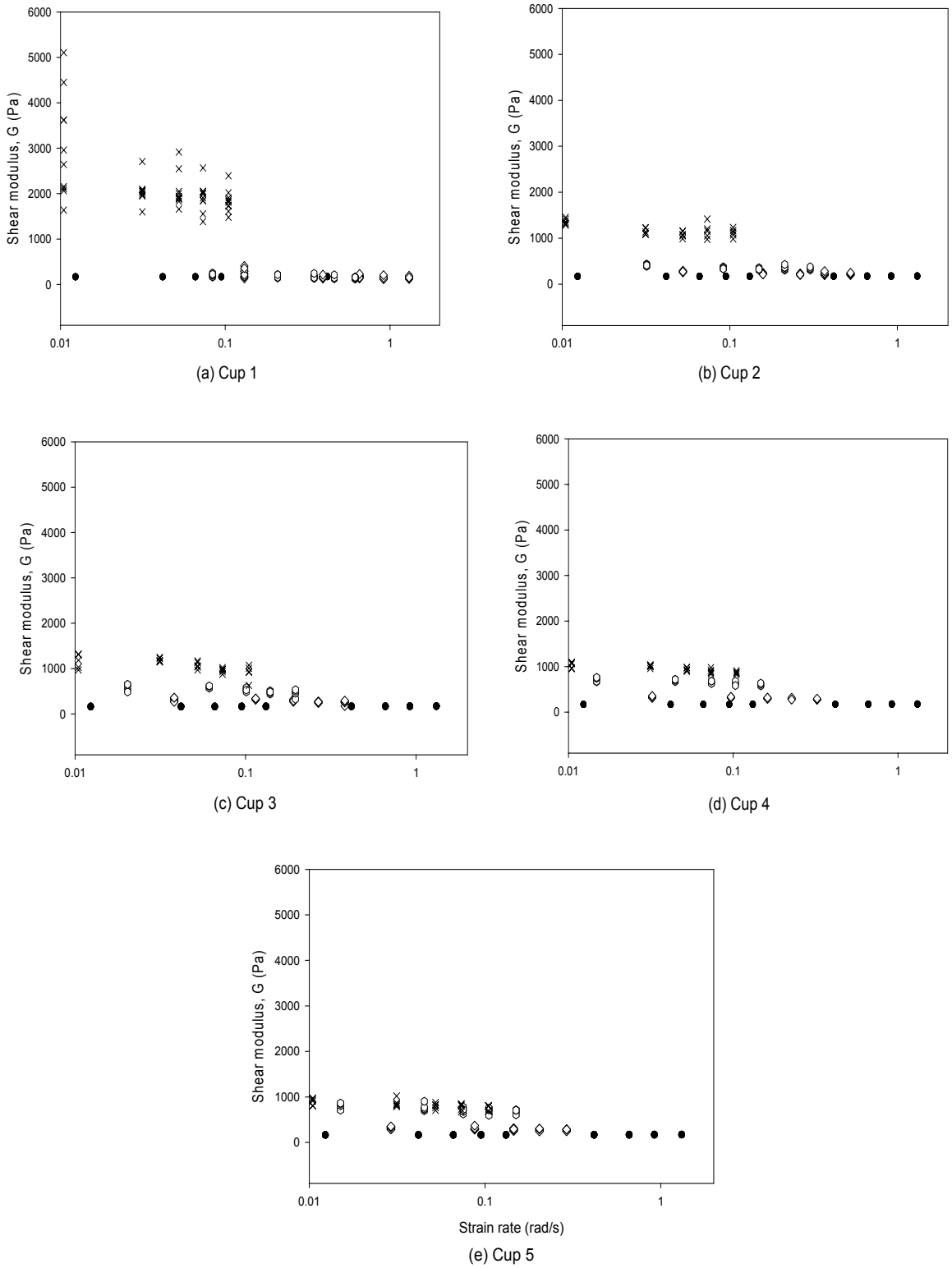
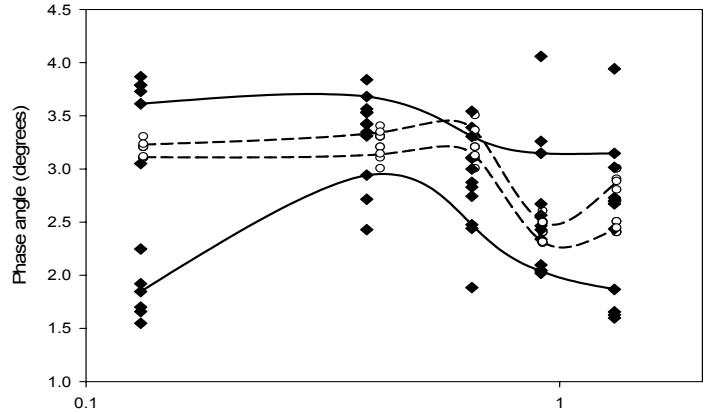
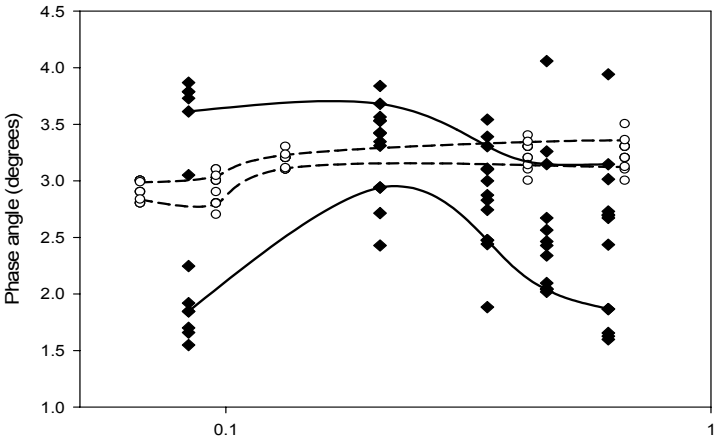


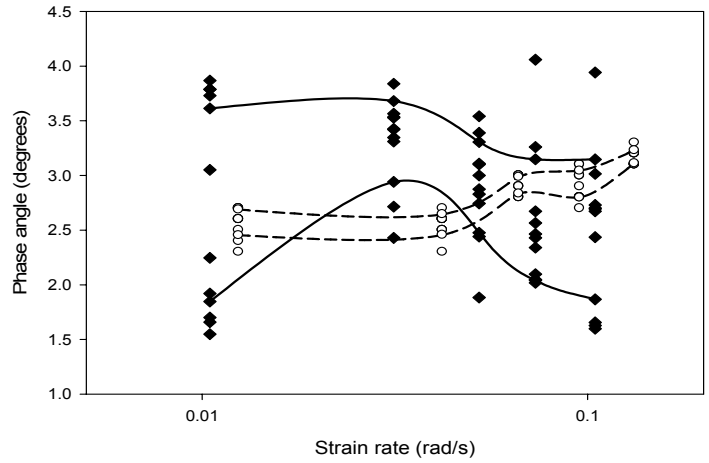
Fig. 3.13 Gelatin 4% - shear moduli data for various cups for all three approaches; • StressTech data;◇ Alderman approach;⎔ NCSU Approach;× Brookfield Approach



(a) Alderman approach

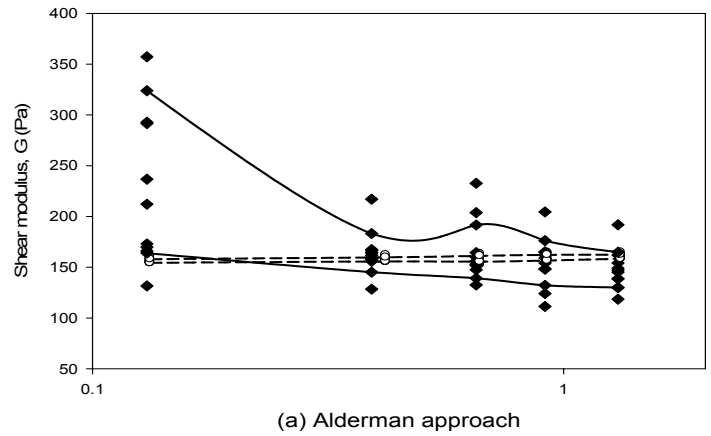


(b) NCSU approach

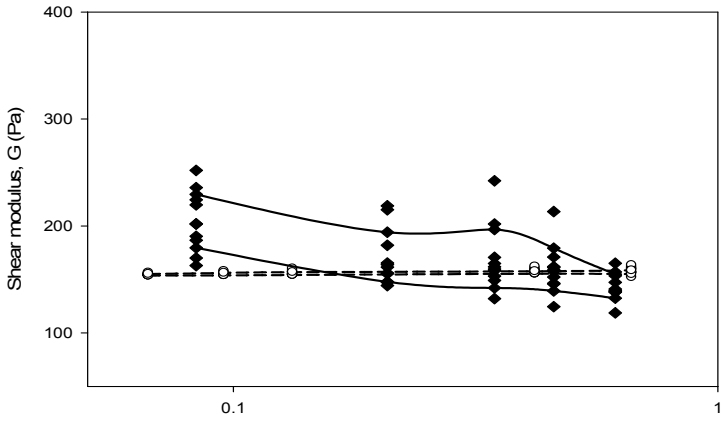


(c) Brookfield approach

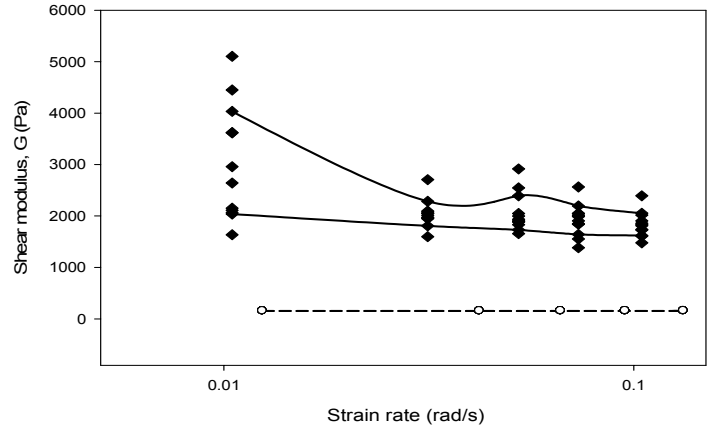
Fig. 3.14 Gelatin 4% - phase angle data for the three approaches for cup 1; ○ StressTech data; ◆ Brookfield data; -⊖- StressTech confidence limits; —◆— Brookfield confidence limits



(a) Alderman approach



(b) NCSU approach



(c) Brookfield approach

Fig. 3.15 Gelatin 4% - shear moduli data for the three approaches for cup ○ StressTech data; ◆ Brookfield data; -⊖- StressTech confidence limits; —◆— Brookfield confidence limits

CHAPTER 4.

DESIGN AND VERIFICATION OF PROTOCOL

4.1 INTRODUCTION

The vane method is an established technique for yield stress determination [1, 2, 3, 4, 5, 6]. Methods to estimate shear modulus of materials by using the vane technique were previously developed by Alderman et al. (1990), Sherwood and Meeten (1991) and Bagdassarov and Pinkerton (2004) [7, 8, 9]. In the previous chapter, a new approach (the NCSU approach) for the estimation of shear modulus for small strains using a deformation zone concept was introduced. Moreover, a novel method for the determination of phase angle and thereby the viscoelastic properties of materials was demonstrated. Observations and conclusions obtained from different model systems helped devise a protocol to use with the Brookfield YR-I vane rheometer (Brookfield Engineering, Middleboro, Massachusetts) for the measurement of viscoelastic properties.

Data obtained from the model systems showed agreement between viscoelastic property predictions from the Brookfield YR-I - Cup 1 combination (diameter of the cup 10% greater than the vane diameter) and the StressTech rheometer, a conventional, controlled stress instrument (Rheologica Instruments AB, Lund Sweden). Cups with larger diameters produced results statistically different from the StressTech data. Of all techniques considered, a statistical analysis confirmed the Alderman concept as the optimal approach for shear moduli and rate calculations. Similarly, other observations from the preliminary results (see section 3.5) were used in the development of the following specifications:

- Cup 1 (with diameter 10% greater than vane diameter) should be used with Brookfield YR-I.
- Brookfield YR-I HB series should be used with materials having a yield stress greater than 30 Pa while Brookfield YR-I RV series should be used with materials having a yield stress below 30 Pa.
- Rotational speeds below 1.0 rpm should be used.
- Torque data below 10% of the viscometers full scale torque should be deleted.
- The Alderman approach should be implemented for shear modulus and rate calculations.

The objective of present research was to validate the above stated criteria for the use of Brookfield YR-I as a viscoelastic parameter determining rheometer. To accomplish the objective, several commercial products were evaluated and compared with results obtained from conventional viscoelastic rheometry.

4.2 MATERIALS AND METHODS

4.2.1 COMMERCIAL PRODUCTS AND SAMPLE PREPARATION

To verify the use of the Brookfield YR-I for viscoelastic property measurement, certain commercial products, listed in Table 4.1, were chosen for analysis. All the products were purchased from a local store. Jell-o was melted in a microwave for a minute, in the same container in which it is obtained. Later, the Jell-o was cooled in

the rheometers with attachments inside the cups at room temperature for 6 hours. Thus, a network was present in the material during the test. All other products were placed in a beaker prior to testing and presheared using a spatula to eliminate any network present in the material to establish a baseline shear history. The sheared material was placed in the respective rheometer cups and tested without delay. The same conditions of temperature and pressure were observed with both instruments.

4.2.2 RHEOLOGICAL ANALYSIS

4.2.2.1 STRESSTECH

A serrated bob and cup combination was used with the StressTech rheometer, (Rheological Instruments AB, Lund, Sweden). The linear viscoelastic region of each material was identified for three different frequencies of 0.01, 0.1 and 1.0 Hz. Within the linear viscoelastic region of the material, strain controlled experiments were performed at strain rates between 0.13 to 1.3 rad/s to determine the phase angles and complex moduli. By definition, a linear relationship between stress and strain is invalid beyond the linear viscoelastic region, therefore the equations for computations of the moduli are applicable only in the linear viscoelastic region [10]. Thus, it was necessary to conduct experiments within the linear region. Strain controlled experiments were conducted as they were preferable over the more regular frequency sweeps to obtained desired strains and hence strain rates.

4.2.2.2 BROOKFIELD YR-I

Vane spindle V-72 was used with the Brookfield YR-I, and the established criteria described in the previous section were followed. Thus, for peanut butter with a yield stress above 150 Pa, a Brookfield YR-I HB series was used for testing. The yield stress of all other materials was below 30 Pa and accordingly Brookfield YR-I RV series was chosen for the experiments.

4.2.3 STATISTICAL ANALYSIS

The statistical analysis of the data obtained from the commercial products was similar to the analysis for model systems. A pointwise 95% level confidence intervals were obtained developed for the phase angle and shear moduli data obtained from both Brookfield YR-I and StressTech instruments. A smooth line was used to join the individual points, and overlap of the areas created by the lines connecting the confidence intervals visually signified similarity between the data produced by both the machines, indicating that the Brookfield YR-I rheometer produced similar properties as compared with the StressTech rheometer.

4.3 RESULTS

Figures 4.1 to 4.6 show the phase angles and shear moduli with confidence intervals obtained from both instruments for all commercial products in Table 4.1.

The results are numerically displayed along with the results from model systems in Tables 4.2 and 4.3.

4.3.1 SHEAR MODULUS

The confidence intervals of shear moduli obtained from the StressTech lie within the confidence intervals of Brookfield YR-I for Jell-o and peanut butter. However, yogurt, salad dressing, grape jelly and ketchup, did not display overlapping confidence intervals, so the results were deemed not similar.

4.3.2 PHASE ANGLES

The confidence intervals for gelatin snacks, yogurt, salad dressing, and grape jelly obtained from the StressTech all fell within the confidence intervals obtained from the Brookfield YR-I. However, the confidence intervals for peanut butter were different orders of magnitude for both machines. The phase angle data for ketchup from the Brookfield YR-I was significantly different for the first strain rate (i.e., $0.13s^{-1}$), but for the higher strain rates the data were similar.

4.4 DISCUSSION

The torque response of the vane rheometer is based on the yield stress of the material. Therefore, on the Brookfield YR I, materials with low yield stress produced

a high phase angle and low shear modulus value. Yogurt, salad dressing, grape jelly and ketchup each have a relatively low yield stress value (lower than 30 Pa) and accordingly recorded a high phase angle and low shear modulus value when tested with the Brookfield YR-I. Similarly, peanut butter with a comparatively high yield stress value generated a low phase angle and a high shear modulus with the Brookfield YR-I. However, the StressTech produced a considerably higher value of shear moduli for yogurt, salad dressing, grape jelly and ketchup. Peanut butter showed a considerably higher phase angle when tested on the StressTech than on the Brookfield YR-I.

Results from the model systems (see Figure 3.13) signified the tendency of obtaining higher shear moduli values from the Brookfield YR-I with an increase in the cup size. Therefore, yogurt was tested on Brookfield YR-I with cup 5. The phase angle data obtained from cup 5 was comparable to the data from the StressTech, see Figure 4.6 and as expected, a significant increase in the shear moduli was observed. However, the data was still not comparable to the results obtained from the StressTech, see Figure 4.7. An increase in the cup size decreases the strain value and hence an increase in the shear moduli value, see Eqs. [3.7], [3.9], [3.15] and [3.16]. Thus, a further increase in the cup size may further increase the shear moduli values obtained from the Brookfield YR-I where they are comparable to the data obtained from StressTech.

The significant difference between the phase angle data obtained from both the instruments for peanut butter can be explained based on the assumed Newtonian line of the material. A higher assumed Newtonian line can significantly decrease

the area representing the elastic energy and hence produce a more viscous response with a higher phase angle similar to the StressTech, see Figure 4.8. Therefore, the cup size and the position of the assumed Newtonian line play a significant role in the estimation of the phase angle and shear modulus parameters. However, the present results from Brookfield YR-I with cup 1 exhibit a level of agreement with StressTech. Considering the data obtained from the model systems and the commercial food products, Table 4.4 is an attempt to categorize the pattern of agreement between both machines. This categorization is based on three different levels of phase angle and shear moduli-low, medium and high ranges as indicated on the table. The Brookfield YR-I, along with the stated protocol, was observed to produce viscoelastic parameters that were in agreement with the results obtained from StressTech for materials exhibiting a combination of high shear moduli-low phase angle, medium shear moduli-medium phase angle, low shear moduli-medium phase angle, and low shear moduli-high phase angle.

4.5 SUMMARY

Based on the results obtained from the model systems, a protocol was developed and recommended to use with the Brookfield YR-I to measure viscoelastic properties. The method was further evaluated with commercial products for verification. Jell-o showed a good agreement between the data from both machines. For other materials, either the phase angle or the shear moduli data from the Brookfield YR-I did not correspond with data from the StressTech. One of

the materials, yogurt, was tested on the Brookfield YR-I along with cup 5, and a significant increase in the shear moduli value was observed. A further increase in the cup size may produce shear moduli values corresponding to the StressTech. Meanwhile, the phase angle data remained comparable to the StressTech result. Thus, a selection of appropriate cup size for a material governs the similarity between the results from Brookfield YR-I and StressTech. Considering the data obtained from both the model systems and the commercial products, Brookfield YR-I produced data similar to the StressTech machine for materials with high shear moduli-low phase angle, medium shear moduli-medium phase angle, low shear moduli-medium phase angle, and low shear moduli-high phase angle combinations. All conclusions, however, were based on the assumption that the StressTech produced accurate viscoelastic property values.

Thus, the model systems established Brookfield YR I as a viscometer capable of viscoelasticity measurements. Further research is required to assess the material functions which influence the deformation zone, and thereby the strain calculations. This expanded understanding will advance Brookfield viscometry techniques to the measurement of fundamental viscoelastic property measurements.

4.6 REFERENCES

[2] Barnes H A, The yield stress – a review or ‘παντα ρει’ – everything flows?, J of Non-Newtonian Fluid Mechanics, 81(1&2) (1999) 133

[3] J. R. Stokes, J. H. Telford and A. M. Williamson, The flowability of ice suspensions, J. of Rheology, 49 (1) (2005) 139

[4] L. Zhu et al., A slotted plate device for measuring static yield stress, J. of Rheology, Volume 45 (5) (2001) 1105

[5] H. A. Barnes and Q. D. Nguyen, Rotating vane rheometry — a review, J. Non-Newtonian Fluid Mech, 98(1) (2001) 1

[6] G. H. Meeten, Effects of plate roughness in squeeze-flow rheometry, J. of Non-Newtonian Fluid Mechanics, Volume 124 (2004) 51

[7] Z. Kemblowski, P. Budzynski and P. Owczarz, On-line Measurements of the Rheological Properties of Fermentation Broth, Third European Rheology Conference

[8] N. J. Alderman, G. H. Meeten and J. D. Sherwood, Vane rheometry of bentonite gels, J. Non-Newtonian Fluid Mech., 39 (1991) 291

[9] J.D. Sherwood and G.H. Meeten, The use of the vane to measure the shear modulus of linear elastic solids, J. of Non-Newtonian Fluid Mechanics, Volume 41 (1991) 101 and Golden Jubilee Meeting of the British Society of Rheology (1990) 265 – 300

[10] N. Bagdassarov and H. Pinkerton, A review and investigation of the Non-Newtonian properties of lavas based on laboratory experiments with analogue materials, J. of Volcanology and Geothermal Research, 45 (3) (2004) 197

[11] J.F. Steffe, Rheological Methods in Food Process Engineering, Second Edition, Freeman Press, East Lansing, 1996, p. 2, 158, 200-201, 296, 316-317

Table 4.1. Commercial products used for testing the devised approach

Product	Brand Name and Description	Manufactured/Distributed by	Place
Gelatin Snacks	Jell-o Sugar Free Low Calorie Gelatin Snacks	Kraft Food North America	Tarrytown, New York
Yogurt	Food Lion Plain Nonfat Yogurt	Food Lion	Sablisbury, North Carolina
Salad Dressing	Food lion fat free Ranch	Food Lion	Salisbury, North Carolina
Peanut Butter	Skippy Creamy Peanut butter	Unilever Best Foods	New Jersey
Grape Jelly	Smucker's Concord Grape Jelly	The J.M. Smucker Company	Orrville, Ohio
Ketchup	Heinz Tomato Ketchup	H.J. Heinz Company	Pittsburg, Pennsylvania

Table 4.2. Pointwise 95% Confidence Interval of the phase angle data obtained from Brookfield YR-I and StressTech and agreement between the two instruments

Material	StressTech	Brookfield	Agreement
10% Polyacrylamide	**0.30** ± 0.07 to **0.72** ± 0.06	**0.40** ± 0.04 to **0.71** ± 0.05	Yes
5% Polyacrylamide	**1.44** ± 0.12 to **1.71** ± 0.05	**0.12** ± 0.11 to **1.74** ± 0.11	Yes
4% Gelatin	**2.4** ± 0.13 to **3.24** ± 0.11	**2.51** ± 0.73 to **3.51** ± 0.42	Yes
1.75% Gelatin	**7.25** ± 0.48 to **9.09** ± 0.54	**6.82** ± 0.86 to **8.74** ± 1.22	Yes
1.5% Gelatin	**19.20** ± 0.2 to **23.72** ± 1.41	**10.01** ± 8.85 to **29.26** ± 7.01	Yes
Gelatin Snacks	**9.80** ± 0.16 to **11.26** ± 0.1	**8.86** ± 0.87 to **11.07** ± 1.33	Yes
Yogurt	**13.74** ± 0.13 to **20.5** ± 0.16	**13.48** ± 2.52 to **15.54** ± 3.34	Yes
Salad Dressing	**19.44** ± 0.15 to **21.62** ± 0.27	**18.80** ± 0.31 to **21.65** ± 0.87	Yes
Peanut Butter	**39.45** ± 1.12 to **46.28** ± 0.85	**1.39** ± 0.68 to **2.86** ± 0.48	No
Grape Jelly	**6.56** ± 0.24 to **13.66** ± 0.25	**6.69** ± 1.22 to **13.04** ± 2.99	Yes
Ketchup	**23.52** ± 1.24 to **27.2** ± 0.97	**18.80** ± 0.31 to **82.48** ± 3.52	Yes (Partially)

Table 4.3. Pointwise 95% Confidence Interval of the shear moduli data obtained from Brookfield YR-I and StressTech and agreement between

Material	StressTech	Brookfield	Agreement
10% Polyacrylamide	**1700** to **1800**	**825.47** ± 65.43 to **1736**.94 to 99.22	Yes
5% Polyacrylamide	**700**	**216.26** ± 21.81 to **955.39** ± 299.72	Yes
4% Gelatin	**156.09** ± 2.29 to **160.35** ± 2.09	**147.41** ± 19.82 to **243.86** ± 91.26	Yes
1.75% Gelatin	**8.27** ± 0.15 to **10.46** ± 1.32	**8.07** ± 0.69 to **9.73** ± 0.99	Yes
1.5% Gelatin	**1.82** ± 0.07 to **3.84** ± 0.25	**2.68** ± 1.21 to **10.78** ± 7.42	Yes
Gelatin Snacks	**5.33** ± 0.14 to **6.26** ± 0.16	**7.03** ± 1.04 to **8.25** ± 3.95	Yes
Yogurt	**68.78** ± 2.20 to **82.37** ± 2.85	**4.57** ± 1.04 to **5.90** ± 1.11	No
Salad Dressing	**29.35** ± 0.42 to **45.65** ± 0.29	**3.24** ± 0.25 to **3.74** ± 0.36	No
Peanut Butter	**395.98** ± 155.19 to **583.34** ± 081.28	**148.34** ± 18.34 to **493.92** ± 426.40	Yes
Grape Jelly	**94.09** ± 0.87 to **125.58** ± 0.78	**5.62** ± 0.69 to **8.99** ± 1.05	No
Ketchup	**145.06** ± 14.83 to **201.10** ± 08.66	**0.93** ± 0.62 to **3.74** ± 0.36	No

Table 4.4. Categorization of the agreement between data obtained from Brookfield YR-I and StressTech
"Yes": Agreement between the Brookfield YR-I and StressTech
"No": Disagreement between the Brookfield YR-I and StressTech

Phase Angle / Shear Moduli	Low (1 – 5)	Medium (5 – 15)	High (15 – 25)
Low (1 – 10)	---	**Yes** (Gelatin Snacks)	**Yes** (1.5% Gelatin)
Medium (10 – 100)	---	**Yes** (1.75% Gelatin)	No (Salad Dressing, Yogurt)
High (100 – 1000)	**Yes** (10% and 5% Polyacrylamide, 4% Gelatin)	No (Grape Jelly)	No (Ketchup, Peanut Butter)

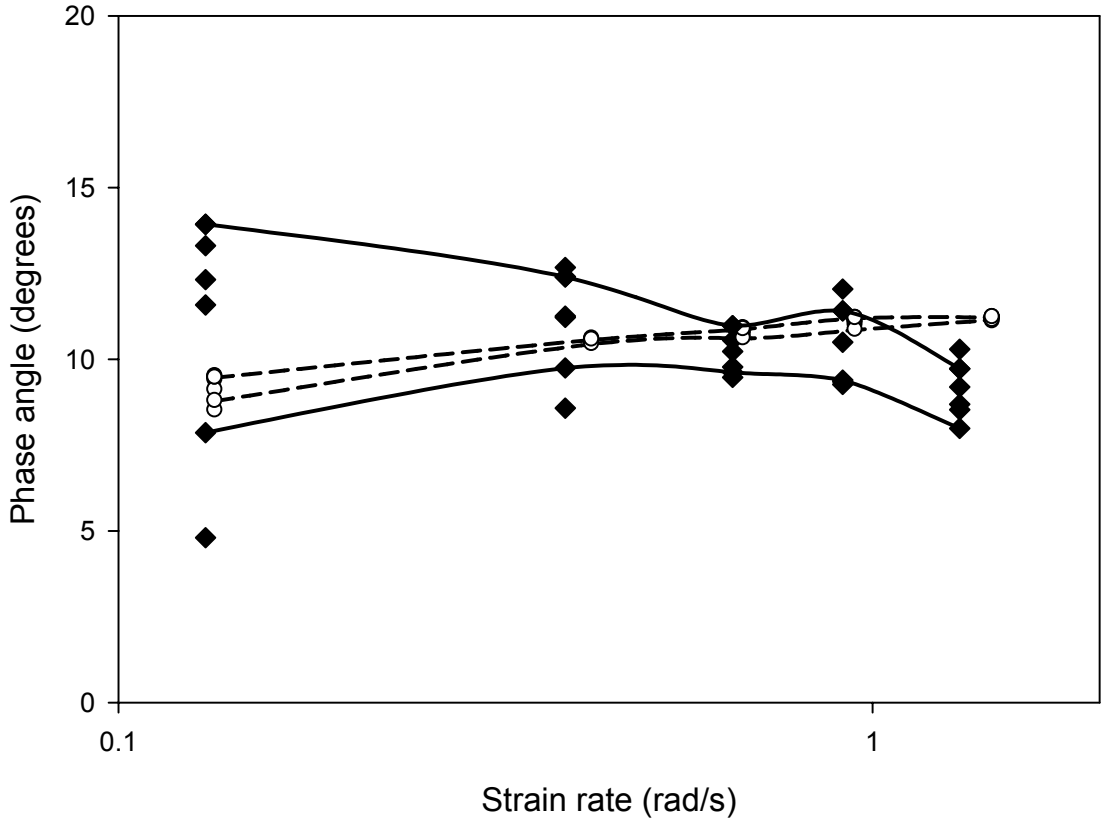


Fig 4.1a. Phase Angle Data for Jell-o (Gelatin Snacks); ○ Stress Tech phase angles; ◆ Brookfield phase angles; –○– Stress Tech confidence limits; –◆– Brookfield confidence limits

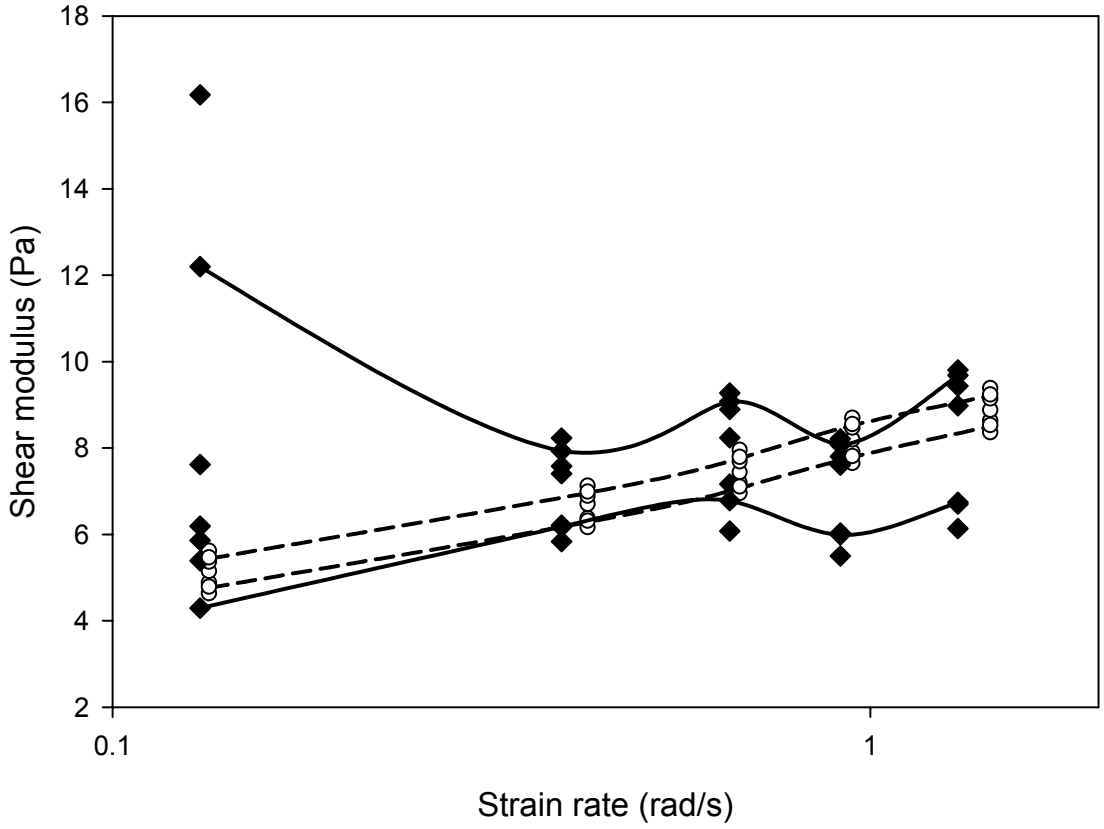


Fig 4.1b. Shear Moduli Data for Jell-o (Gelatin Snacks); ○ Stress Tech shear moduli; ◆ Brookfield shear moduli; —○— Stress Tech confidence limits; —◆— Brookfield confidence limits

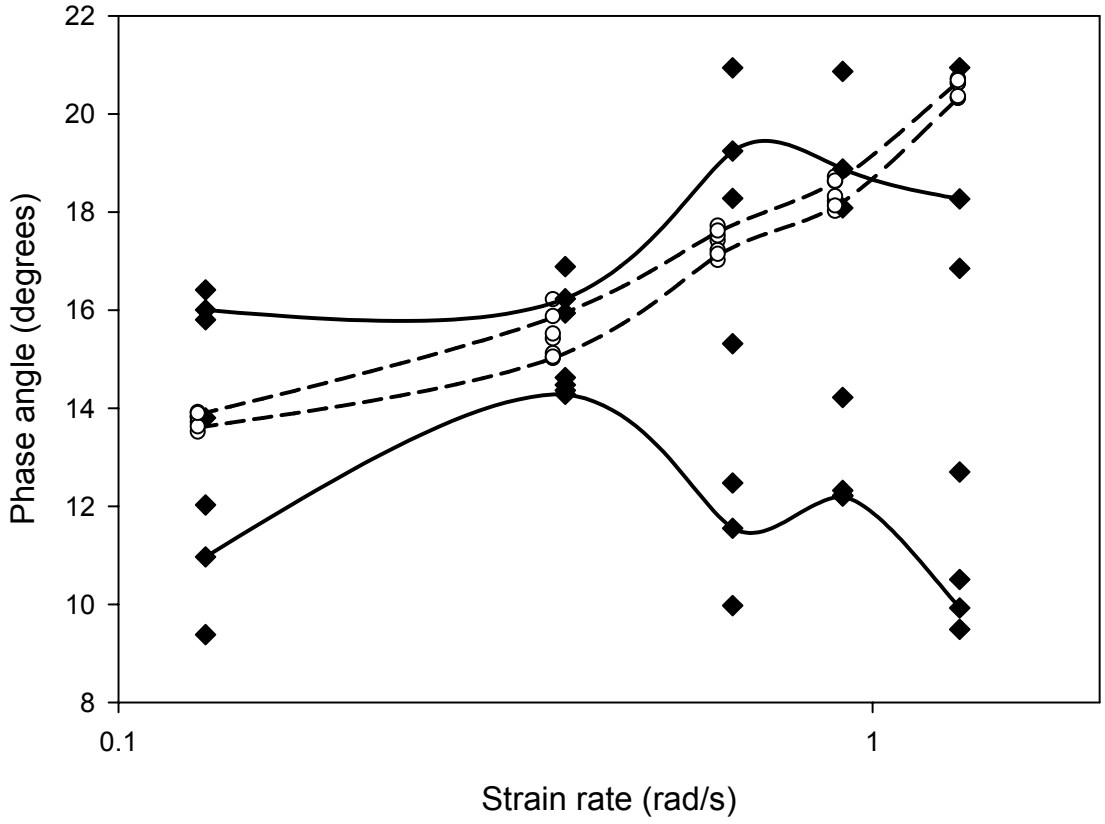


Fig 4.2a Phase Angle Data for Yogurt; ○ Stress Tech phase angles;
◆ Brookfield phase angles; —○— Stress Tech confidence limits;
—◆— Brookfield confidence limits

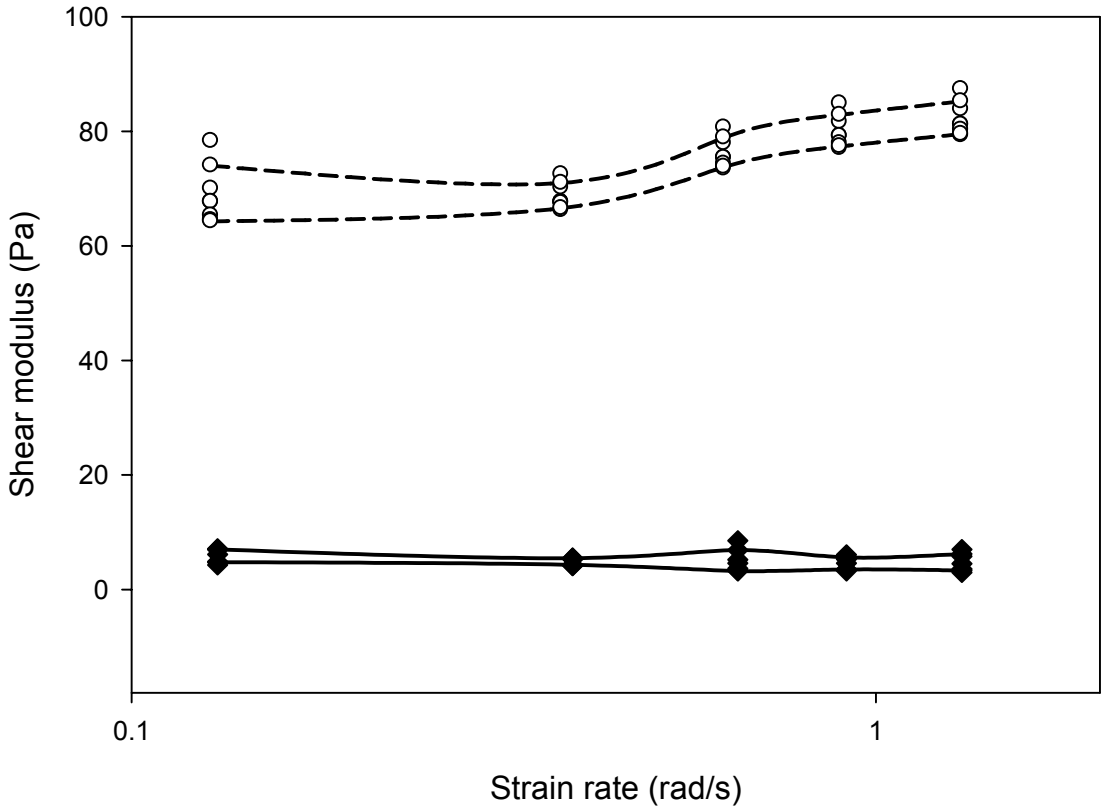


Fig 4.2b Shear Moduli Data for Yogurt; ○ Stress Tech shear moduli; ◆ Brookfield shear moduli; –○– Stress Tech confidence limits; –◆– Brookfield confidence limits

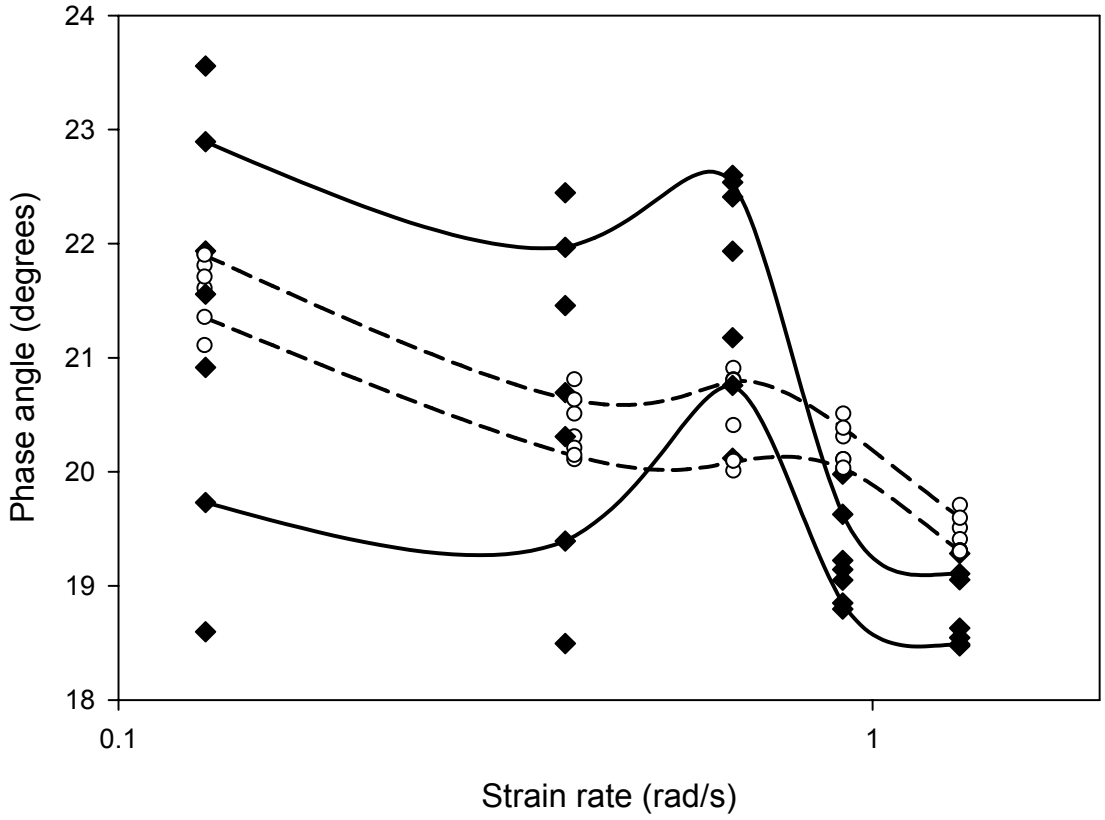


Fig 4.3a. Phase Angle Data for Salad Dressing; ○ Stress Tech phase angles; ◆ Brookfield phase angles; –○– Stress Tech confidence limits; –◆– Brookfield confidence limits

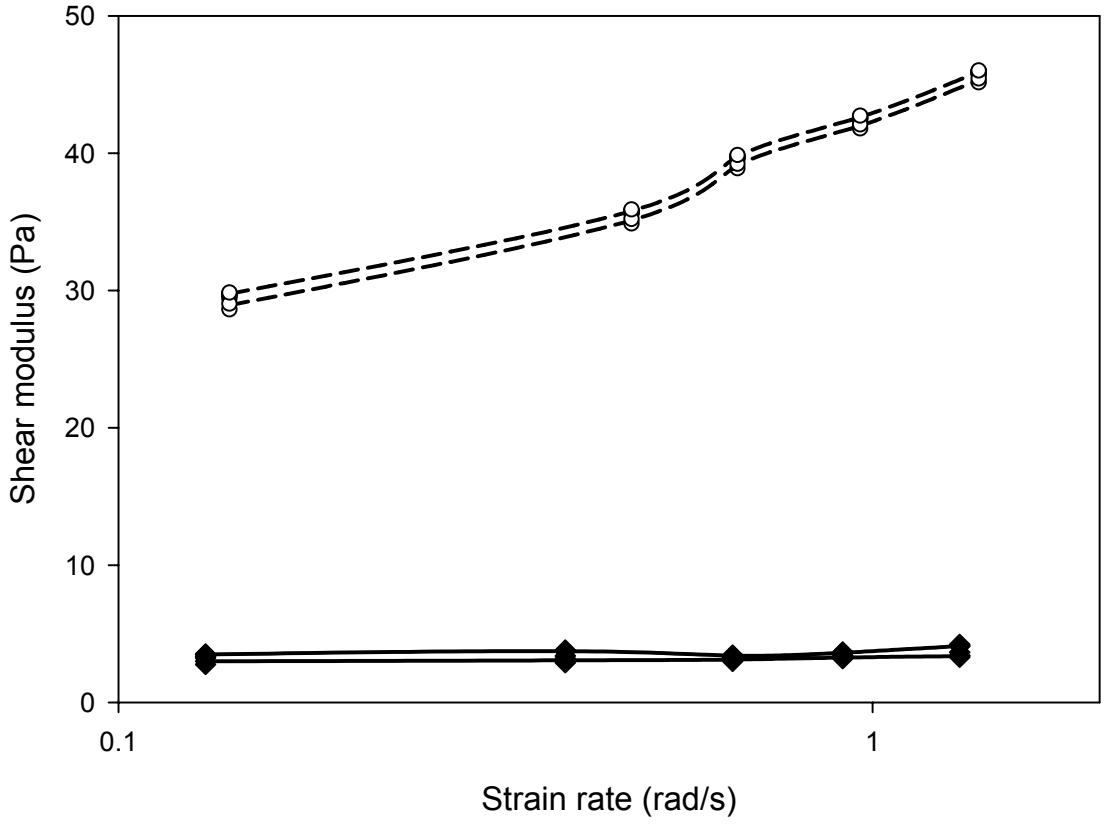


Fig 4.3b. Shear Moduli Data for Salad Dressing; ○ Stress Tech shear moduli; ◆ Brookfield shear moduli; —○— Stress Tech confidence limits; —◆— Brookfield confidence limits

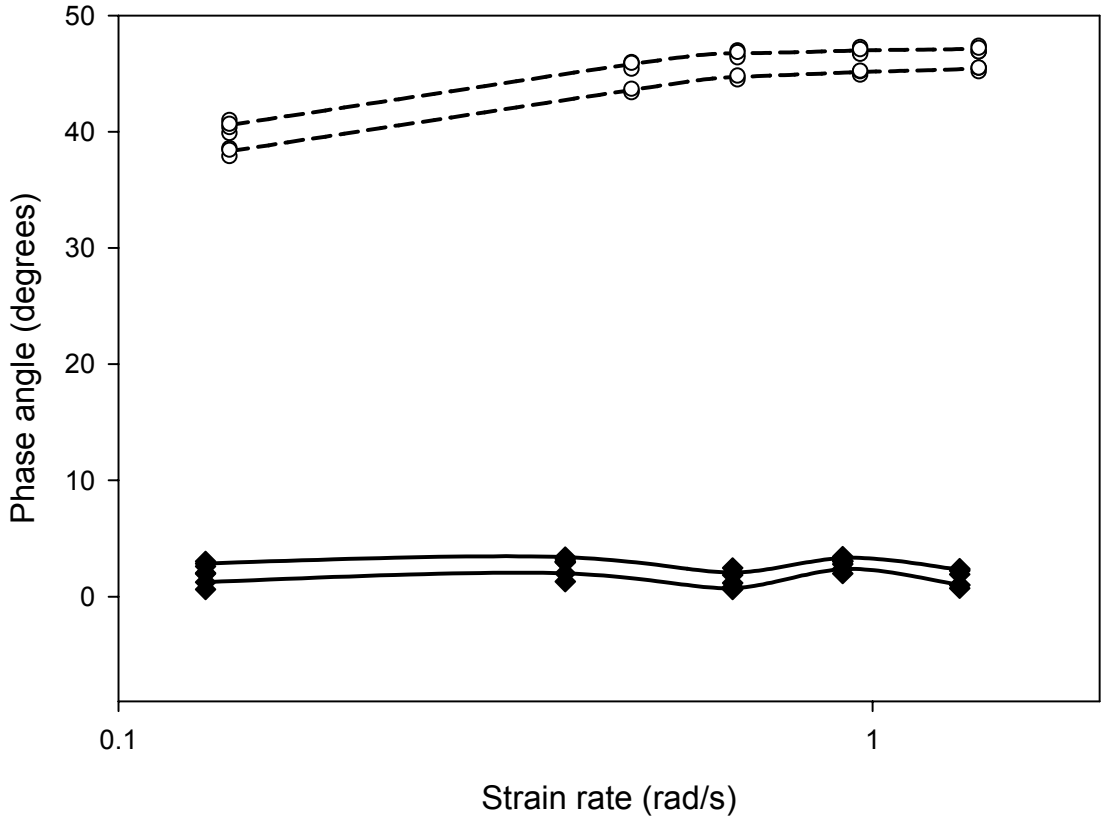


Fig 4.4a. Phase Angle Data for Peanut Butter; ○ Stress Tech phase angles; ◆ Brookfield phase angles; –○– Stress Tech confidence limits; –◆– Brookfield confidence limits

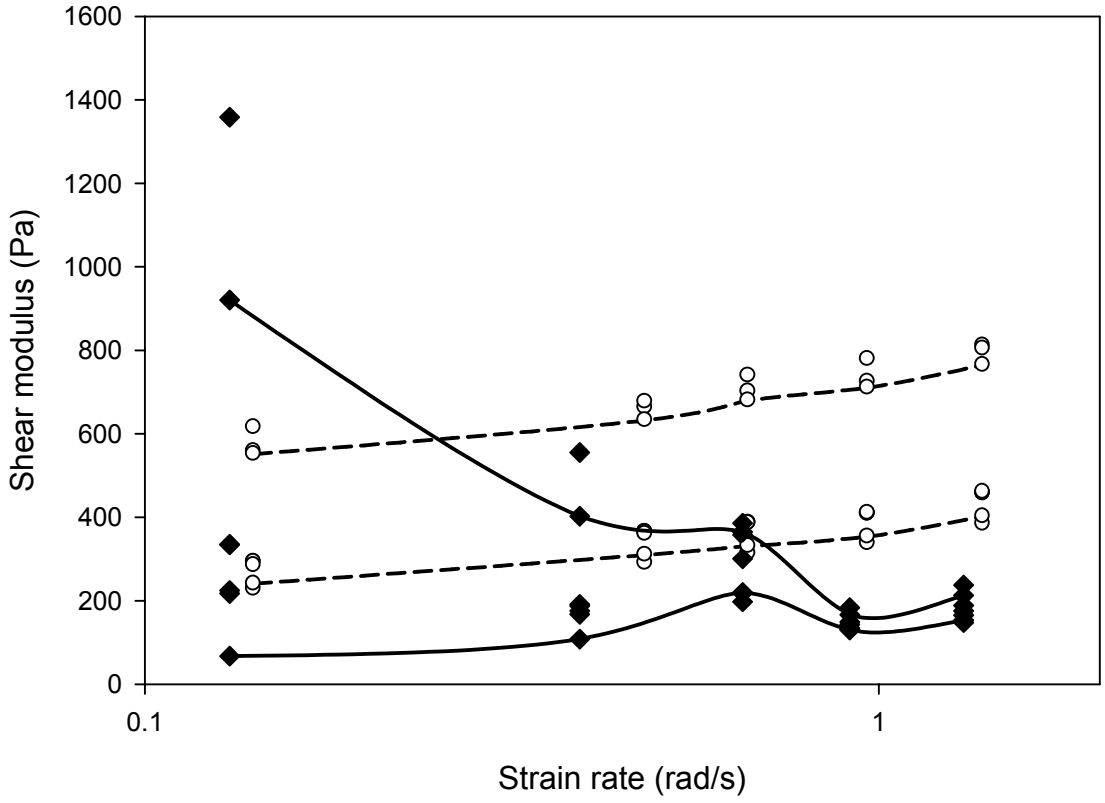


Fig 4.4b. Shear Moduli Data for Peanut Butter; ○ Stress Tech shear moduli; ◆ Brookfield shear moduli; –○– Stress Tech confidence limits; ○ Brookfield confidence limits

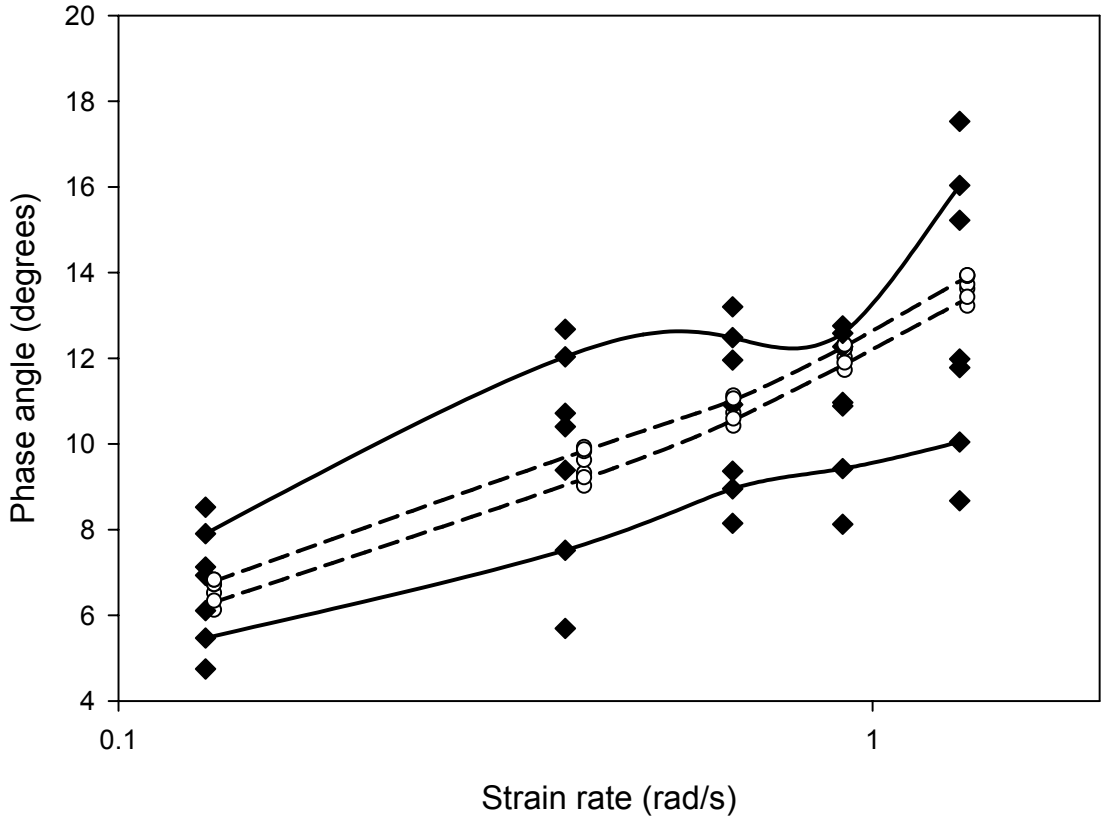


Fig 4.5a. Phase Angle Data for Grape Jelly; ○ Stress Tech phase angles; ◆ Brookfield phase angles; –○– Stress Tech confidence limits; –◆– Brookfield confidence limits

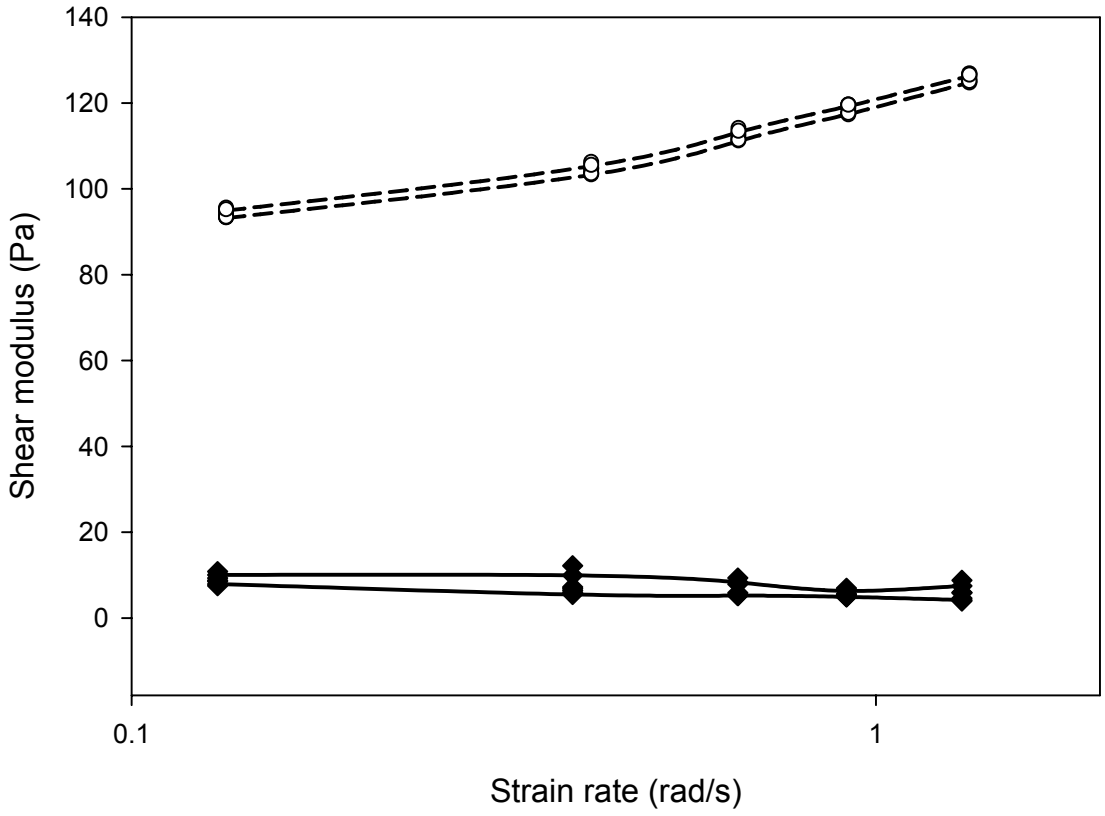


Fig 4.5b. Shear Moduli Data for Grape Jelly; ○ Stress Tech shear moduli; ◆ Brookfield shear moduli; —○— Stress Tech confidence limits; —◆— Brookfield confidence limits

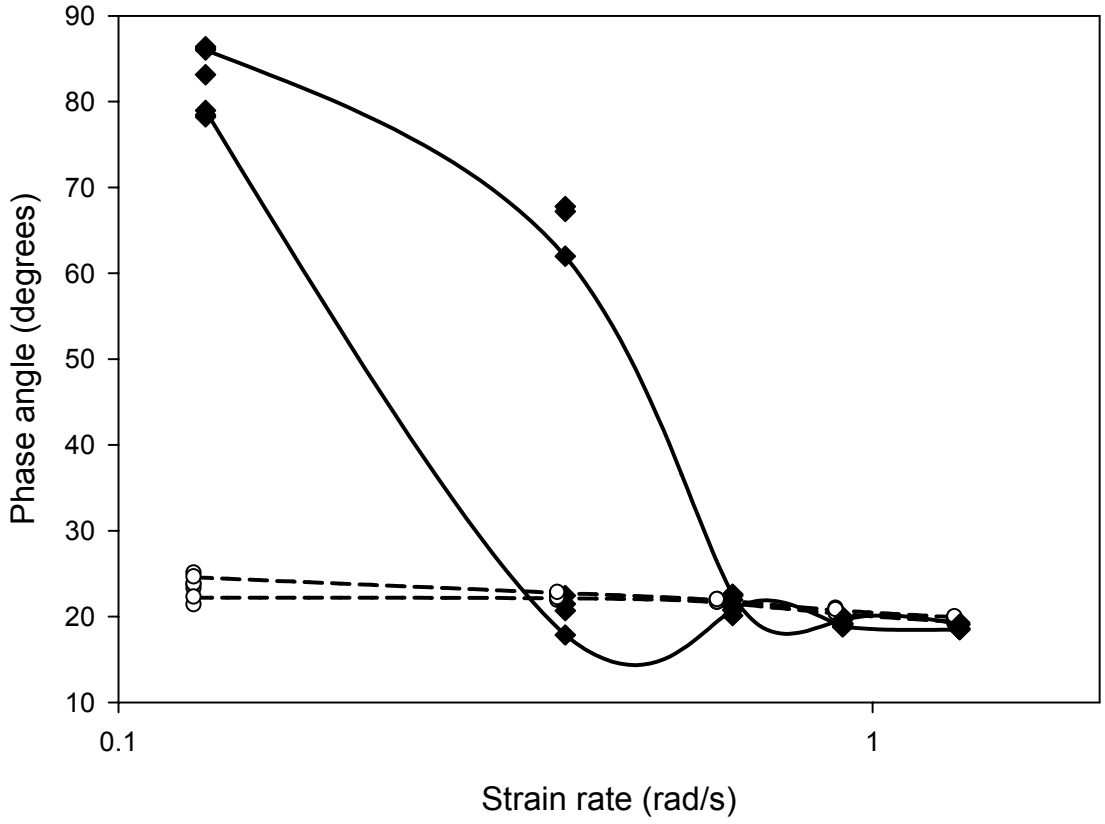


Fig 4.6a. Phase Angle Data for Ketchup; ○ Stress Tech phase angles; ◆ Brookfield phase angles; –○– Stress Tech confidence limits; –◆– Brookfield confidence limits

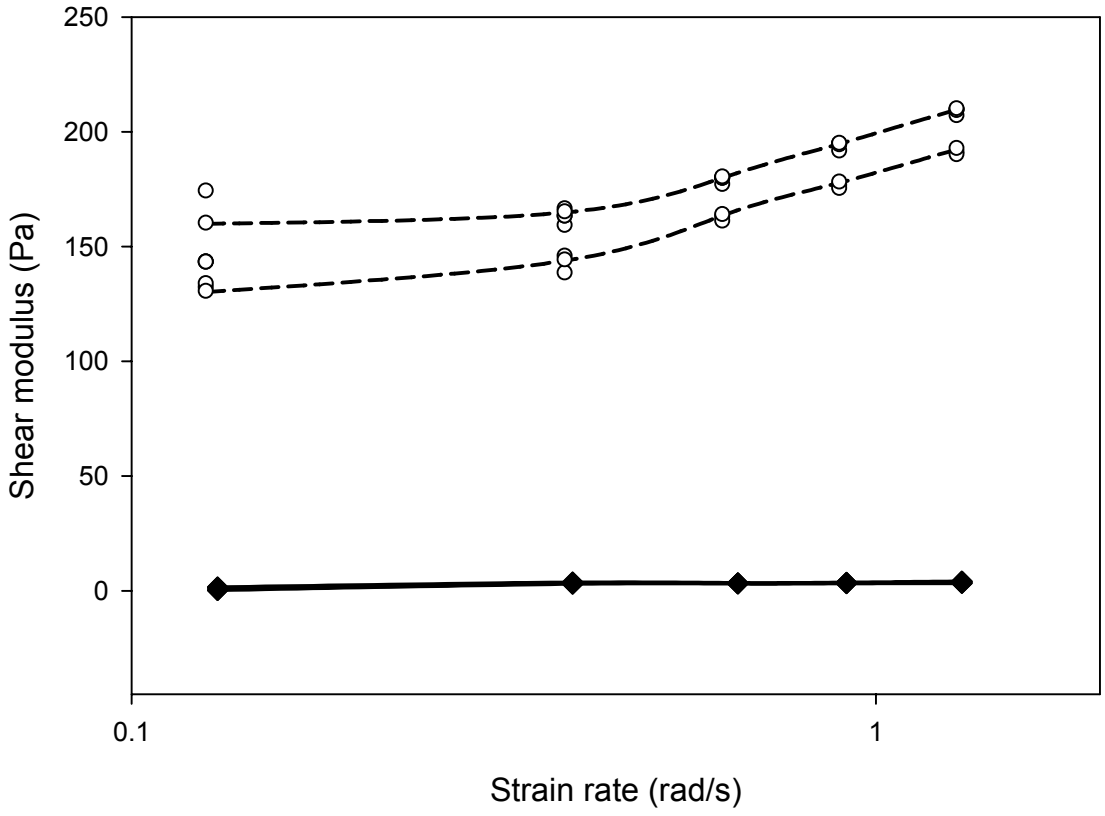


Fig 4.6b. Shear Moduli Data for Ketchup; ○ Stress Tech shear moduli; ◆ Brookfield shear moduli; –○– Stress Tech confidence limits; –◆– Brookfield confidence limits

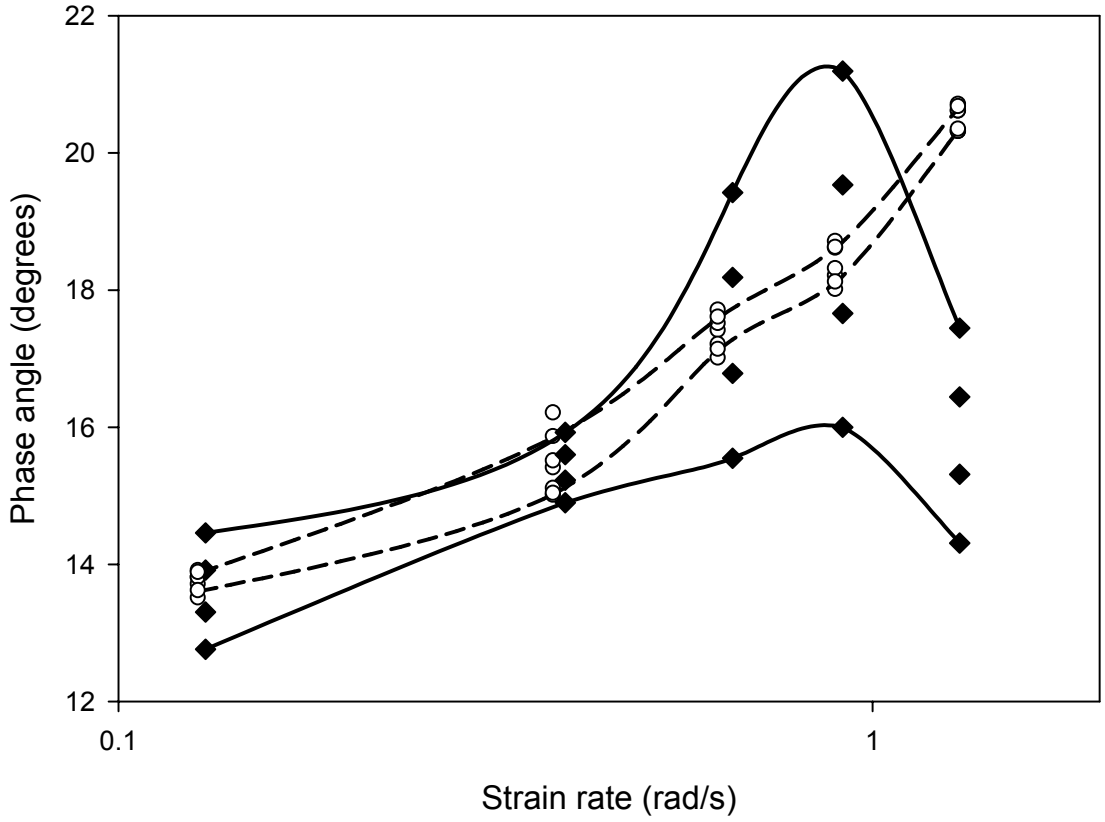


Fig 4.7a. Phase Angle Data for Yogurt in cup 5; ○ Stress Tech phase angles; ◆ Brookfield phase angles; –○– Stress Tech confidence limits; –◆– Brookfield confidence limits

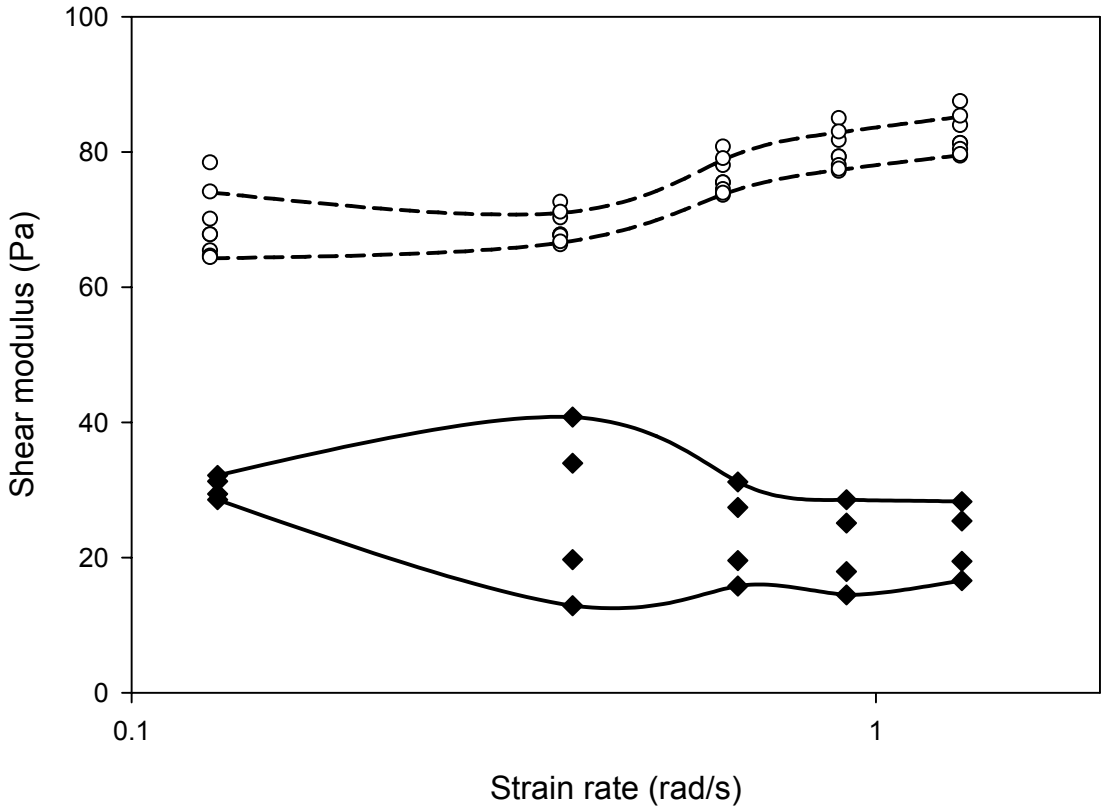


Fig 4.7b. Shear Moduli Data for Yogurt in cup 5; ○ Stress Tech shear moduli; ◆ Brookfield shear moduli; —○— Stress Tech confidence limits; —◆— Brookfield confidence limits

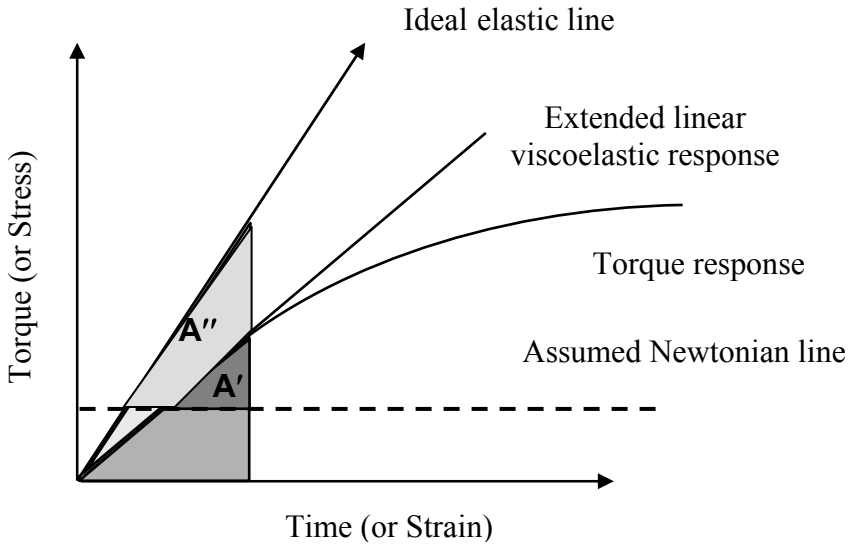


Fig. 4.8 Effect of Assumed Newtonian Line

APPENDIX

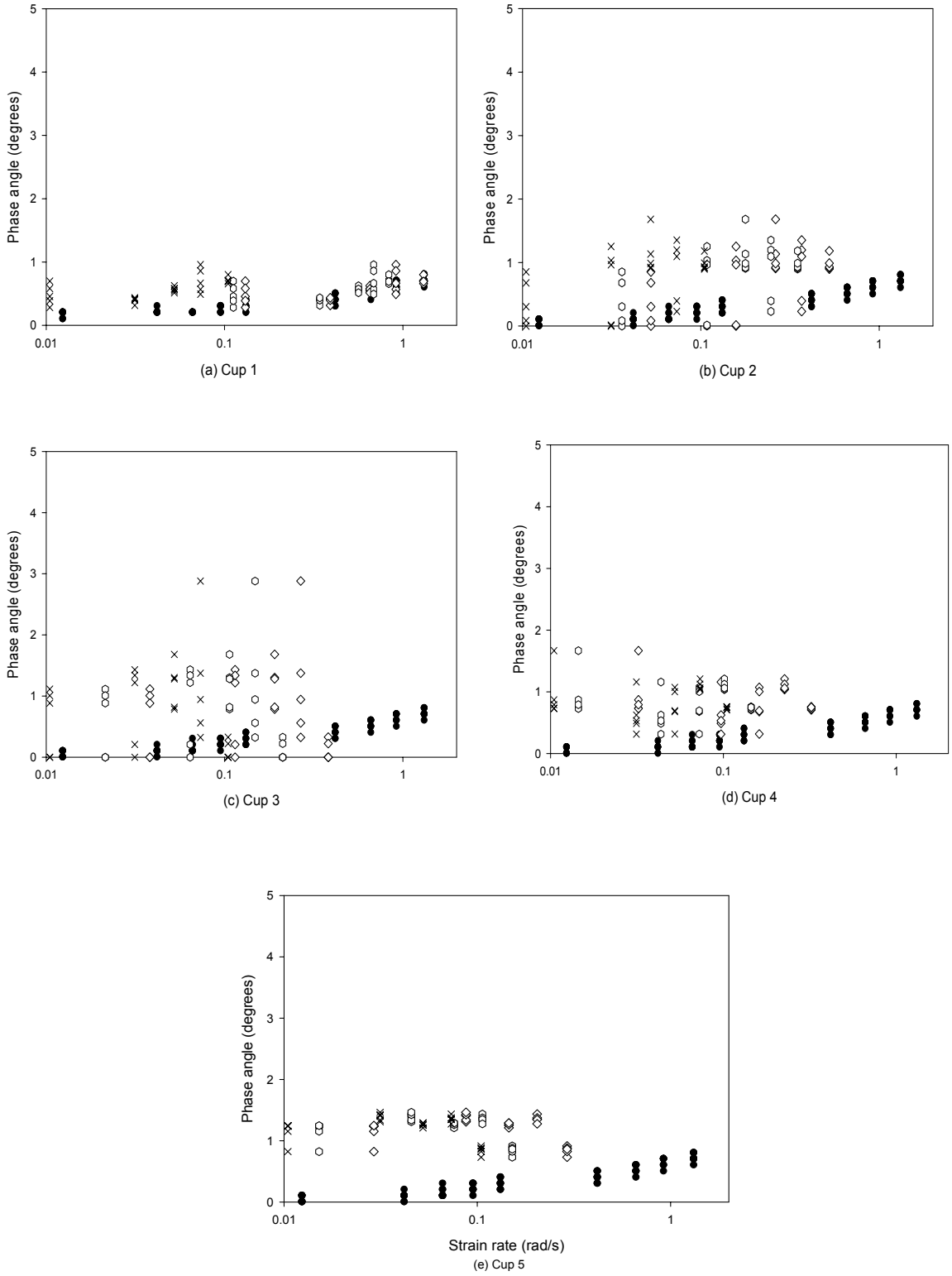


Fig. A.1 Polyacrylamide 10% gels phase angle data for various cups for all three approaches; • StressTech data;◇ Alderman approach;⎔ NCSU Approach; × Brookfield Approach

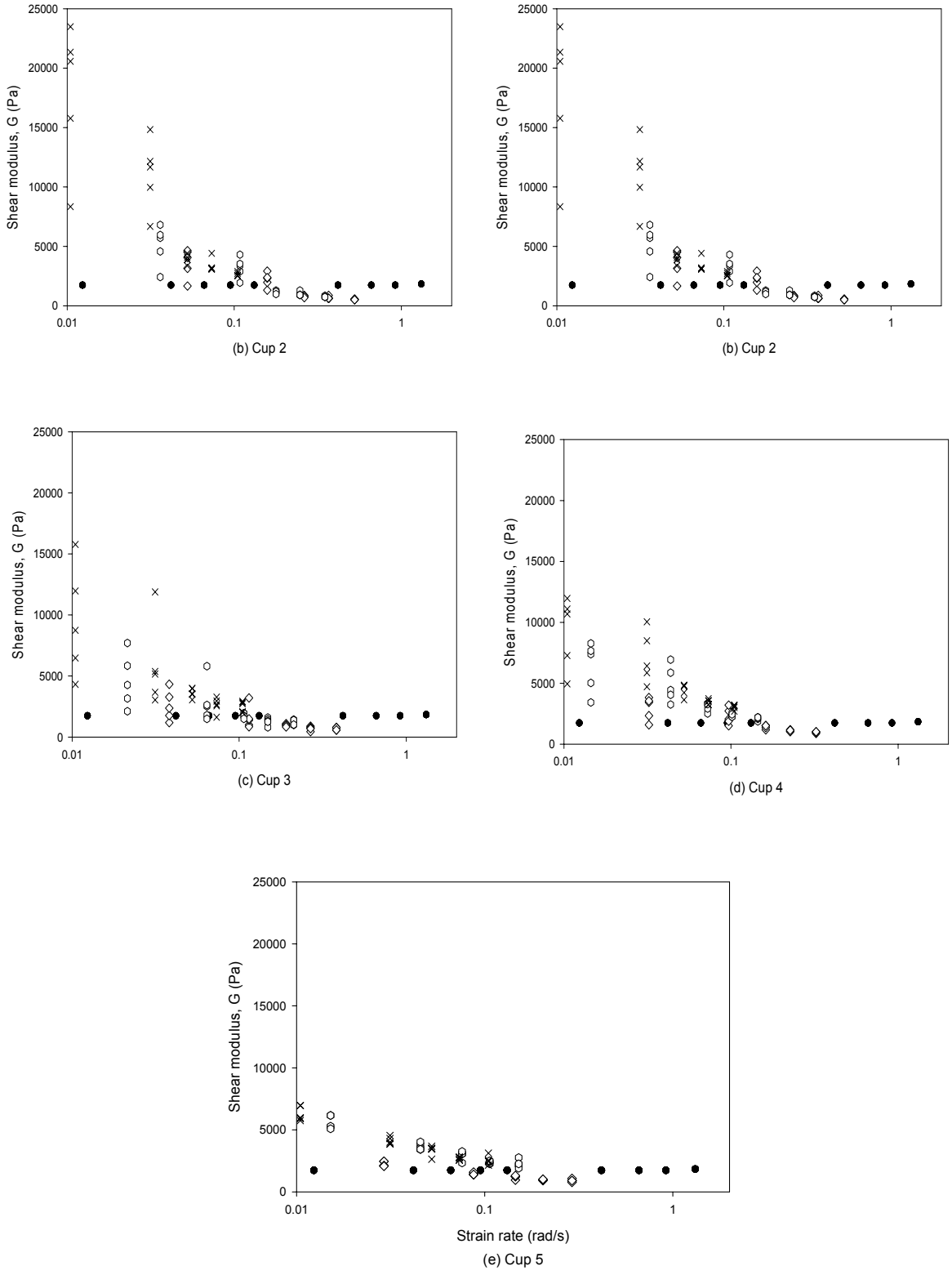


Fig. A.2 Polyacrylamide 10% gels shear moduli data for various cups for all three approaches; • StressTech data; ◇ Alderman approach; ⎔ NCSU Approach; × Brookfield Approach

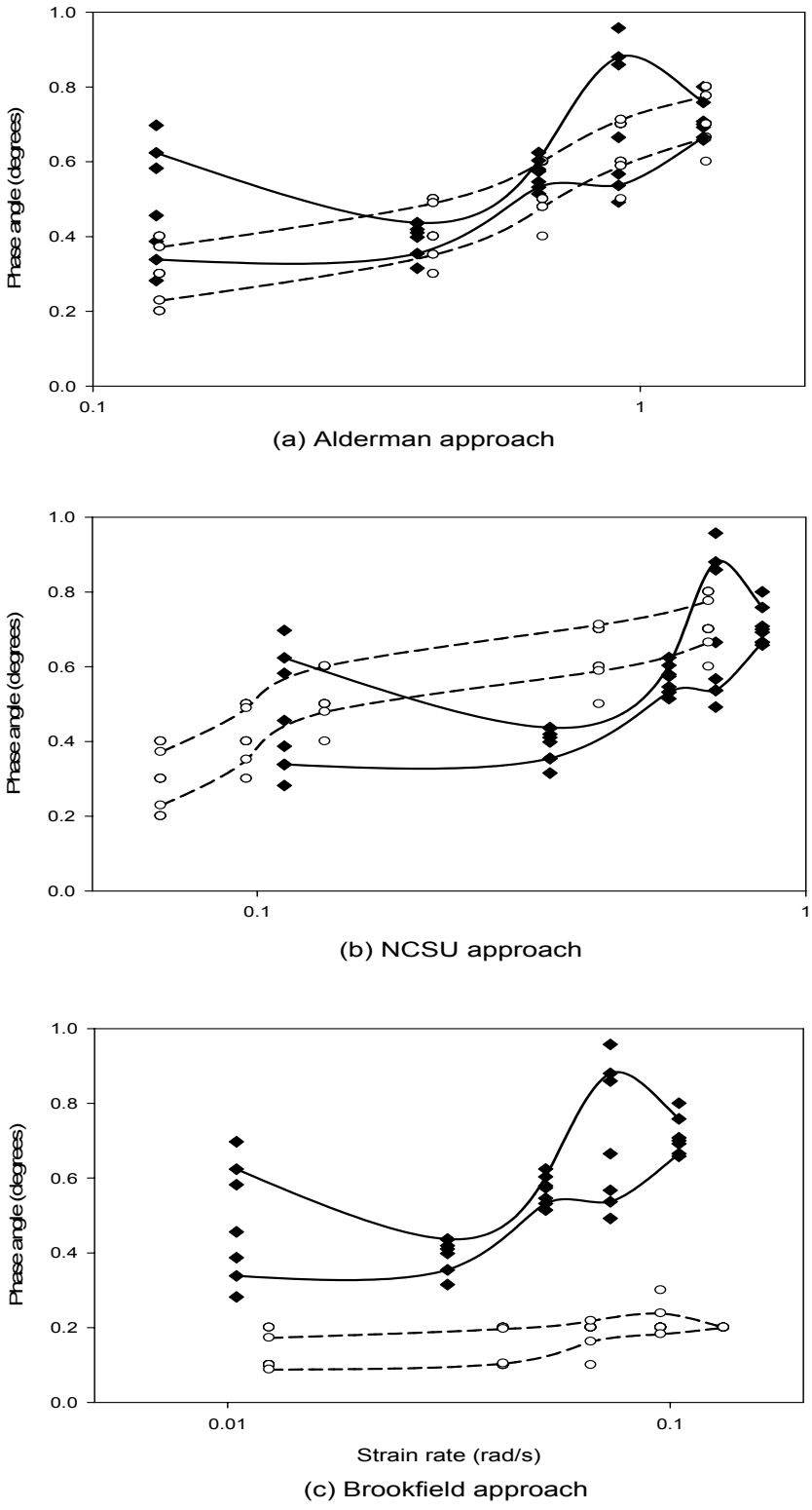


Fig. A.3 Polyacrylamide 10% phase angle data for the three approaches for cup 1; ○ StressTech data; ◆ Brookfield data; --⊖-- StressTech confidence limits; —◆— Brookfield confidence limits

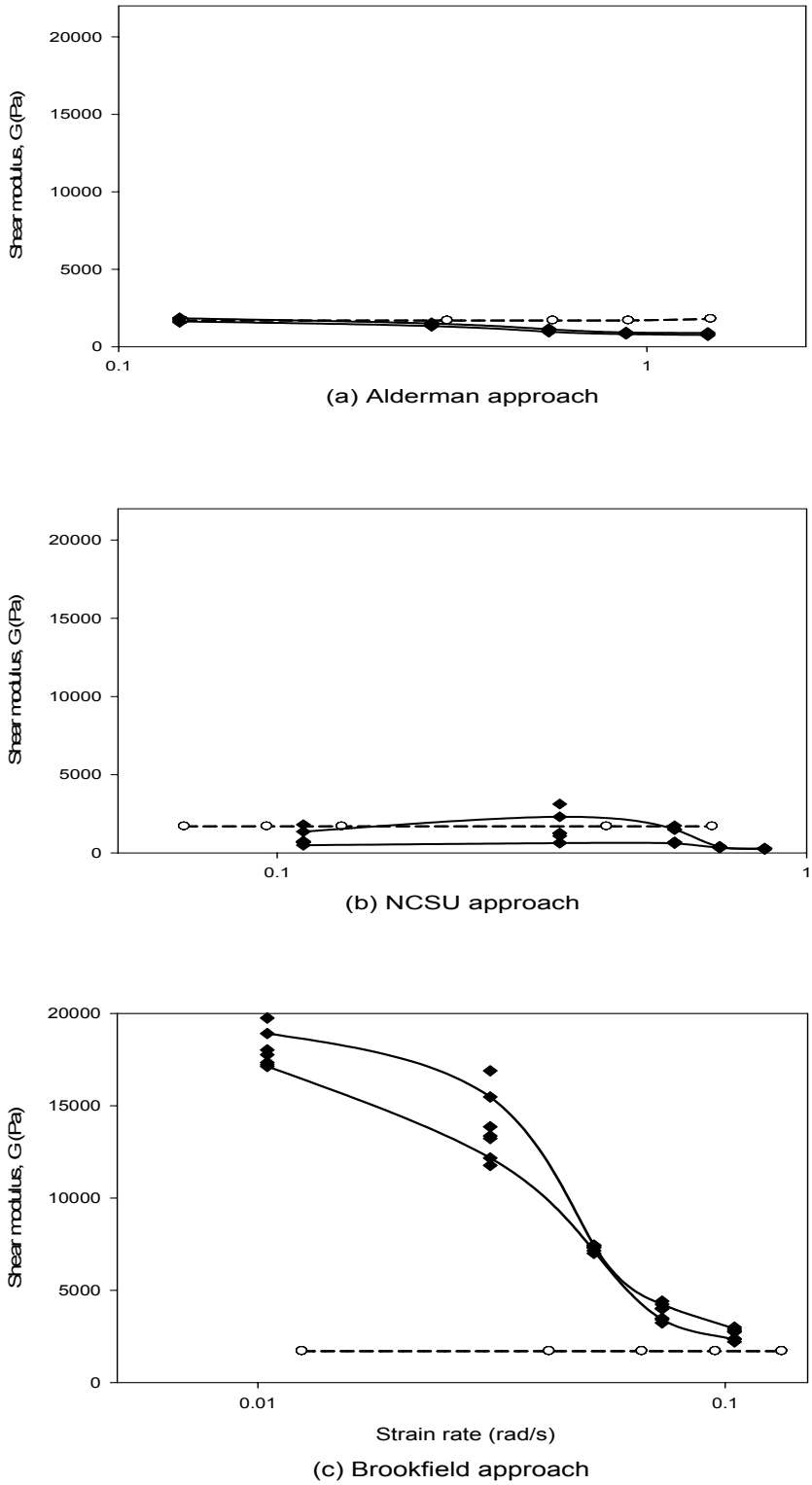


Fig. A.4 Polyacrylamide 10% shear moduli data for the three approaches for cup 1; ○ StressTech data; ◆ Brookfield data; -⊖- StressTech confidence limits; —◆— Brookfield confidence limits

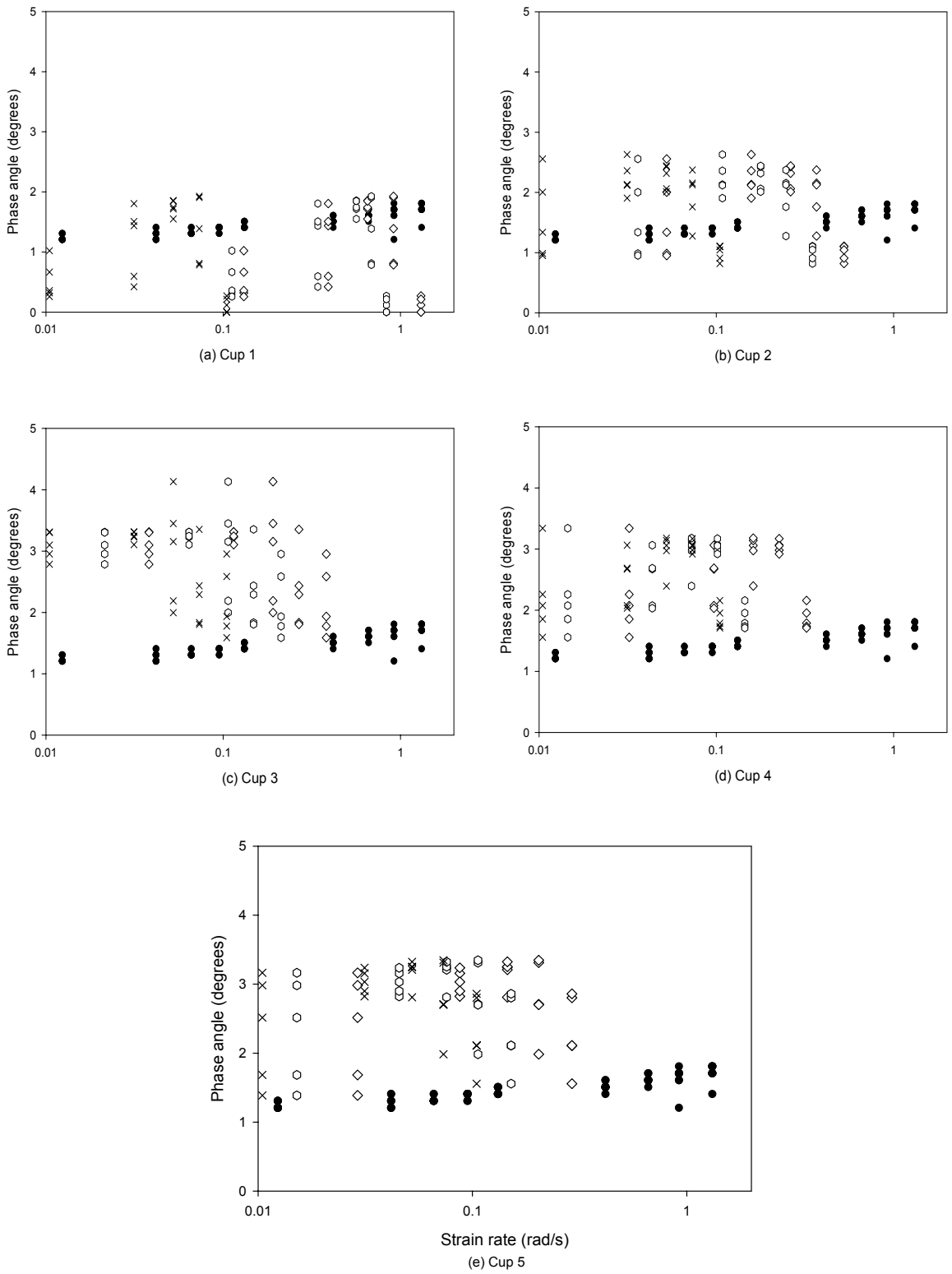


Fig. A.5 Polyacrylamide 5% phase angle data for various cups for all three approaches; • StressTech data;◇ Alderman approach;⎔ NC State Approach; × Brookfield Approach

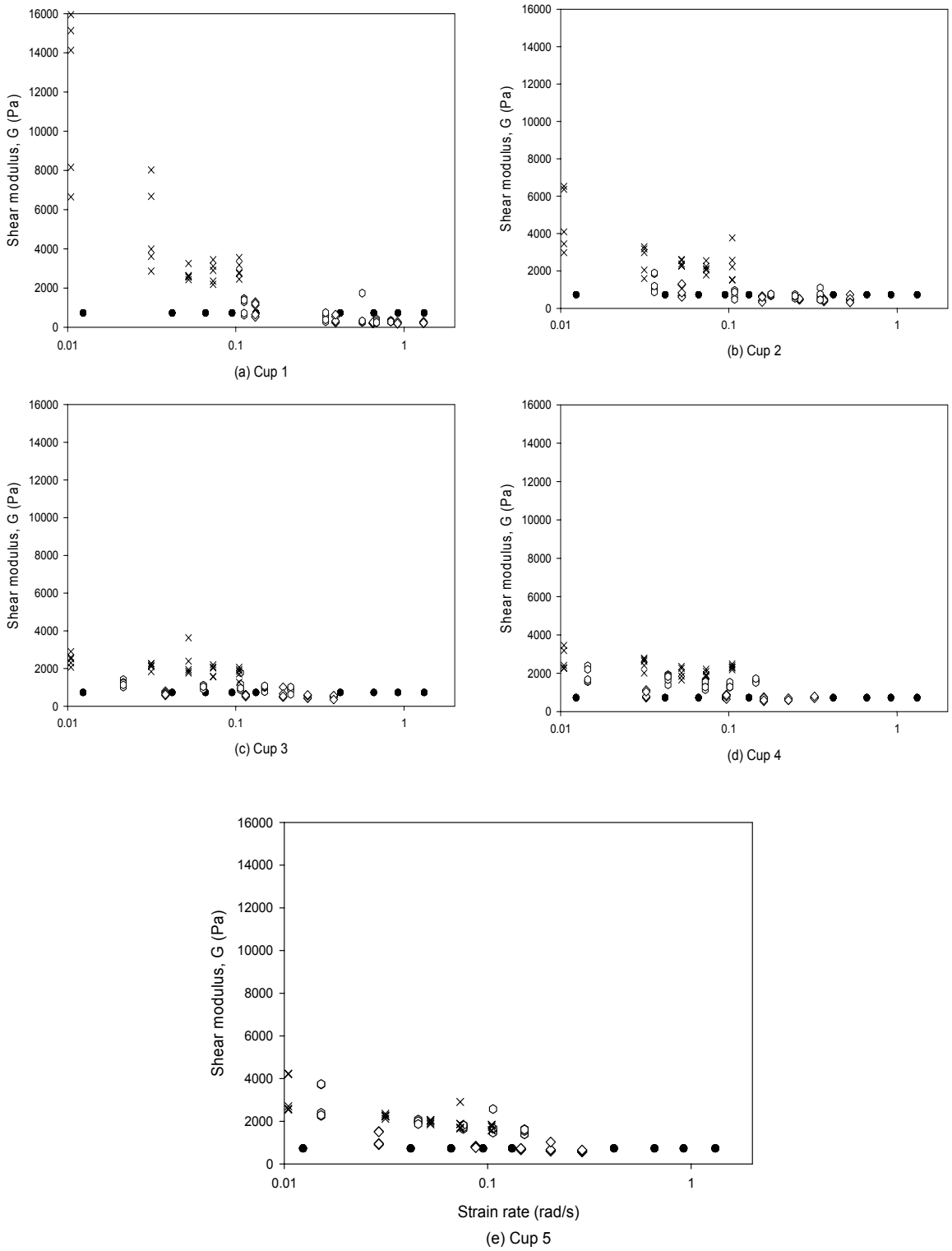
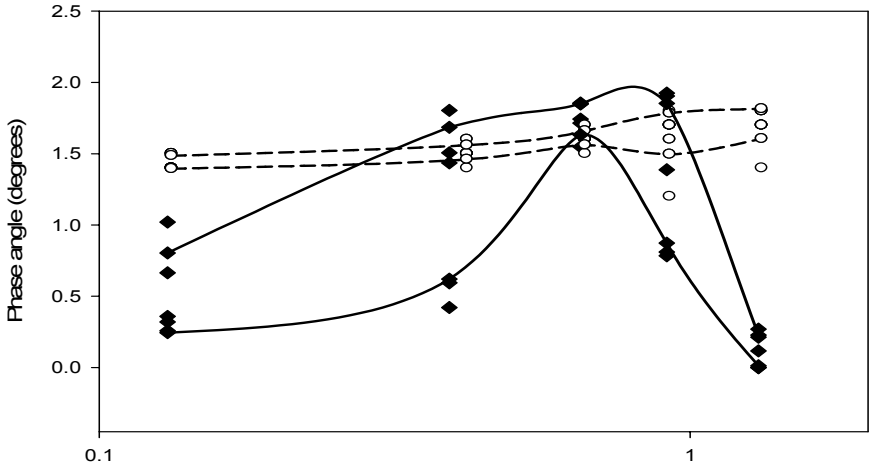
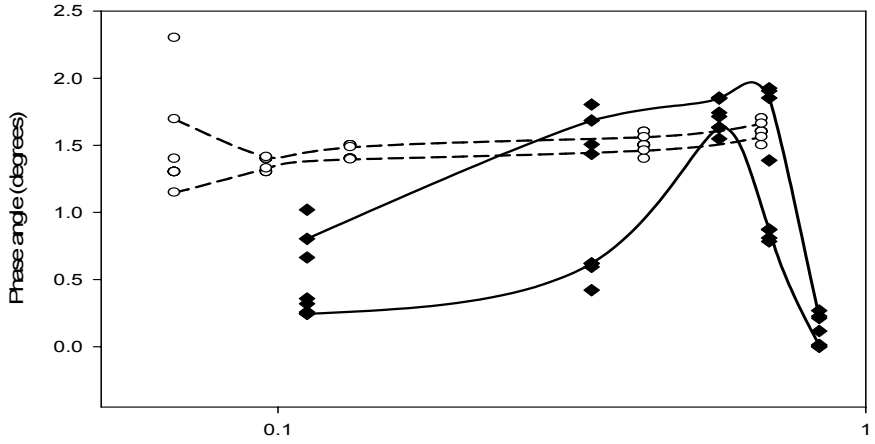


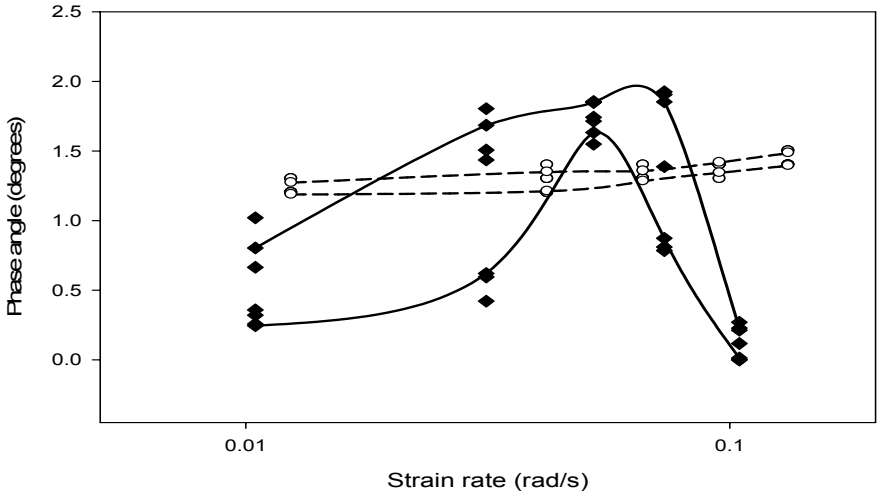
Fig. A.6 Polyacrylamide 5% shear moduli data for various cups for all three approaches; • StressTech data; ◇ Alderman approach; ⎔ NC State Approach; × Brookfield Approach



(a) Alderman approach



(b) NCSU approach



(c) Brookfield approach

Fig. A.7 Polyacrylamide 5% phase angle data for the three approaches for cup 1; ○ StressTech data; ◆ Brookfield data; -⊖- StressTech confidence limits; —◆— Brookfield confidence limits

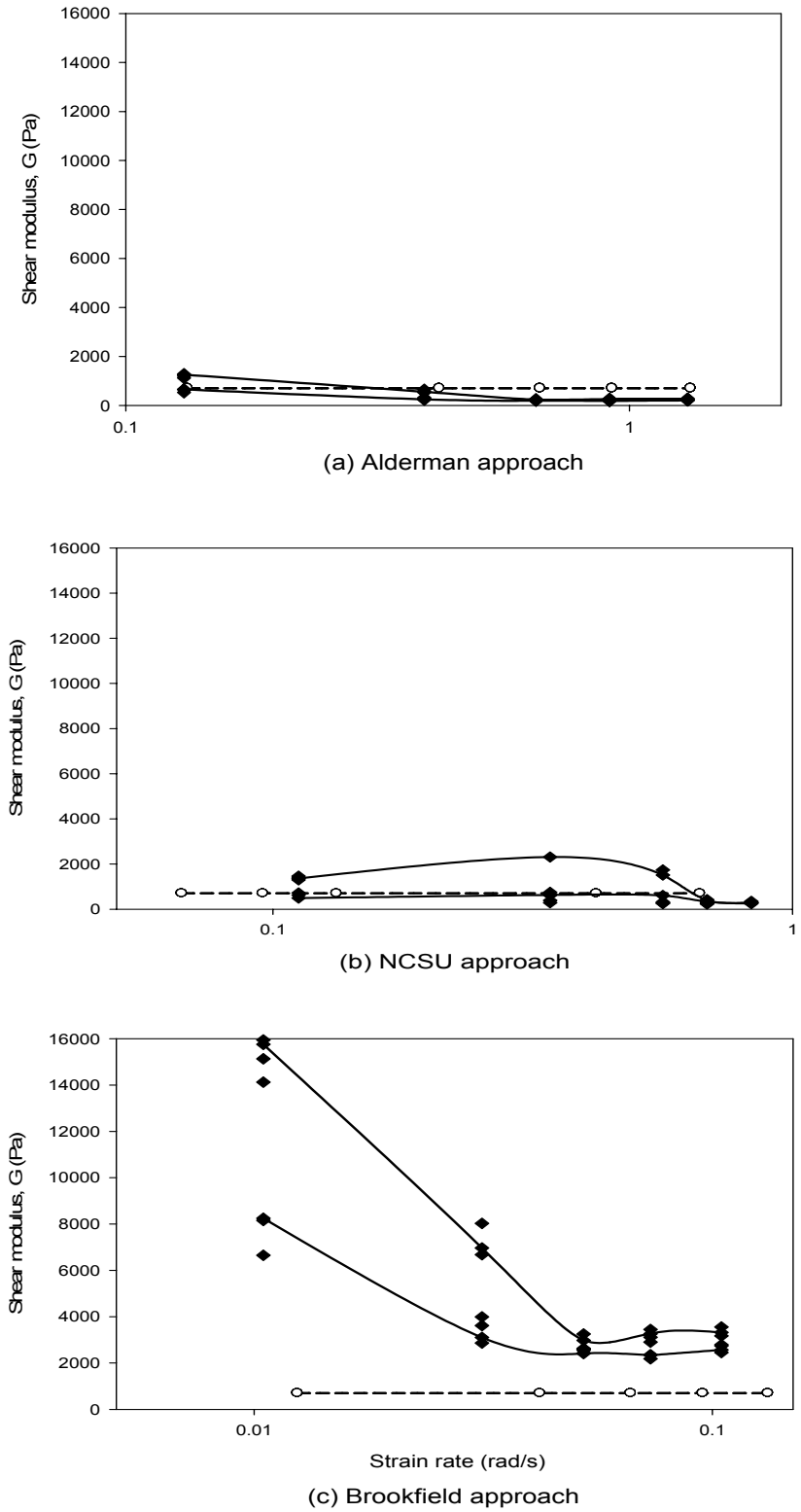


Fig. A.8 Polyacrylamide 5% shear moduli data for the three approaches for cup 1; ○ StressTech data; ◆ Brookfield data; - -⊖- - StressTech confidence limits; —◆— Brookfield confidence limits

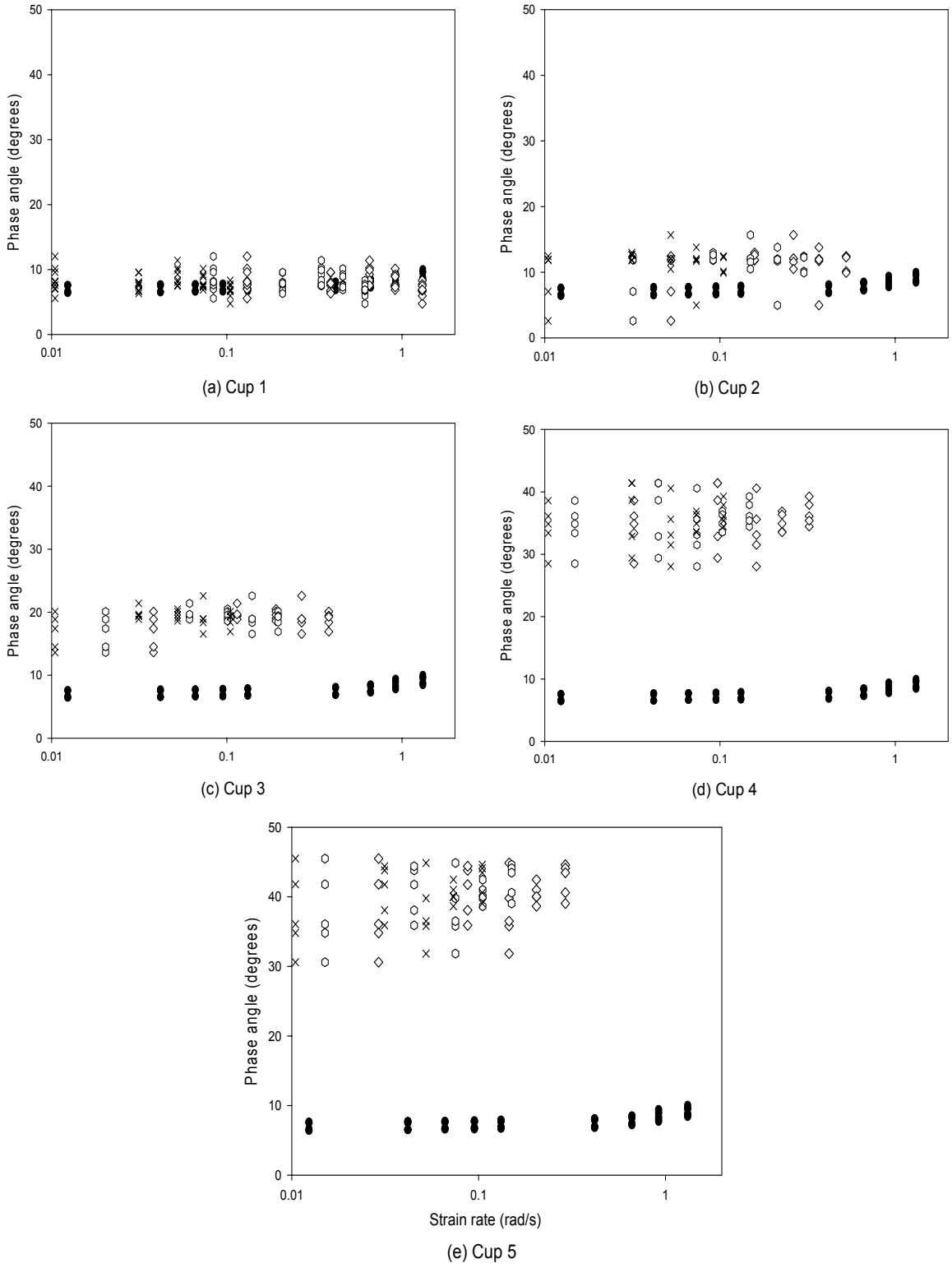


Fig. A.9 Gelatin 1.75% gels phase angle data for various cups for all three approaches; • StressTech data;◇ Alderman approach;⎔ NC State Approach; × Brookfield Approach

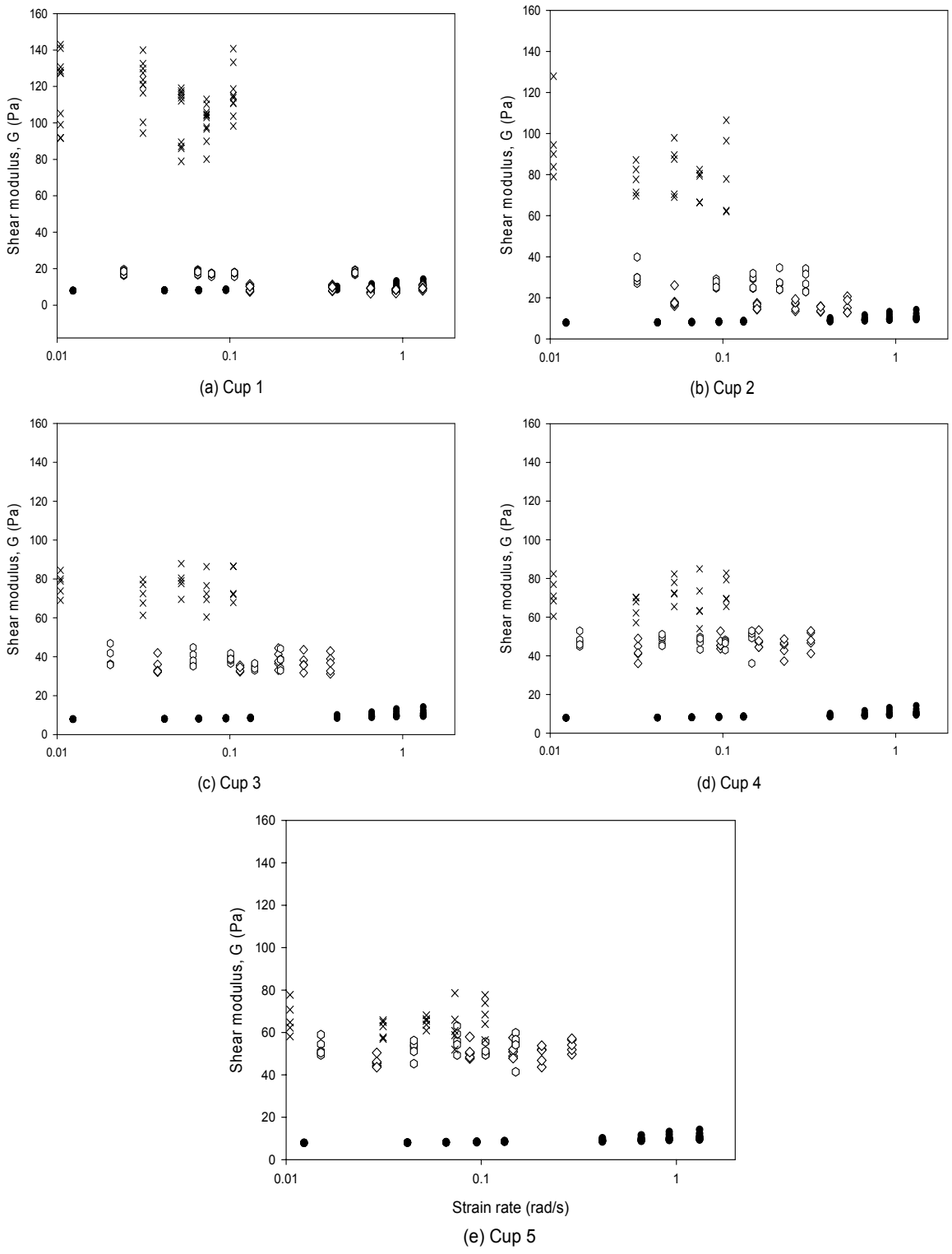


Fig. A.10 Gelatin 1.75% gels shear moduli data for various cups for all three approaches; • StressTech data; ◇ Alderman approach; ⎔ NC State Approach; × Brookfield Approach

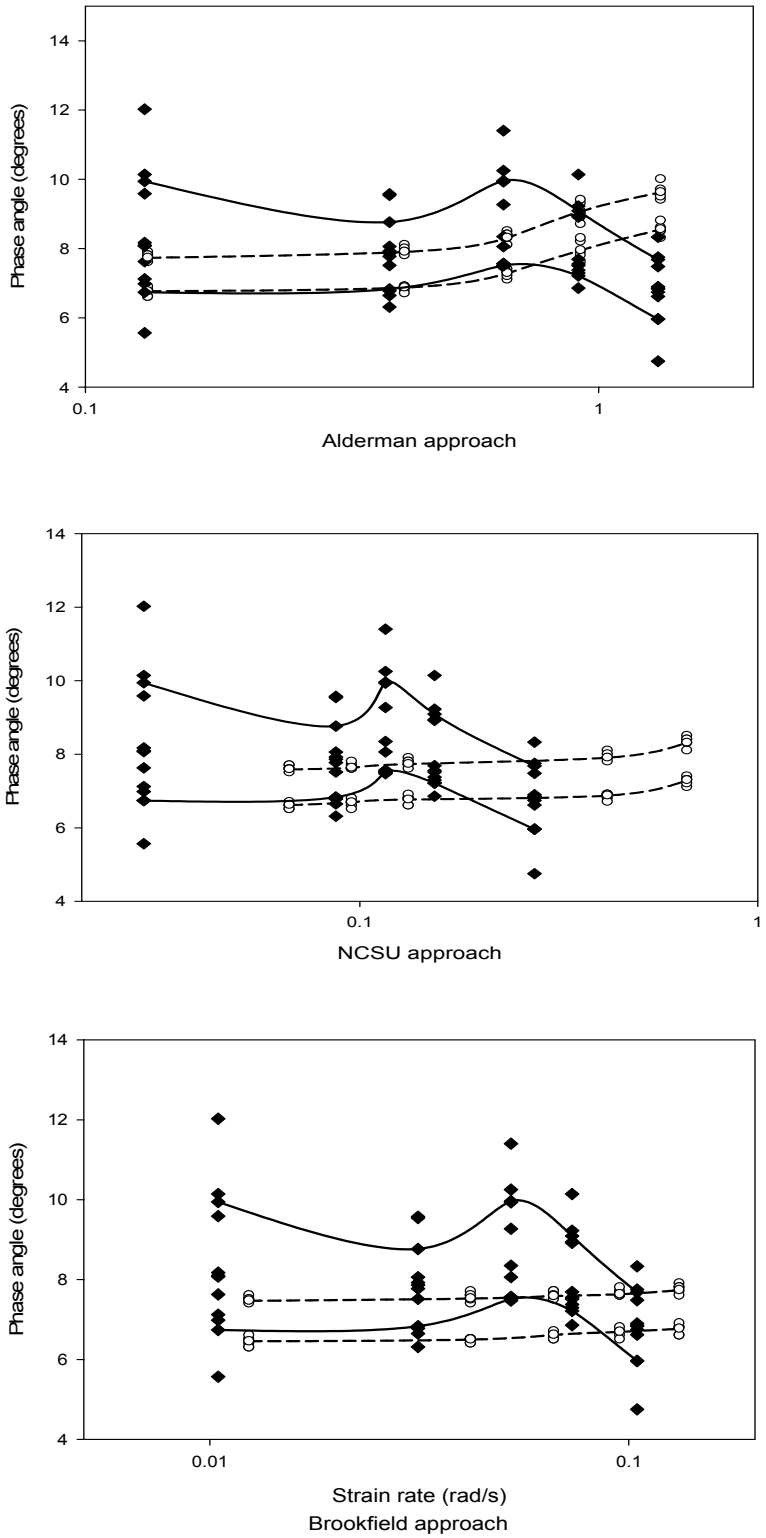


Fig. A.11 Gelatin 1.75% gels phase angle data for the three approaches for cup 1; ○ StressTech data; ◆ Brookfield data; --⊖-- StressTech confidence limits; —◆— Brookfield confidence limits

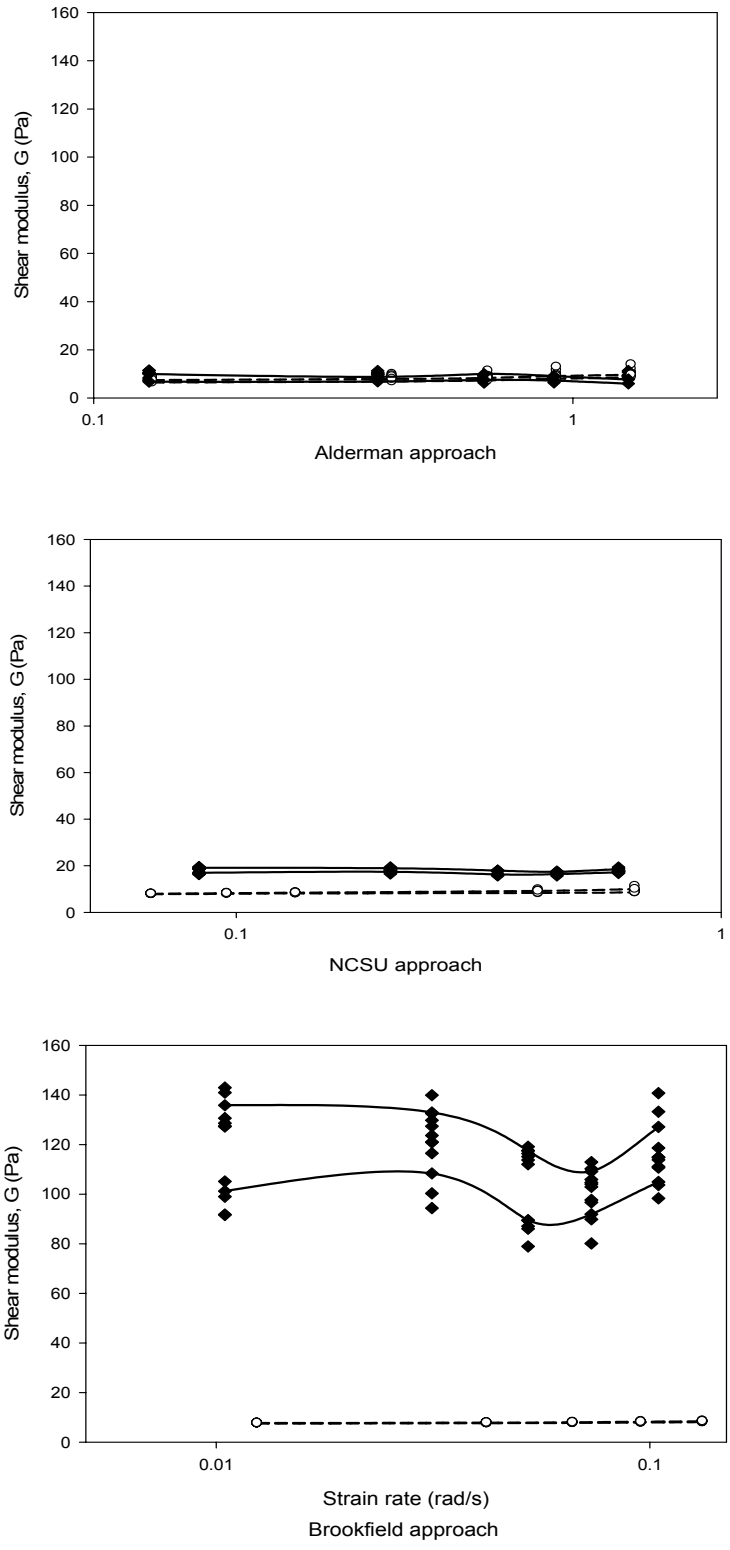


Fig. A.12 Gelatin 1.75% gels shear moduli data for the three approaches for cup 1;○ StressTech data; ◆ Brookfield data; -⊖- StressTech confidence limits; —◆— Brookfield confidence limits

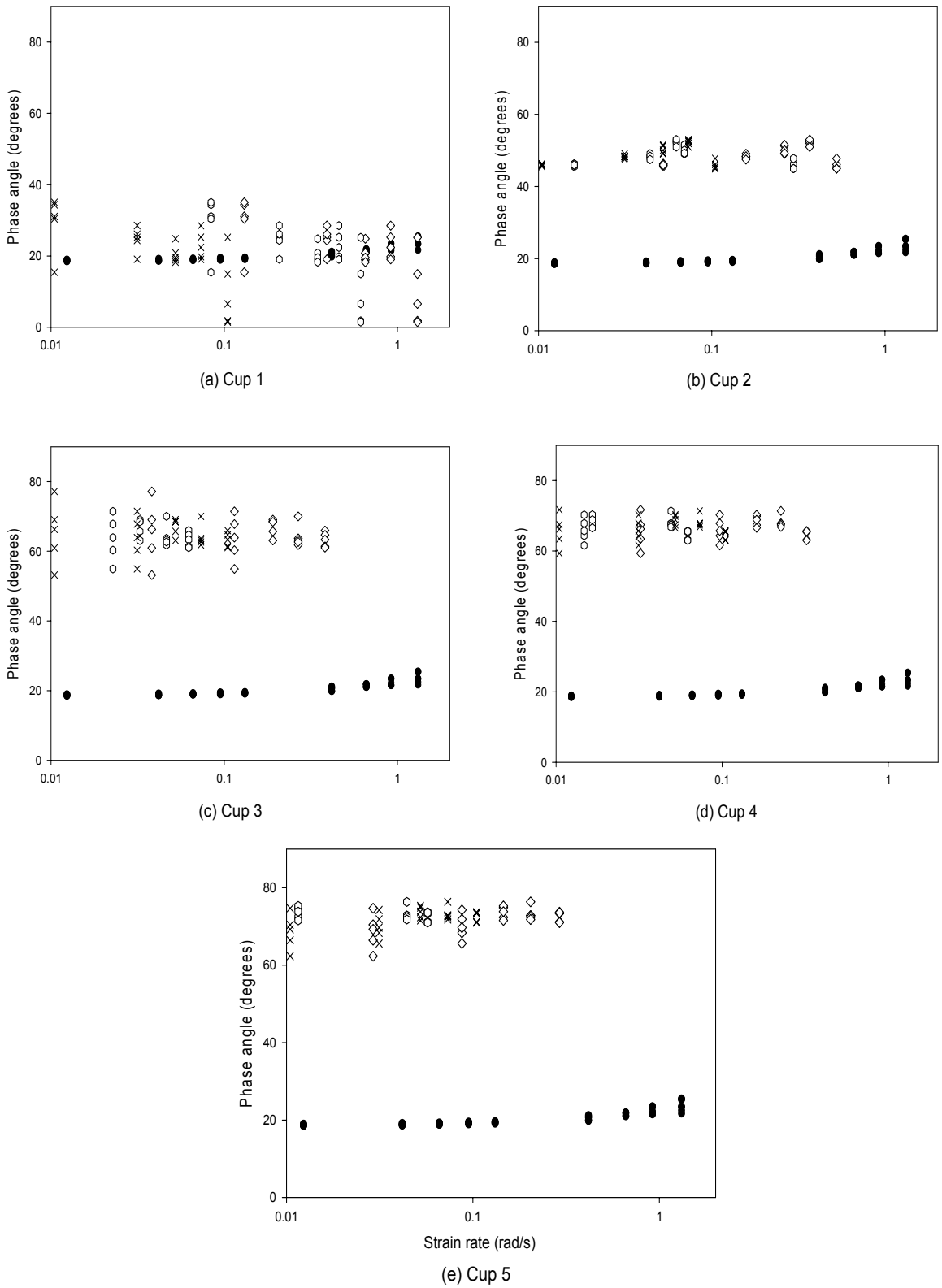


Fig. A.13 Gelatin 1.5% gels phase angle data for various cups for all three approaches; • StressTech data;◇ Alderman approach;⎔ NC State Approach; × Brookfield Approach

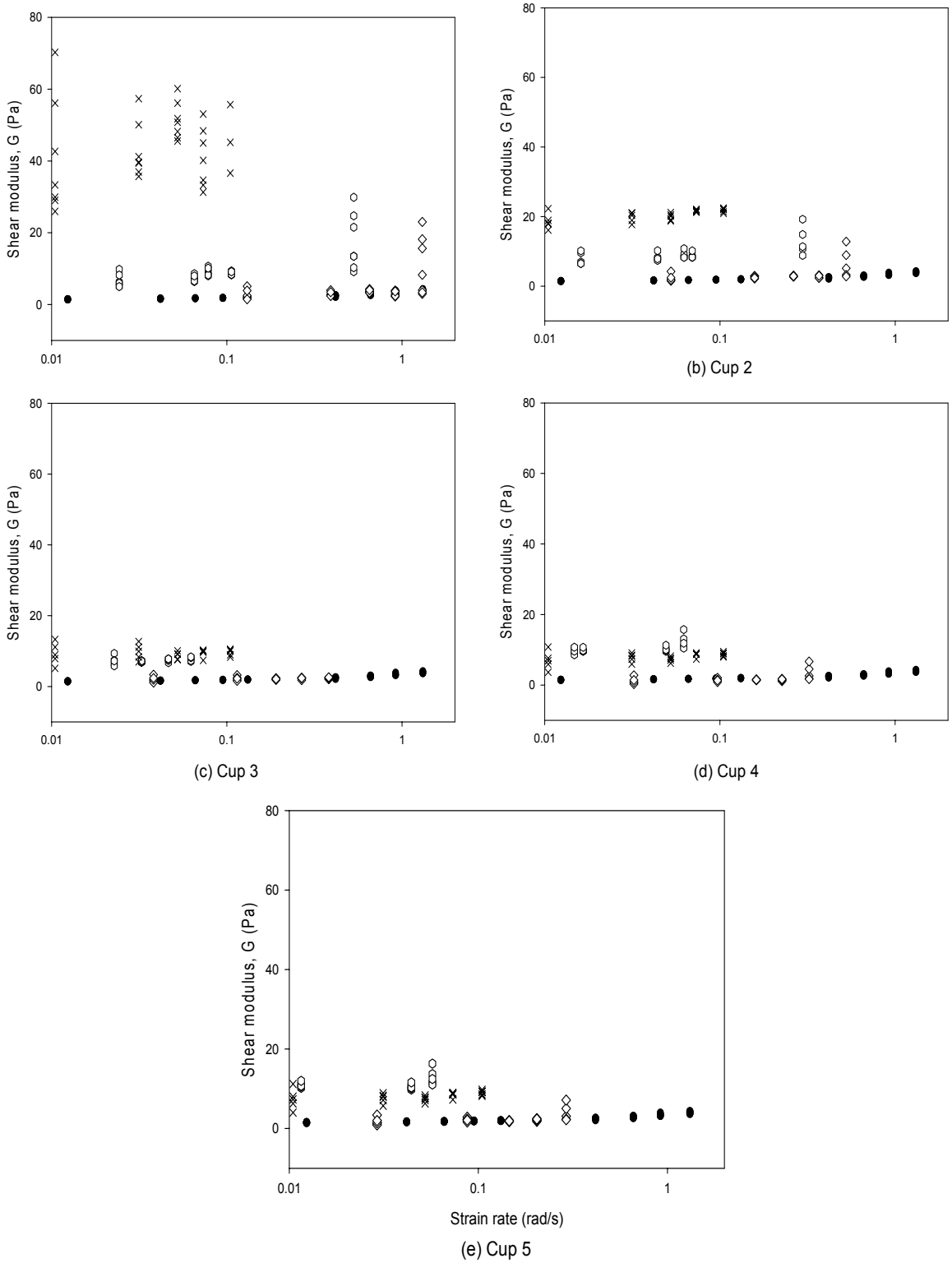


Fig. A.14 Gelatin 1.5% gels shear moduli data for various cups for all three approaches; • StressTech data;◇ Alderman approach;⎔ NC State Approach; × Brookfield Approach

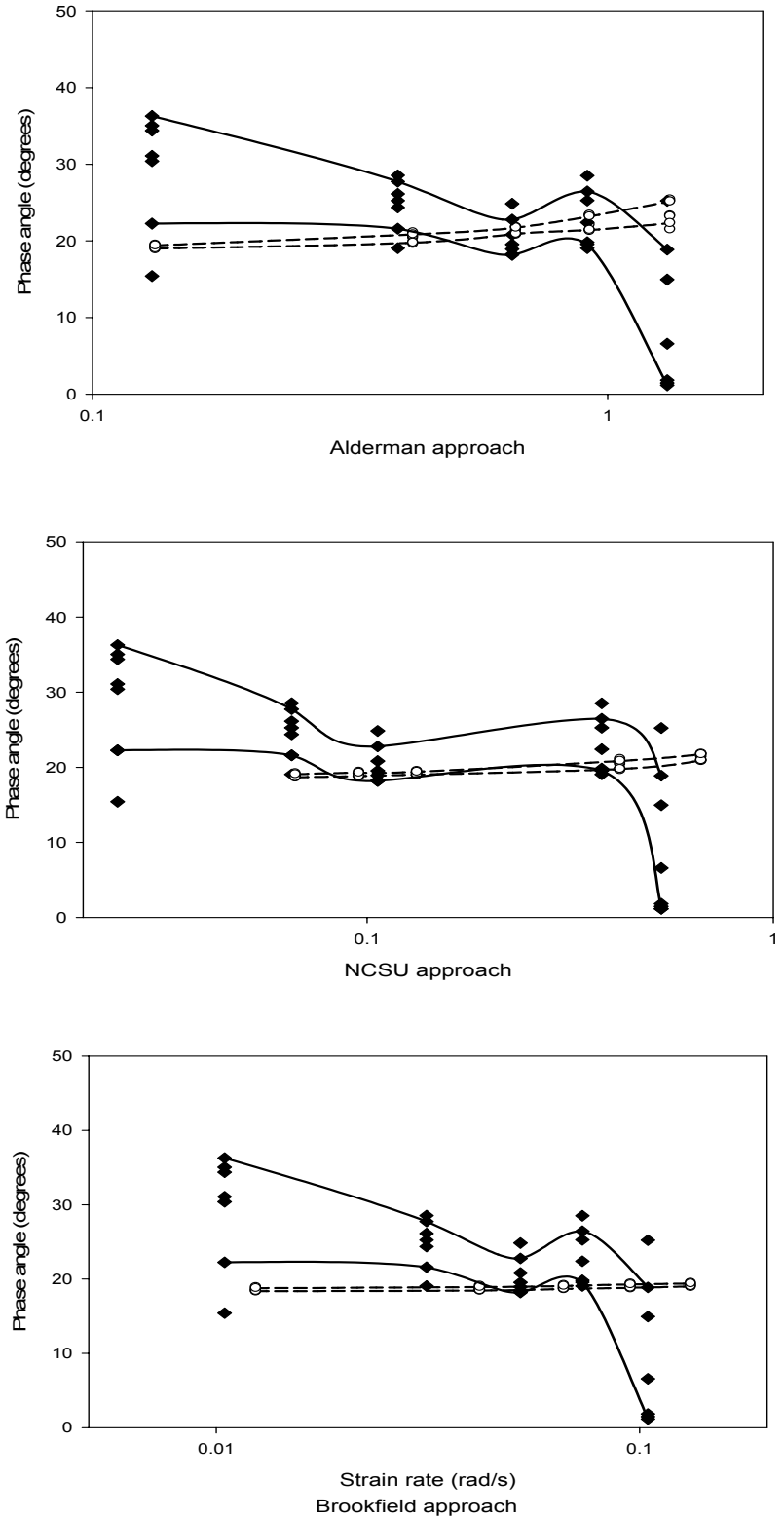


Fig. A.15 Gelatin 1.5% gels phase angle data for the three approaches for cup 1; ○ StressTech data; ◆ Brookfield data; -⊖- StressTech confidence limits; —◆— Brookfield confidence limits

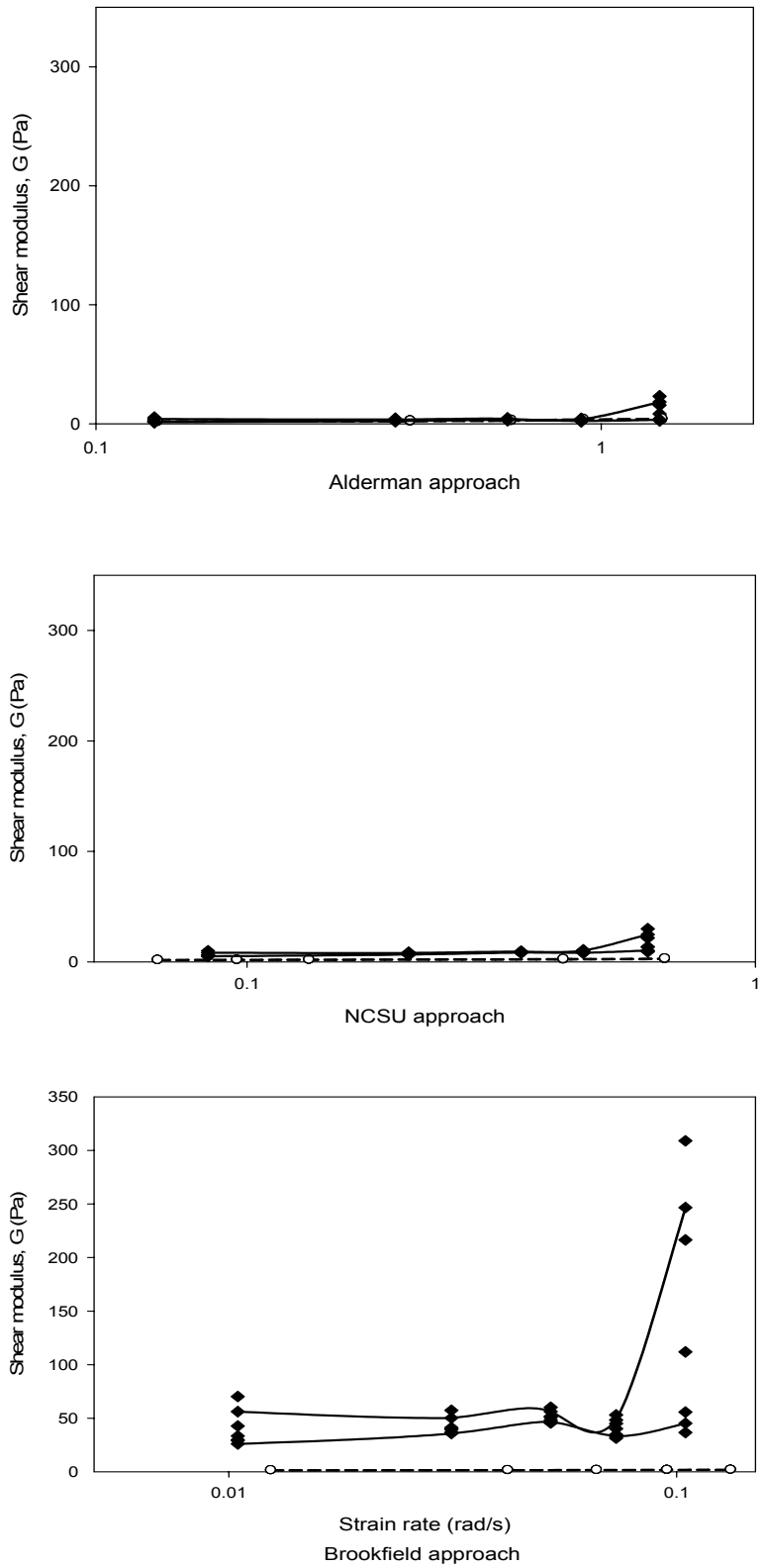


Fig. A.16 Gelatin 1.5% gels shear moduli data for the three approaches for cup 1; ○ StressTech data; ◆ Brookfield data; - -⊖- - StressTech confidence limits; —◆— Brookfield confidence limits